ELEMENTAL ANALYSIS AND MICROSCOPICAL STUDIES

OF THE MATURE SEEDS OF ELEVEN SPECIES OF <u>PINUS</u>

By

MARIA MARCIA WEST, B.Sc

A Thesis

Submitted to the School of Graduate Studies

in Partial Fulfilment of the Requirements

for the Degree

Master of Science

McMaster University

MASTER OF SCIENCE (1992)   McMASTER UNIVERSITY
(Biology)   Hamilton, Ontario

TITLE: Elemental Analysis and Microscopical Studies of the
       Mature Seeds of Eleven Species of <u>Pinus</u>.

AUTHOR: Maria Marcia West, B.Sc.
       (McMaster University)

SUPERVISOR : Dr. J. N. A. Lott

NUMBER OF PAGES: xiv, 178

ABSTRACT

The storage reserves in the mature seeds of eleven
species of <u>Pinus</u> were investigated. Lipids and proteins,
sequestered in lipid vesicles and protein bodies respectively,
were found to be the major storage reserves of pine seeds.
All seed tissues of mature <u>Pinus</u> seeds contained protein
bodies with one or more protein crystalloids and/or one or
more globoid crystals. Energy dispersive x-ray (EDX) analysis
of globoid crystals in all species of <u>Pinus</u> that were studied
revealed the presence of P, K and Mg, a fact that is
consistent with globoid crystals being phytate-rich. Traces
of Ca and Fe were also detected in the globoid crystals of
some seed tissues.

High levels of Fe and significant levels of P, K and
Mg were detected in small (often ≤ 0.33 μm), naturally
electron-dense particles that were distributed throughout the
tissues of the embryo and female gametophyte. Unlike
conventional phytate-rich globoid crystals, these Fe-rich
particles were not contained in the proteinaceous matrix of
typical protein bodies. Instead, the particles were contained
within membrane-bound structures resembling plastids.

Neutron activation analysis and spectrophotometric
phosphorus analysis were used to provide a quantitative

determination of elements in whole female gametophyte and embryo tissue samples. High levels of P, K, Mg and S and significant levels of Cl, Ca, Mn, Zn and Fe were detected in pine seed tissues. Environment and growth conditions under which the seed developed did not appear to affect the total mineral nutrient levels of mature pine seeds.

Seed size and weight varied greatly between the eleven species of _Pinus_ investigated. A major focus of this study was to determine whether seed size was correlated to the distribution of minerals in pine seeds. Previous studies showed that mineral distribution was related to seed size in cucurbits. Phosphorus, Mg and Ca concentrations in globoid crystals and Fe concentrations in electron-dense particles of _Pinus_ seed tissue were found to be negatively correlated with seed size.

A comparative study of nutrient reserves in haploid female gametophyte tissue versus diploid embryo tissues was made. Within each species of _Pinus_, the total mineral nutrient concentrations in whole female gametophyte samples were similar to total mineral nutrient concentrations within whole embryo samples. Protein body structure and the types of mineral nutrients stored in globoid crystals of protein bodies were also similar between female gametophytes and their corresponding embryos.

ACKNOWLEDGEMENTS

I wish to thank my supervisor Dr. J. Lott for encouraging me to pursue a graduate degree and for his patience, guidance and continual encouragement while I have been in his lab. I would also like to thank the members of my supervisory committee Dr. E. Weretilnyk and Dr. G. Leppard for their helpful advice.

I would like to thank Dr. L. Barber and Dr. I. Ockenden for their encouraging words and technical advice, and A. Pidruczny for technical assistance with neutron activation analysis procedures. Thank you to K. Schultes and D. Flannigan who also aided in various aspects of this work.

Finally, I would like to thank my family and friends for their support and encouragement to finish what I started. Thank you to my husband Jamie for understanding the pressures of deadlines and doing all he could to make things easier for me.

TABLE OF CONTENTS

LIST OF TABLES

that were generated by EDX analysis of globoid crystals (≥0.33 μm) or electron-dense particles (≤0.33 μm) in P. resinosa seed tissues.

crystals (≥0.33 μm) or electron-dense particles (≤0.33 μm) in P. strobus seed tissues.

($\leq$0.33 μm) in P. coulteri seed tissues.

LIST OF FIGURES

Chapter 1

INTRODUCTION

Pinus is the largest and most important genus of
conifers, comprising approximately 90 species in the northern
hemisphere of which 35 species are native to North America and
9 commonly occur in Canada (Hosie, 1979). The pines are
evergreen, resin-yielding trees and are distinguished from
other conifers by having their needles borne in fascicles or
bundles of usually 2-5, united at the base of a small branch
with a sheath of bundle scales (Little and Critchfield, 1969).
Pinus is a genus of tremendous economic importance having
species which yield timber, pulp, resins, essential oils and
edible seeds. Many species have been adopted as ornamentals.

Pinus seeds are composed of an outer seed coat that
surrounds a haploid female gametophyte tissue within which
lies a relatively small, straight, diploid embryo. In many
species, each seed has a wing to aid in wind dispersal. The
unfertilized female gametophyte tissue develops independently
and before fertilization of the egg cell (Jensen and Berthold,
1989) which results in formation of the zygote and eventually
the embryo. A fully developed embryo is composed of a whorl
of cotyledons surrounding a shoot apex, a short hypocotyl and
a radicle.

1

In addition to cytoplasm and cell wall constituents, seed tissues in general contain various storage reserves. Seed storage reserves primarily consist of lipids, proteins and carbohydrates. During germination these reserves are hydrolyzed and used by the developing seedling. Although all three types of storage reserves occur in most seeds, their relative concentrations vary from species to species. Seed reserves are present in both the female gametophyte and embryo tissues of pine seeds with the bulk of the reserves being localized in the larger female gametophyte region of the seed.

Starch is the major storage form of carbohydrates in many seeds. Starch consists of a combination of two polymers of D-glucose namely; amylose which consists of a straight chain of 300-400 glucose residues and amylopectin, a multi-branched polymer, which consists of many amylose chains joined by α-1,6 linkages (Copeland, 1976). In seed tissues starch is deposited in discrete subcellular bodies called starch granules which can vary in size and shape from species to species, and even within the seed tissues of one species (West et al., 1992). Less common seed carbohydrates include hemicellulose, amyloids and galactomannans. These carbohydrates are usually found in thickened cell walls of the endosperm or cotyledons. Starch is only a minor constituent of the storage reserves in Pinus seeds (Winton and Winton, 1932; Simola, 1974).

Each lipid or triglyceride molecule is composed of one

glycerol combined with three fatty acids. Lipids are water insoluble but soluble in a number of organic solvents such as ether, chloroform, benzene or hexane (Copeland, 1976). In seed tissues lipid reserves are stored in lipid vesicles or spherosomes that some researchers believe are bounded by half-unit membranes (Yatsu and Jacks, 1972). Pine seeds have a high content of neutral lipids (typically 45-60% of dry wt), mainly located in the female gametophyte tissue (Winton and Winton, 1932; Lopez-Perez et al., 1974; Simola, 1974; Gori, 1979). Commonly a high seed lipid content is associated with a high seed protein content.

Seed storage proteins account for the major portion of the proteins in seeds and have been defined by Higgins (1984) as any protein accumulated in significant quantities in the developing seed which is rapidly hydrolyzed during seed germination to provide reduced nitrogen to the developing seedling. Consistent with their role as nitrogenous reserves, storage proteins tend to be rich in asparagine, glutamine and arginine or proline (Higgins, 1984). These proteins are synthesized on the rough ER and are transported to the protein bodies. Seed storage proteins are differentially distributed both quantitatively and qualitatively throughout the embryo tissues of a seed. The synthesis and tissue-specific expression of seed storage proteins is assumed to be controlled by plant hormones (Higgins, 1984).

Total protein concentrations range from 10-25% of the

total seed weight in several <u>Pinus</u> species (Gifford, 1988) and are especially concentrated (typically 15-35% of dry weight) in the female gametophyte tissues (Salmia and Mikola, 1975). The major storage proteins of <u>Pinus</u> seeds are water-insoluble crystalloid proteins. They constitute 50-80% (varies with species) of the major protein reserves in the mature seed and are soluble in buffers only if sodium dodecyl sulphate (SDS) or urea is present (Gifford, 1988). The subunits of these proteins were found to be heterodimers made up of polypeptides linked by disulfide bonds (Gifford, 1988). They are rapidly hydrolyzed during germination confirming their role as storage reserves. Similar seed proteins have been found to a lesser extent in <u>Picea glauca</u> (Gifford and Tolley, 1989), as well as in some angiosperm seeds (O'Kennedy <u>et al</u>., 1979; Lalonde <u>et al</u>., 1984). Lectins, which form an important class of seed proteins in many angiosperm seeds (Barondes, 1981) were not found in seeds of <u>Pinus</u> (Gifford, 1988).

The storage proteins of seeds have long been known to be stored primarily in protein bodies (Bewley and Black, 1985). Protein bodies were first demonstrated by Hartig in 1855. Since then, protein bodies have been found in haploid, diploid and triploid tissues of both angiosperm and gymnosperm seeds. Protein bodies are spherical or oval structures bound by a single membrane and variable in size and internal structure. The internal structure of protein bodies may vary from species to species, tissue to tissue, cell to cell and

even within one cell (Lott 1981). A protein body may consist only of a homogeneous proteinaceous matrix or it may contain a combination of one or more inclusion types, such as globoid crystals, protein crystalloids and less commonly, druse or rosette crystals of calcium oxalate. This variability in internal structure provides a basis for protein body classification as outlined by Lott (1980). Generally, protein bodies are composed of storage proteins, salts of phytic acid, hydrolytic enzymes and cations. As well, small amounts of carbohydrates, oxalic acid salts and lipids may be present (Pernollet, 1978).

The protein crystalloid inclusion appears to be an ordered, partly crystalline protein deposit (Ashton, 1976) usually composed of globulin, while the globoid crystal is a phytate storage inclusion. Phytic acid or myo-inositol hexaphosphoric acid is the major storage form of phosphorus in seeds representing 60-90% of total seed P (Raboy, 1990). The term phytin refers to the mixed Mg, K and Ca cation salts of phytic acid, while phytate is a general term used to describe any salt of phytic acid. Due to its cation-chelation capabilities, phytic acid is also a form of inorganic cation storage. Phytin is principally located in the globoid crystals of protein bodies (Pernollet, 1978). The site of phytin biosynthesis is not clearly understood. Evidence has been presented that the phosphorylation of myo-inositol can occur in isolated protein bodies, therefore the protein bodies

may act as the sites of phytin biosynthesis (Sobolev and Rodionova, 1966; Tanaka et al., 1976). However, phytin particles have been found in the cytoplasm of castor beans at the time of globoid synthesis, suggesting that phytin is produced in the cytoplasm before concentrating in the protein bodies as globoid crystals (Greenwood and Bewley, 1984). During germination phytic acid is dephosphorylated, by enzymes such as phytase, into inorganic phosphorus and myo-inositol (Ashton and Williams, 1958; Ergle and Guinn, 1959; Hall and Hodges, 1966; Kikunaga et al., 1991). Although present, phytase is inactive in dry or dormant seeds (Maga, 1982).

Eleven species of Pinus, with seed sizes ranging from the species with the smallest seeds in this group (P. banksiana) to a species with one of the largest seeds (P. sabiniana) were investigated in this study. Seed size probably represents a compromise between requirements for dispersal and for establishment (Fenner, 1983). Small seed size facilitates wind dispersal over long distances while the considerable storage reserves of larger seeds improves the successful establishment of the species. There are many reports of correlations between seed size and early seedling size and vigor in the literature. The significance of seed size has been found to vary with the species and with the conditions of seedling cultivation. Spurr (1944) showed that seedling size for P. strobus was positively correlated with seed size for at least three years with the strength of the

relationship diminishing each year as seedlings became established. In general, within a species, large seeds have been found to germinate faster than smaller seeds and to produce seedlings whose initial growth is greater. Other reports of positive correlations between seed size and seedling size and vigor for _Pinus_ species include _P. sylvestris_ (Langdon, 1958), _P. elliottii_ (Shoulders, 1961), _P. banksiana_ (Yeatman, 1966), _P. taeda_ (Perry, 1976), _P. radiata_ (Wilcox, 1983) and _P. caribaea_ (Toon _et al._, 1991).

Fenner (1983) found that in general, large and small seeds differed not only in size but were also quantitatively different. Even with the seed coat taken into account, larger seeds had a lower mineral concentration in their embryos than small seeds. Seed size may also influence globoid crystal composition. Lott and Buttrose (1978) determined that Ca is usually present in the globoid crystals of _Cucurbita_ species with small seeds but absent or present only in low amounts in the globoid crystals of species with large seeds.

According to the systematics of Critchfield and Little (1966) the genus _Pinus_ contains 3 subgenera (Ducampopinus, Strobus Lemm., and Pinus), 5 sections and 15 subsections. In the subgenus Ducampopinus there is only one section (Ducampopinus) and one subsection (Krempfianae). The subgenus Strobus has two sections, Strobus and Parrya. Section Strobus has two subsections; Cembrae and Strobi while section Parrya has three subsections; Cembroides, Gerardianae and

Balfourianae. The subgenus Pinus has two sections, Pinea and Pinus. Section Pinea has three subsections; Leiophyllae, Canarienses and Pineae, while section Pinus has six subsections; Sylvestres, Ponderosae, Australes, Sabinianae, Contortae and Oocarpae.

Two of the three subgenera of <u>Pinus</u> are represented by the eleven species that were investigated in this study. <u>P</u>. <u>banksiana</u>, <u>P</u>. <u>contorta</u>, <u>P</u>. <u>resinosa</u>, <u>P</u>. <u>sylvestris</u>, <u>P</u>. <u>mugo</u>, <u>P</u>. <u>nigra</u>, <u>P</u>. <u>ponderosa</u>, <u>P</u>. <u>coulteri</u> and <u>P</u>. <u>sabiniana</u> belong to the subgenus Pinus and section Pinus. <u>P</u>. <u>banksiana</u> and <u>P</u>. <u>contorta</u> are further categorized into the subsection Contortae. <u>P</u>. <u>resinosa</u>, <u>P</u>. <u>sylvestris</u>, <u>P</u>. <u>mugo</u> and <u>P</u>. <u>nigra</u> belong in the subsection Sylvestres. <u>P</u>. <u>ponderosa</u> belongs in the subsection Ponderosae, while <u>P</u>. <u>coulteri</u> and <u>P</u>. <u>sabiniana</u> belong in the subsection Sabinianae. <u>P</u>. <u>strobus</u> and <u>P</u>. <u>koraiensis</u> belong to the subgenus Strobus Lemm. and section Strobus. These two species are further categorized into different subsections, namely; Strobi and Cembrae respectively.

<u>Pinus banksiana</u>, <u>P</u>. <u>contorta</u>, <u>P</u>. <u>resinosa</u>, <u>P</u>. <u>strobus</u>, and <u>P</u>. <u>ponderosa</u> are all pine species that are native to Canada and/or the United States. <u>P</u>. <u>banksiana</u> (jack pine) is characteristically a tree of the boreal forest region (Hosie, 1979). Its full range extends from the northeastern coast of North America to the Mackenzie River valley in northwestern Ontario (Yeatman, 1966). <u>P</u>. <u>contorta</u> (lodgepole pine) ranges

over most of British Columbia, much of Alberta and parts of southwestern Saskatchewan (Hosie, 1979). P. resinosa (red pine) is found from the Atlantic coast to southern Manitoba and is especially abundant in the Great Lakes-St. Lawrence forest region (Hosie, 1979). P. strobus (eastern white pine) is also abundant in the Great Lakes-St. Lawrence forest region but its range extends throughout most of eastern Canada into the southeastern parts of the boreal forest region, eastward into the Acadian forest region and south throughout the deciduous forest region (Hosie, 1979). In the United States it ranges through the Lake States, south to Iowa and Illinois, throughout much of the northeast, and south in the Appalachian Mountains to Georgia (Critchfield and Little, 1966). P. ponderosa (ponderosa pine/western yellow pine) is distributed over a large area both geographically and altitudinally throughout the western part of the United States (Buchholz and Stiemert, 1945) as well as drier portions of the southern interior of British Columbia (Canada Dept. of Mines and Resources, 1939).

Pinus sylvestris, P. mugo and P. nigra are not native to Canada but have been introduced to this country and are commonly planted here. P. sylvestris (scots/scotch pine) is the dominant forest tree species within the boreal zone and has a wider world-wide distribution than any other pine (Ingestad, 1979). Its natural area stretches longitudinally from Scotland and the Iberian peninsula to the Pacific coast

of Siberia and latitudinally from Norway to Spain (Pardos, 1990). P. mugo (mugho pine) commonly grows in the mountains of central and southern Europe, Rumania, Bulgaria, central Italy, Germany, Poland and Spain (Critchfield and Little, 1966). P. nigra (Austrian pine) is an eastern and southern European pine from Spain to Austria and throughout most of the Balkan peninsula. This species is found as far east as southern Russia and south to Turkey as well as on the islands of Cyprus, Sicily and Corsica (Critchfield and Little, 1966).

Pinus coulteri and P. sabiniana are native to California (Webster, 1896). P. coulteri (coulter pine) commonly grows in the southern and central mountains of California, while P. sabiniana (digger pine) is found in the coast range and in the foothills of the Sierra Nevada (Critchfield and Little, 1966).

Pinus koraiensis (Korean pine) is native to Korea and eastern Manchuria into southeastern Siberia, with outliers on the Japanese islands of Honshu and Shikoku (Critchfield and Little, 1966).

The objectives of this study were:

1) to examine protein body structure in the mature seeds of the eleven Pinus species using transmission electron microscopy (Chapter 2).

2) to determine whether or not the mineral nutrient content of mature seeds varies between species of Pinus through the

use of spectrophotometric phosphorus analysis (Chapter 3) and neutron activation analysis (Chapter 4).

3) to use energy dispersive x-ray (EDX) microanalysis to study where elements of importance as mineral nutrients are stored in protein bodies of mature pine seeds (Chapter 5).

4) to study the distribution of EDX analyzable elements in various seed tissues of mature pine seeds and to determine if mineral nutrient distribution can be related to seed tissue weight and size measurements (Chapter 5).

Chapter 2

IMAGE ANALYSIS MEASUREMENTS AND TRANSMISSION ELECTRON MICROSCOPY OBSERVATIONS OF PINUS SEEDS.

Introduction

Image analysis is a versatile tool that readily provides objective interpretations and quantitative analyses of selected parameters in a computer image. For storage in a computer, an image must be digitized ie. divided into individual pixels, the size of which defines the spatial resolution of the image (Hader, 1988). Each square pixel has a numerical value that represents the average brightness of the original image in that particular square area (Russ, 1990). The number of possible grey-level values also affects the image resolution. A typical computer has a capacity for 256 grey-levels while the human eye can only distinguish 20-30 grey-levels in a monochrome image (Russ, 1990). Quantitative measurements are based on the number and area of pixels that compose a selected feature of the image. This ensures accuracy and reproducibility of measurements without human bias.

Image analysis techniques have previously been used in biological sciences for many studies including counting and sizing bacteria (Estep and MacIntyre, 1986), to evaluate the

shape of plants in several stages (Ninomiya and Shigemori, 1991), to measure morphology characteristics of various cereal grains such as size, shape (Symons and Fulcher, 1988) and colour (Neuman et al., 1989) and to discriminate between cereal grains and weed grains (Chen et al., 1989).

Resolution is the ability to distinguish two adjacent structures. The resolution of a light microscope is limited by the wave diffractive properties of visible light, which acts as the source of illumination. The resolving power of a light microscope is approximately 0.2 μm. In contrast, a resolving power of 1 nm can routinely be achieved by a transmission electron microscope (TEM). The source of illumination in an electron microscope is a beam of fast-moving electrons. The electron has a much shorter wavelength than visible light, therefore diffraction limitations are reduced. The TEM has magnification and resolution capabilities that are over 1000 times greater than those of a light microscope (Bozzola and Russell, 1992).

In this study image analysis has been used to measure area, length, width and the elongation ratio (width:length) of whole seeds, female gametophyte tissues and embryos of the Pinus species being studied. Transmission electron microscopy was used to examine the ultrastructure of mature seed tissues of Pinus.

Materials and Methods

Sources of seeds

The Ontario Tree Seed Plant (Ministry of Natural Resources, Angus, Ont.) provided seeds of P. banksiana, P. resinosa, P. mugo (sample A and sample B), P. strobus (sample A and sample B) and P. nigra that were used in this study. P. strobus (sample A) seeds had been collected in 1959 in northwestern Ontario. The P. banksiana and P. mugo (sample A) seeds had been collected in 1968 and 1982 respectively from eastern Ontario surrounding Lake Ontario. P. strobus (sample B) and P. resinosa (sample A) seeds were collected in 1969 and 1970 respectively from the Algonquin region of Ontario. P. resinosa (sample B) and P. nigra seeds were collected in southwestern Ontario in 1970 and 1975 respectively. P. mugo (sample B) seeds were collected from Eastern Ontario near Peterborough in 1973. P. contorta, P. sylvestris and P. ponderosa seeds were provided by the Petawawa National Forestry Institute (Chalk River, Ont.). P. koraiensis seeds came from the National Tree Seed Laboratory (Dry Branch, Georgia). P. coulteri seeds also came from the National Tree Seed Laboratory and had been collected in California, Seed Zone 997, in 1978. P. sabiniana seeds were collected at Lake Beryesa, California in 1988 and P. mugo (sample C) seeds were collected in Hamilton, Ont. in 1992.

Seed weight measurements

Whole seed mean weights were calculated by

individually weighing 100 seeds of each species of <u>Pinus</u> under investigation in this study. Similarly, embryo mean weights for <u>P</u>. <u>strobus</u>, <u>P</u>. <u>nigra</u>, <u>P</u>. <u>ponderosa</u>, <u>P</u>. <u>coulteri</u>, <u>P</u>. <u>sabiniana</u>, and <u>P</u>. <u>koraiensis</u> were obtained from individual weights of 100 embryos of each species. Due to their small size, 100 embryos of <u>P</u>. <u>banksiana</u>, <u>P</u>. <u>contorta</u>, <u>P</u>. <u>resinosa</u>, <u>P</u>. <u>sylvestris</u> and <u>P</u>. <u>mugo</u> were weighed four at one time rather than individually. Embryo mean weights were then calculated from the 25 average weight values. Female gametophyte mean weights were calculated by subtracting embryo mean weights from the mean weights of female gametophyte + embryo tissues for 100 seeds of each species.

Statistical Analysis

In order to determine if differences in means were significant, MINITAB'S analysis of variance (ANOVA) test was employed. ANOVA tests the null hypothesis H_o: $\mu_1 = \mu_2 = \ldots = \mu_k$, where k is the number of experimental groups or samples. When the null hypothesis is rejected at a 5% level of significance, then a multiple comparison test can be applied to determine which means significantly differ from one another. The multiple comparison test used in this study was the Tukey test. Procedures for the Tukey test were followed as outlined by Zar (1984) and a confidence level of 95% was used. MINITAB was used to perform correlations on sets of means once the null hypothesis for the means was rejected by ANOVA testing.

Moisture content values

Aluminum pans were dried in an oven, allowed to cool in a desiccator, and then weighed. Air-dried female gametophyte and embryo tissue samples were weighed into the aluminum pans. The tissue samples were transferred to an oven and dried at 85±2°C for 2-24 h until a constant weight was attained. Each sample was then cooled in a desiccator and weighed. The moisture content for each sample was calculated using the formula suggested by Allen (1974) so that the percentage moisture is equal to the loss in weight of the sample on drying divided by the initial sample weight, then multiplied by 100.

Image analysis

Prior to collecting seed images, a calibration file was created by collecting the image of a square on graph paper, then calibration software was used to indicate the correct measurement and units between numbered points at the square's corners. The aspect ratio (the image's ratio of height to width) was calibrated by collecting images of round coins after the diameters were measured with vernier callipers. The aspect ratio was then adjusted until the diameter of each coin was the same around the entire circumference and equalled that of the manually measured value.

One hundred P. banksiana seeds were laid out on a copy stand so that no two seeds were touching. An image of the

seeds was transmitted onto the CRT screen of a monitor using a video camera (MTI-65, Dage-MTI Inc., Michigan City, IN) mounted above the copy stand. The lights of the copy stand and brightness and contrast of the CRT screen were adjusted to remove shadows and optimize the image. This image was transferred to the monitor of a PGT IMIX-II Sun computer as a grey-tone digital image. Brightness and contrast were adjusted to augment the captured computer image. A painter program was used to create a binary colour image by means of grey-level conversion. Once a binary image was made, feature analysis software was used to measure area, length, width and elongation ratio (ratio of width to length) of each seed based on the number of coloured pixels that incorporated each seed image. Similar binary images were created for 100 female gametophytes and 100 embryos of P. banksiana. The same procedure was then followed for 100 seeds, female gametophytes and embryos of each Pinus species under investigation in this study.

Transmission electron microscopy

Female gametophyte and embryo tissues of a few seeds of each Pinus species were cut up into approximately 1 mm^3 blocks and fixed in 3% glutaraldehyde in 0.05 M cacodylate buffer (pH 7.2) for 2 h. The tissue blocks were post-fixed in 2% OsO$_4$ in buffer for 2 h, then dehydrated through an EtOH series (50%, 60%, 70%, 80%, 90%, 100%, 100%) over 30 minute intervals. The tissue samples were further dehydrated in 100%

propylene oxide and embedded in Spurr's resin following a propylene oxide:Spurr's resin series (3:1, 2:1, 1:1, 1:2, 1:3, 100% Spurr's, 100% Spurr's) for 24 h periods. Ultra-thin sections were cut with glass knives on a Reichert OM U2 Ultramicrotome. The sections were post-stained with uranyl acetate followed by Reynold's lead citrate and examined with a JEOL JEM-1200 EX-2 TEMSCAN microscope.

Results

Figure 1 illustrates whole seed and female gametophyte size differences between the eleven species of <u>Pinus</u> that were investigated. Whole seed, female gametophyte + embryo, female gametophyte, and embryo weights for the eleven species are listed in Table 1. The order in which the species have been arranged in Table 1 and all subsequent tables is according to increasing female gametophyte + embryo weight. Whole seed weight and size measurements were included in this study for completeness and interest. Whole seed weight, area, length and width measurements (Table 1 and 2) were found to be positively correlated with each other (see Appendix A for correlation data). Likewise, whole seed measurements were positively correlated with weight measurements obtained for female gametophyte + embryo tissues (Table 1), as well as weight, area, length and width measurements obtained for female gametophyte tissues (Table 3) and embryo tissues (Table 4). The correlations of whole seed weight and size measurements with analysis data will not be discussed as the seed coats were always removed prior to analysis of elements in the remaining seed tissues.

Elongation ratios are provided for whole seeds (Table 2), female gametophyte tissues (Table 3) and embryos (Table 4). The whole seeds of <u>P</u>. <u>banksiana</u>, <u>P</u>. <u>mugo</u>, <u>P</u>. <u>ponderosa</u> and <u>P</u>. <u>koraiensis</u> have similar ratios of 0.7 indicating that these species are similar in their shape. <u>P</u>. <u>contorta</u>, <u>P</u>.

Figure 1.   **Mature Seeds and Female Gametophytes of Eleven
             Pinus Species**

             Species are arranged in order of increasing
             female gametophyte + embryo weight. This
             illustration shows the size differences between
             whole seeds and female gametophytes of the
             Pinus species that were investigated.
             Magnification = 1.25x.

P. banksiana

P. contorta

P. resinosa

P. sylvestris

P. mugo

P. strobus

P. nigra

P. ponderosa

P. coulteri

P. sabiniana

P. koraiensis
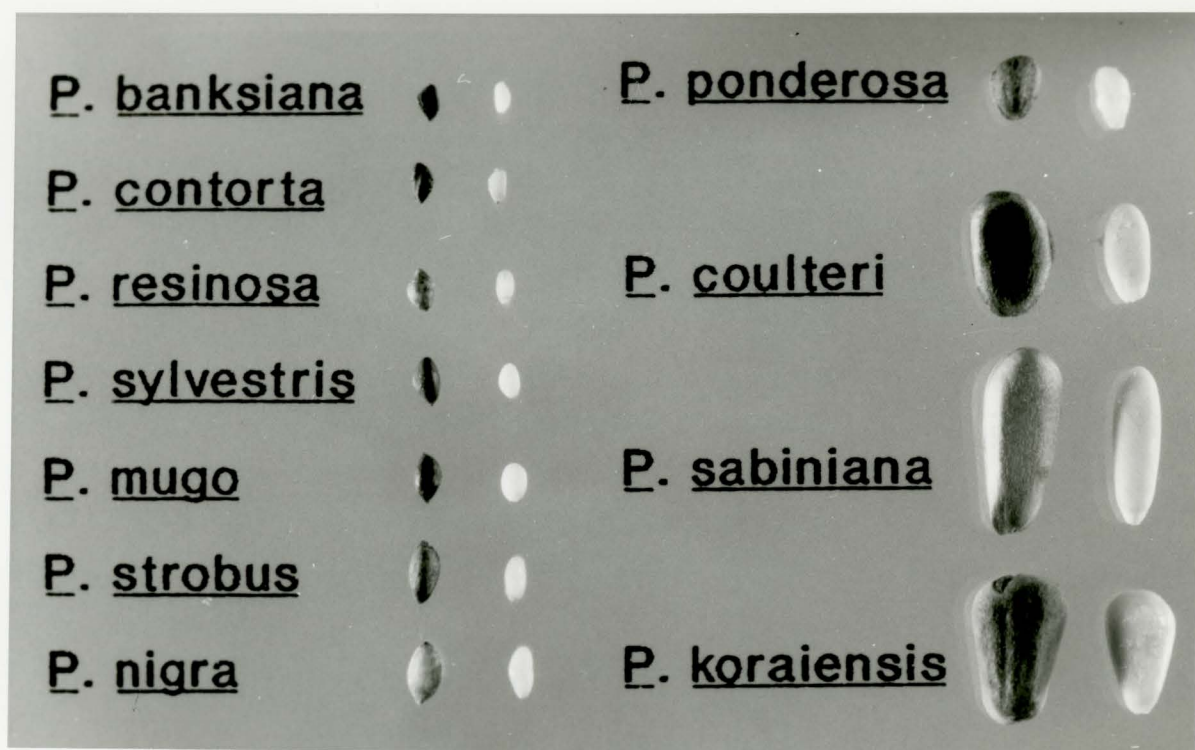
Table 1. Mean measurements (± SD) of whole seed weight, female
gametophyte + embryo weight, female gametophyte weight and
embryo weight of various <u>Pinus</u> species.

Species N= 100	Weight (mg)			
	Whole seed	Female gametophyte + embryo	Female gametophyte	Embryo
<u>P</u>. <u>banksiana</u>	3.9 ± 0.7e	3.0 ± 0.4g	2.7 ± 0.4g	0.3 ± 0.1d
<u>P</u>. <u>contorta</u>	4.3 ± 0.9e	3.6 ± 0.5fg	3.1 ± 0.5fg	0.5 ± 0.1d
<u>P</u>. <u>resinosa</u>	8.9 ± 1.4e	5.9 ± 1.0fg	5.3 ± 1.0fg	0.6 ± 0.1d
<u>P</u>. <u>sylvestris</u>	7.0 ± 1.5e	5.9 ± 1.2fg	5.2 ± 1.5fg	0.7 ± 0.1d
<u>P</u>. <u>mugo</u>	7.5 ± 2.1e	6.5 ± 1.6fg	5.9 ± 1.6fg	0.6 ± 0.1d
<u>P</u>. <u>strobus</u>	17.6 ± 3.8e	12.2 ± 2.8ef	11.3 ± 2.8ef	0.9 ± 0.2d
<u>P</u>. <u>nigra</u>	23.8 ± 4.6de	16.1 ± 3.5e	14.3 ± 3.5e	1.8 ± 0.2cd
<u>P</u>. <u>ponderosa</u>	46.9 ± 9.8d	27.9 ± 6.4d	24.5 ± 6.4d	3.4 ± 0.6c
<u>P</u>. <u>coulteri</u>	269.7 ± 52.7c	79.1 ± 18.7c	72.7 ± 19.0c	6.4 ± 3.1b
<u>P</u>. <u>sabiniana</u>	577.3 ± 158.3a	109.7 ± 27.8b	100.2 ± 28.1b	9.5 ± 4.2a
<u>P</u>. <u>koraiensis</u>	453.6 ± 104.4b	163.2 ± 38.3a	157.7 ± 38.3a	5.5 ± 1.3b

Note: Values within the same column that are followed by the same
letter are not significantly different at P>0.05.

Table 2. Mean (±SD) measurements obtained by image analysis of whole Pinus seeds.

Species N= 100	Area (mm^2)	Length (mm)	Width (mm)	Elongation ratio
P. banksiana	7.6 ± 1.1f	4.2 ± 0.4h	2.7 ± 0.3g	0.7 ± 0.1a
P. contorta	8.0 ± 1.1f	4.4 ± 0.4gh	2.7 ± 0.2g	0.6 ± 0.1b
P. resinosa	9.2 ± 1.3f	4.6 ± 0.3fg	2.9 ± 0.3fg	0.6 ± 0.1b
P. sylvestris	10.0 ± 1.9f	4.9 ± 0.5f	3.1 ± 0.3f	0.6 ± 0.1b
P. mugo	10.0 ± 1.7f	4.7 ± 0.4fg	3.1 ± 0.4f	0.7 ± 0.1a
P. strobus	19.4 ± 2.7e	6.8 ± 0.6e	4.1 ± 0.4e	0.6 ± 0.1b
P. nigra	19.5 ± 3.6e	6.8 ± 0.7e	4.1 ± 0.4e	0.6 ± 0.1b
P. ponderosa	29.9 ± 5.9d	7.8 ± 0.8d	5.4 ± 0.6d	0.7 ± 0.1a
P. coulteri	97.2 ± 16.8c	14.4 ± 1.4c	9.2 ± 1.0c	0.6 ± 0.1b
P. sabiniana	158.1 ± 21.0a	20.9 ± 1.0a	10.0 ± 0.9b	0.5 ± 0.0c
P. koraiensis	122.8 ± 32.3b	15.7 ± 2.4b	10.6 ± 1.6a	0.7 ± 0.1a

Note: Values within the same column that are followed by the same letter are not significantly different at P>0.05.

Table 3. Mean (±SD) measurements obtained by image

analysis of _Pinus_ female gametophytes.

Species N= 100	Area (mm^2)	Length (mm)	Width (mm)	Elongation ratio
P. banksiana	4.7 ± 0.8f	3.4 ± 0.3i	2.1 ± 0.2h	0.6 ± 0.1a
P. contorta	5.7 ± 1.0f	3.7 ± 0.3hi	2.3 ± 0.3gh	0.6 ± 0.1a
P. resinosa	6.5 ± 1.1f	4.0 ± 0.3gh	2.4 ± 0.3fg	0.6 ± 0.1a
P. sylvestris	7.2 ± 1.4f	4.2 ± 0.4g	2.6 ± 0.3f	0.6 ± 0.1a
P. mugo	7.2 ± 1.4f	4.1 ± 0.4g	2.6 ± 0.3f	0.6 ± 0.1a
P. strobus	10.3 ± 1.9e	5.2 ± 0.5f	2.9 ± 0.3e	0.6 ± 0.1a
P. nigra	13.7 ± 2.4d	5.9 ± 0.6e	3.3 ± 0.4d	0.6 ± 0.1a
P. ponderosa	19.1 ± 3.4c	6.6 ± 0.6d	4.1 ± 0.5c	0.6 ± 0.1a
P. coulteri	45.3 ± 7.4b	11.2 ± 1.0c	5.6 ± 0.6b	0.5 ± 0.1b
P. sabiniana	63.6 ± 13.9a	16.0 ± 1.7a	5.6 ± 0.9b	0.4 ± 0.0c
P. koraiensis	62.3 ± 12.5a	12.4 ± 1.2b	6.9 ± 0.9a	0.6 ± 0.1a

Note: Values within the same column that are followed by the

same letter are not significantly different at P>0.05.

Table 4. Mean (±SD) measurements obtained by image analysis of Pinus
embryos.

Species N= 100	Area (mm^2)	Length (mm)	Width (mm)	Elongation ratio
P. banksiana	2.2 ± 0.7g	2.8 ± 0.4i	1.3 ± 0.2ef	0.5 ± 0.1a
P. contorta	2.9 ± 0.7fg	3.2 ± 0.4ghi	1.4 ± 0.2de	0.5 ± 0.1a
P. resinosa	2.1 ± 0.6g	3.0 ± 0.4hi	1.2 ± 0.2f	0.4 ± 0.1b
P. sylvestris	3.5 ± 0.8f	3.6 ± 0.4g	1.5 ± 0.2cd	0.4 ± 0.1b
P. mugo	2.9 ± 0.7fg	3.4 ± 0.4gh	1.4 ± 0.2de	0.4 ± 0.1b
P. strobus	3.5 ± 0.9f	4.1 ± 0.6f	1.4 ± 0.2de	0.3 ± 0.1c
P. nigra	5.1 ± 1.3e	5.1 ± 0.7e	1.6 ± 0.3c	0.3 ± 0.1c
P. ponderosa	8.0 ± 1.6d	6.0 ± 0.6d	2.2 ± 0.3b	0.4 ± 0.0b
P. coulteri	14.9 ± 3.9b	9.1 ± 1.4b	2.6 ± 0.4a	0.3 ± 0.0c
P. sabiniana	18.2 ± 5.3a	10.7 ± 2.1a	2.7 ± 0.4a	0.3 ± 0.0c
P. koraiensis	9.7 ± 2.4c	7.3 ± 1.0c	2.3 ± 0.4b	0.3 ± 0.0c

Note: Values within the same column that are followed by the same letter
are not significantly different at P>0.05.

resinosa, P. sylvestris, P. strobus, P. nigra and P. coulteri have ratios approximating 0.6, while P. sabiniana with a ratio of 0.5 is elongated in its shape with the length of the seed twice as long as the width. Female gametophyte elongation ratios ranged from 0.4 for P. sabiniana to 0.7 for P. sylvestris and P. mugo denoting an oval to slightly oblong female gametophyte shape for the eleven species. Embryo elongation ratios ranged from 0.3 to 0.5 indicating that embryo length was at least twice as great as embryo width for all Pinus species investigated.

Moisture content values for female gametophyte and embryo tissues of the eleven species studied are listed in Table 5. These values were used to calculate dry weight element concentrations that are presented in Chapter 3 and 4.

Cells of similar tissue regions and organs were comparable in appearance from species to species. The cells contained numerous protein bodies surrounded by lipid vesicles or spherosomes (Figs. 2, 3). The protein bodies varied in size and internal composition. Large protein bodies (1.0-3.5 μm in diameter) were observed in the female gametophyte and ground meristem tissues of the embryo. These large protein bodies often contained one or more globoid crystals and/or protein crystalloids (Figs. 2, 3). Globoid crystals appeared as naturally, electron-dense particles when viewed by the TEM (Fig. 4). Smaller protein bodies (0.5-1.0 μm in diameter) were also observed in these tissues and commonly contained one

Table 5. Moisture content values (%) for female
          gametophyte and embryo tissues of various <u>Pinus</u>
          seeds.

Species	Female gametophyte	Embryo
<u>P</u>. <u>banksiana</u>	5.0	5.0
<u>P</u>. <u>contorta</u>	5.0	3.0
<u>P</u>. <u>resinosa</u>	5.0	4.3
<u>P</u>. <u>sylvestris</u>	4.5	4.5
<u>P</u>. <u>mugo</u>	5.4	4.1
<u>P</u>. <u>strobus</u>	4.0	4.0
<u>P</u>. <u>nigra</u>	4.5	5.0
<u>P</u>. <u>ponderosa</u>	5.6	5.0
<u>P</u>. <u>coulteri</u>	4.7	4.5
<u>P</u>. <u>sabiniana</u>	3.9	3.6
<u>P</u>. <u>koraiensis</u>	2.8	3.1

or more protein crystalloids and/or small globoid crystals. Protein bodies of the protoderm, procambium or shoot apex were routinely small and rarely contained globoid crystals (Fig. 5). Protein crystalloids were more commonly found in the protein bodies of these embryo regions.

Small ($\leq$ 0.33 μm in diameter), naturally electron-dense particles were observed throughout the female gametophyte and embryo tissues of pine seeds (Figs. 5, 6, 7) and were especially prevalent in the protoderm, procambium and shoot apex of the embryo. The number of particles appeared to be higher within the cells of tissues of smaller-sized seeds than larger-sized seeds. Unlike conventional globoid crystals, these electron dense particles were not found in the proteinaceous matrix of traditional protein bodies. These particles were however, contained within membrane-bound structures of variable shape and size. The shape of the bounding structures appeared to be governed by surrounding cytoplasmic storage reserves (Fig. 5). Often these structures were observed to be associated with stacks of rough ER (Fig. 6) and commonly contained a substance that closely resembles sections of starch as viewed by TEM (Fig. 7). Except in the membrane-bound structures, these deposits were not observed elsewhere in the sections of female gametophyte and embryo tissues.

Figure 2.   **Transmission Electron Micrograph of a P.**
             banksiana Embryo Protein Body.

             Thin section fixed by glutaraldehyde, post-fixed
             by OsO$_4$, and stained by uranyl acetate and lead
             citrate showing the internal composition of a
             protein body surrounded by lipid vesicles (L)
             within the cotyledon ground meristem tissue.
             Note one large protein crystalloid (PC) and
             a globoid cavity (GC) within the proteinaceous
             matrix (PM) of the protein body.
             Scale bar = 1 μm.

Figure 3.   **Transmission Electron Micrograph of a P. contorta**
             Embryo Protein body.

             Thin section fixed by glutaraldehyde, post-fixed
             by OsO$_4$, and stained by uranyl acetate and lead
             citrate showing lipid vesicles (L) surrounding a
             protein body in the cotyledon ground meristem
             tissue. Three protein crystalloids (PC) and one
             globoid cavity (GC) can be observed within the
             proteinaceous matrix (PM) of the protein body.
             Scale bar = 0.5 μm.

Figure 4.   **Scanning Transmission Electron Micrograph of**
             Globoid Crystals in Embryo Tissue of P. Mugo.

             Thick section fixed by low-water-content
             procedures (see Chapter 5) showing naturally
             electron-dense globoid crystals (G) contained
             within protein bodies and smaller electron-dense
             particles (DP) not found in protein bodies.
             Scale bar = 5 μm.

Figure 5.   **Transmission Electron Micrograph of Protoderm**
             Tissue of P. sylvestris.

             Thin section fixed by glutaraldehyde, post-fixed
             by OsO$_4$, and stained by uranyl acetate and lead
             citrate showing the storage reserves in a
             protoderm cell of the hypocotyl. Lipid vesicles
             (L), protein bodies (PB) and electron-dense
             particles (DP) are visible.
             Scale bar = 1 μm.

Figure 6.   **Transmission Electron Micrograph of an Electron-Dense Particle in Root Apex Cell of P. mugo.**

Thin section fixed by glutaraldehyde, post-fixed by OsO_4, and stained by uranyl acetate and lead citrate showing membrane-bound structure (indicated by arrows) that surrounds electron-dense particles (DP). Stacks of rough endoplasmic reticulum (ER) are commonly observed near the particles. Lipid vesicles (L) and a protein body with one globoid cavity (GC) are visible.
Scale bar = 0.5 μm.

Figure 7.   **Transmission Electron Micrograph of an Electron-Dense Particle in Cotyledon Ground Meristem Cell of P. ponderosa.**

Thin section fixed by glutaraldehyde, post-fixed by OsO_4, and stained by uranyl acetate and lead citrate showing an electron-dense particle (DP) surrounded by a membrane-bound structure (indicated by arrows), within which lies a starch deposit (S). Note the cavity (DC) left by another electron-dense particle that was removed from the section during sectioning.
Scale bar = 1 μm.
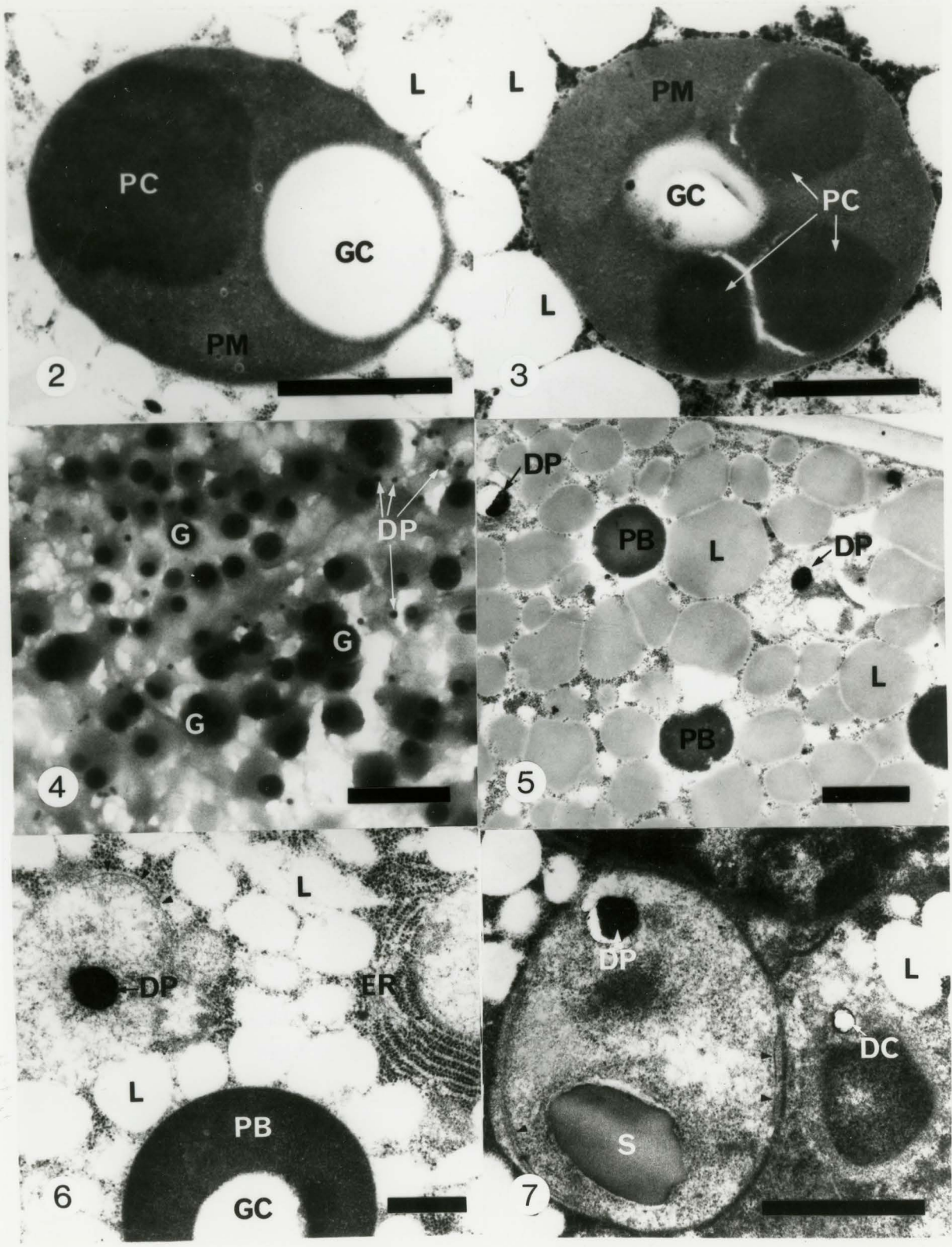
Discussion

In the eleven _Pinus_ species investigated, whole seed weight and size varied over a large range. Even with seed coats removed, the differences in female gametophyte weights and sizes were still great. It was determined that female gametophyte and embryo weights and sizes were strongly related to the size of the whole seed from which they came ie., larger seeds had larger female gametophytes and embryos. Buchholz (1946) found similar correlations between seed size, female gametophyte size and embryo size in _P_. _ponderosa_. Unlike the angiosperms where some seeds may become larger due to vigorous embryo growth, the seeds of gymnosperms are fully grown with hardened seed coats prior to fertilization (Buchholz and Stiemert, 1945). Thus embryo growth does not affect final seed size. Since the female gametophyte is fully formed prior to embryo development and surrounds the embryo, female gametophyte size does appear to influence final embryo size (Buchholz and Stiemert, 1945).

Embryo and female gametophyte cells were similar in storage reserves as observed by electron microscopy. This fact confirms previous observations of seeds of _P_. _sylvestris_ and _P_. _pinea_ (Simola, 1974; Fernandez Garcia de Castro and Martinez-Honduvilla, 1984). For all eleven species investigated, embryo and female gametophyte cells contained large numbers of lipid vesicles. Lipid is the major storage reserve in _Pinus_ seeds. Lipids have been found to account for

up to 50% of the cross-sectional area of pine seeds (Flinn et al., 1989). Numerous protein bodies, comparable in structure for similar tissue regions and organs, were observed in seeds of the eleven species. Gori (1979) determined that lipids and proteins were the main storage substances in the female gametophyte of P. pinea. The presence of a small amount of starch within pine seed tissue was confirmed using Lugol's iodine on ground tissue pieces. In sections viewed by TEM, trace amounts of starch were observed only in membrane-bound structures that surrounded the electron-dense particles throughout the tissues of the embryo and the female gametophyte of the species investigated in this study, indicating it is only a minor storage reserve constituent of pine seeds.

Protein crystalloids and globoid crystals were commonly observed within the proteinaceous matrix of protein bodies throughout the tissues of the embryo and the female gametophyte. These protein body inclusions were previously noted in P. sylvestris seed tissues (Simola, 1974) and in the female gametophyte of P. pinea seeds (Gori, 1979). Although not commented on by the authors, the micrographs of Durzan et al. (1971) clearly showed similar inclusions in the protein bodies of P. banksiana seeds. Due to the density of globoid crystals, they are difficult to fix and infiltrate with resin. Therefore, globoid crystals are commonly pulled out or chemically extracted from seed tissues during sectioning,

leaving a hole or globoid cavity in the proteinaceous matrix of protein bodies.

As previously indicated, the major female gametophyte and embryonic axis proteins were shown to be located in protein crystalloids (Gifford, 1988). These water-insoluble proteins constitute 50% of the total storage reserves in pine seeds. In mature P. contorta seeds the protein crystalloids accounted for approximately 70% of the water-insoluble protein fraction; of this, 90-95% was in the female gametophyte and the remainder in the embryonic axis (Lammer and Gifford, 1989). The differences in solubility between the matrix and crystalloid proteins effectively compartmentalize them within the protein bodies.

Small electron-dense particles were observed to be surrounded by membrane-bound structures in embryos and female gametophytes of all eleven pine species examined. These particles were commonly found in close proximity to the nuclei of cells and frequently observed to be associated with stacks of rough ER. The matrix of the membrane-bound structures did not appear to be as dense as the matrix of traditional protein bodies. I believe that these structures are proplastids but it will require further study to confirm the origin and function of the structures. Proplastids are precursor structures which can develop into plastids with specialized biochemical characteristics (Gunning and Steer, 1975). Simola (1974) indicated that proplastids with electron-translucent

starch grains were visible in P. sylvestris seeds especially near the nucleus of a cell. Simola did not report that electron-dense particles were present within the observed proplastids. Proplastids were found in the cotyledon cells of P. banksiana (Durzan et al., 1971).

Chapter 3

MEASUREMENT OF PHOSPHORUS IN FEMALE GAMETOPHYTE AND EMBRYO TISSUES OF _PINUS_ SEEDS BY SPECTROPHOTOMETRIC PHOSPHORUS ANALYSIS.

Introduction

Spectrophotometry is one of the most popular techniques for phosphorus determination. The principle of spectrophotometry is based on the conversion of a particular constituent of a matrix into a product whose solution or suspension is strongly coloured and shows differential absorption of light of different wavelengths (Sandell, 1950). In spectrophotometry, the photo-electric cells of a spectrophotometer are used to measure the intensity of incident light transmitted by a coloured solution that is subjected to light consisting of a narrow band of wavelengths.

Most of the procedures for the spectrophotometric determination of inorganic phosphate in solution have been based on the formation of heteropolyacids such as molybdophosphate and vanadomolybdophosphate in an acidic medium. It has been found that the molybdophosphate reduction method provides better sensitivity in phosphorus measurement than the procedure involving the formation of the

vanadomolybdophosphate complex, especially for samples with lower phosphorus contents (Tušl, 1972).

In an acidic solution of ammonium molybdate, orthophosphate ions condense with molybdate ions to give molybdophosphoric acid $H_3[P(Mo_3O_{10})_4]$. This heteropoly complex has a yellow colour. The reduction of molybdophosphoric acid by hydroquinone in the presence of sodium sulfite results in the formation of an intensely blue complex that is proportional to the inorganic phosphorus present (Briggs, 1924). Excess molybdic acid is not reduced in this reaction and a colour reaction does not occur when ammonium molybdate, hydroquinone and sodium sulfite are mixed in the absence of inorganic phosphate. With such a blue molybdophosphoric acid complex, a detection limit of 0.05 μg/ml can be attained using spectrophotometry (Štupar et al., 1987).

Only orthophosphates react with molybdate to form molybdophosphate (Motomizu et al., 1983). Therefore, a number of procedures must be performed to break up the organic matter of samples and convert phosphorus-containing constituents to orthophosphates prior to analysis. There are two methods for the destruction of biological samples; 1- wet-ashing, the digestion of a sample by an acid or a base; or 2- dry-ashing, the destruction of organic material by high temperature.

Although there seems to be considerable controversy on this subject in the literature, it is generally agreed that wet and dry-ashing give comparable results for a number of

elements and substances (Weissflog and Mengdehl, 1933; Ashton, 1936; Isaac and Johnson, 1975; Lambert, 1976). Some studies have concluded that organic phosphorus (5-20%) can be lost during dry-ashing and recommend acid digestion for phosphorus determination (Stuffins, 1967; Hiriart et al., 1977; Štupar et al., 1987). However, many other studies have shown that dry-ashing provides better results than wet-ashing for phosphorus analysis (Gorsuch, 1959; Lambert, 1976; Mika, 1977; Munter et al., 1979; Suzutani, 1980; Clegg et al., 1981).

Ashing of the organic matrix is one of the most critical steps in analysis of trace elements in biological materials. The ashing method employed must effectively and efficiently remove the organic material of a matrix, while allowing the element to be measured to remain available in its original quantity for analysis.

Wet-ashing procedures often involve the potentially dangerous method of digesting organic material in heated perchloric acid which is extremely explosive when dry. Therefore, although a slower method, dry-ashing was employed in this study. Dry ashing enables many samples to be treated simultaneously. In the first stages of oxidation, samples are heated slowly to allow moisture and volatile materials to evaporate without igniting, a situation which could cause loss of material. The samples are then oxidized at higher temperatures (commonly 450-550°C) until all organic matter is destroyed.

Close to the end of the ashing process, ashing aids are often used to expedite the decomposition of organic material in samples and to improve the recovery of the element to be measured. Nitric acid is a common ashing aid and acts as a strong oxidant to remove carbonaceous material from sample ashes (Gorsuch, 1970). Mengdehl (1933) showed that by boiling ash in dilute hydrochloric acid, the pyro- and metaphosphate salts in the ash could be converted to orthophosphate. Both nitric acid and hydrochloric acid were used in this study to improve phosphorus recovery from each seed tissue sample.

Materials and Methods

Sample preparation

       The seed coats of 30-40 seeds of each species of pine were removed and female gametophyte tissues were separated from embryo tissues. For each of the eleven species, pooled female gametophyte tissue and pooled embryo tissue samples were ground with a mortar and pestle to ensure an even distribution of phosphorus throughout the sample. From each pooled sample, at least two subsamples of female gametophyte tissue and two subsamples of embryo tissue were obtained.

Dry ashing

       To minimize any contamination of the samples, all crucibles, glassware and pipettes were acid washed and thoroughly rinsed with distilled water and deionized water prior to being used. Each subsample was weighed into an oven-dried porcelain crucible (Coors Porcelain, Golden, Co.) and charred on a hot plate at approximately 450°C until no smoke was observed being released from the charring sample (approximately 45 minutes). To increase the temperature in the last minutes of charring the crucibles were covered with a piece of tin foil. The crucibles were then transferred to a Blue M Electric Company (Blue Island, Illinois) muffle furnace and ashed at 550°C for 4 h. Blank crucibles were ashed with each set of samples.

       To break up insoluble components in the ash that might contain phosphorus, the samples were post-ash treated with 1.5

ml 1:2 V/V nitric acid (Aristar, BDH) and water and heated to dryness, then treated with 1.5 ml 1:1 V/V hydrochloric acid and water and heated to dryness once again.

The ash residue was taken up in 1% hydrochloric acid and diluted to give a final volume of 10, 25 or 50 ml depending on the initial weight of the sample. The sample extracts were centrifuged for 2-3 min to remove remaining insoluble portions of the ash and then stored for 24-48 h in scintillation vials at approximately 8°C until they could be analyzed.

Preparation of Reagents for P analysis (Isaac, 1990)

Phosphorus standard solution:

30 ml of phosphate volumetric standard (1 ml= 0.5 mg PO_4^{3-}) (Aldrich, Milwaukee) was diluted to 200 ml with deionized water to give 0.0245 mg P/ml.

Ammonium molybdate solution:

25 g NH_4 molybdate was dissolved in 300 ml deionized H_2O.

75 ml H_2SO_4 was diluted to 200 ml with deionized H_2O and added to the NH_4 molybdate solution and stirred until the crystals were dissolved.

Hydroquinone solution:

0.5 g hydroquinone was dissolved in 100 ml of deionized H_2O and one drop of H_2SO_4 was added to the solution to retard oxidation.

Sodium sulfite solution:

20 g Na_2SO_3 was dissolved in deionized H_2O and diluted to 100

ml.

Phosphorus analysis

One ml of sample extract was pipetted into a 10 ml volumetric flask. In succession one ml ammonium molybdate, one ml hydroquinone and one ml sodium sulphite was added to the volumetric flask with agitation after each addition. The sample was then diluted to volume with deionized water, mixed by inversion and allowed to stand approximately 30 min. for colour production. A reagent blank, containing all of the above solutions except the sample extract, was prepared with each set of samples to monitor possible reagent contamination.

The percent transmittance of each sample was measured by a Zeiss PMQ II Spectrophotometer set for a wavelength of 650 nm and adjusted to read 100% transmittance for the reagent blank. A standard curve was prepared for each run by the same procedure, substituting aliquots of the phosphate standard solution for the sample aliquots. The point at which a sample's transmittancy reading crosses the standard curve indicates the phosphorus concentration of that sample. Final phosphorus concentrations are presented on a dry weight basis.

Results

Element concentrations (μg.g^{-1} dry weight)

Phosphorus concentrations for the female gametophyte and embryo tissues of the eleven <u>Pinus</u> species investigated are presented in Table 6 on a per gram dry weight basis and in Table 7 on a per tissue basis. The female gametophyte of <u>P. coulteri</u> with 15600 ± 1200 ppm of phosphorus appeared to contain the most phosphorus (Table 6) with three times as much as <u>P. koraiensis</u> which had the lowest P concentration in its female gametophyte (5200 ± 400 ppm). In the embryo tissues, the P concentration ranged from 14800 ± 1300 ppm for <u>P. coulteri</u> to 7000 ± 700 ppm for <u>P. koraiensis</u>. For nine species the phosphorus concentration of the female gametophyte and its embryo were not significantly different. In <u>P. contorta</u> the phosphorus concentration was significantly higher in the female gametophyte than in the embryo tissue ($0.05 > p > 0.01$), while in <u>P. koraiensis</u> the phosphorus concentration of the embryo was higher than the female gametophyte ($p < 0.01$). Phosphorus concentration differences between the female gametophytes of seeds of the same species that were collected in different environments were not significant. Similarly, embryo phosphorus concentrations were not significantly different for seeds of the same species from different sources (Table 6).

Female gametophyte + embryo weight was not significantly correlated with either the phosphorus

concentrations of the female gametophyte or embryo tissues (see Appendix A for correlation data). Likewise, female gametophyte measurements and embryo measurements were not correlated with phosphorus concentrations in female gametophyte and embryo tissues, respectively.

Tissue concentrations (μg per tissue)

On a per tissue basis, female gametophyte + embryo weight was significantly correlated with phosphorus concentrations in female gametophytes and embryos (Appendix A). Female gametophyte measurements were significantly correlated with individual female gametophyte phosphorus concentrations, while embryo measurements were significantly correlated with individual embryo phosphorus concentrations. Finally, the phosphorus concentration per individual female gametophyte was determined to be highly correlated with the phosphorus concentration per individual embryo. On a per tissue basis, female gametophyte phosphorus concentrations (Table 7) were determined to be 7-13 times greater than the concentration of phosphorus in their embryo, with the exception of P. koraiensis where the concentration was 21 times greater in the female gametophyte than in its embryo.

Table 6. Mean measurements of phosphorus (± SE) in one gram samples of female gametophyte and embryo tissues of the seeds of various <u>Pinus</u> species based on spectrophotometric analysis.

<u>Pinus</u> species	Phosphorus concentrations (ppm[1])	
	Female gametophyte tissue	Embryo tissue
<u>P</u>. <u>banksiana</u>	14800 ± 200ab N=4	12900 ± 1000abc N=3
<u>P</u>. <u>contorta</u>	13100 ± 1300bc N=4	9900 ± 400d N=4
<u>P</u>. <u>resinosa</u> A	12100 ± 1200c N=5	11200 ± 500cd N=4
<u>P</u>. <u>resinosa</u> B	12400 ± 1500bc N=2	11900 ± 2200bcd N=2
<u>P</u>. <u>sylvestris</u>	12900 ± 700bc N=4	13400 ± 300ab N=4
<u>P</u>. <u>mugo</u> A	11500 ± 900c N=4	12600 ± 400bc N=4
<u>P</u>. <u>mugo</u> B	11100 ± 1600c N=2	10300 ± 1800cd N=2
<u>P</u>. <u>mugo</u> C	11100 ± 500c N=2	12100 ± 100bcd N=2
<u>P</u>. <u>strobus</u> A	11300 ± 600c N=4	11500 ± 400bcd N=4
<u>P</u>. <u>strobus</u> B	10800 ± 400c N=2	10200 ± 1300cd N=2
<u>P</u>. <u>nigra</u>	12500 ± 900bc N=4	11700 ± 1200bcd N=4
<u>P</u>. <u>ponderosa</u>	11800 ± 800bc N=8	12900 ± 1200abc N=3
<u>P</u>. <u>coulteri</u>	15600 ± 1200a N=11	14800 ± 1300a N=5
<u>P</u>. <u>sabiniana</u>	12700 ± 1400bc N=4	11700 ± 900bcd N=6
<u>P</u>. <u>koraiensis</u>	5200 ± 400d N=7	7000 ± 700e N=6

[1]- ppm = μg P/g tissue

Note: Values within the same column that are followed by the same letter are not significantly different at P>0.05.

Table 7. Mean measurements of phosphorus ($\pm$ SE) in the female gametophyte and embryo tissues of the seeds of
various Pinus species based on spectrophotometric analysis.

Pinus species	Phosphorus concentrations	
	μg per female gametophyte	μg per embryo
P. banksiana	40.0 $\pm$ 7.2	3.9 $\pm$ 1.3
P. contorta	40.6 $\pm$ 7.7	5.0 $\pm$ 1.0
P. resinosa A	64.1 $\pm$ 13.8	6.7 $\pm$ 1.2
P. resinosa B	65.7 $\pm$ 14.8	7.1 $\pm$ 1.8
P. sylvestris	67.1 $\pm$ 15.8	9.4 $\pm$ 1.6
P. mugo A	67.9 $\pm$ 19.1	7.6 $\pm$ 1.3
P. mugo B	65.5 $\pm$ 19.9	6.2 $\pm$ 1.5
P. mugo C	65.5 $\pm$ 18.0	7.3 $\pm$ 1.2
P. strobus A	127.7 $\pm$ 32.6	10.4 $\pm$ 2.3
P. strobus B	122.0 $\pm$ 30.9	9.2 $\pm$ 2.4
P. nigra	178.8 $\pm$ 44.7	21.1 $\pm$ 3.1
P. ponderosa	289.1 $\pm$ 77.8	43.9 $\pm$ 8.8
P. coulteri	1134.1 $\pm$ 308.5	94.7 $\pm$ 46.2
P. sabiniana	1272.5 $\pm$ 382.8	111.2 $\pm$ 49.7
P. koraiensis	820.0 $\pm$ 207.4	38.5 $\pm$ 10.0

Discussion

The phosphorus compounds found in seeds may be classified into four groups: phytates, phosphatides, nucleic compounds and inorganic P compounds (Lolas and Markakis, 1975). Of these compounds, phytic acid is the major P store, accounting for 50-90% of the total P present in mature seeds (Greenwood, 1989; Raboy, 1990). The phosphorus of phytin comprises 85-90% of total acid-soluble P in mature seeds. Inorganic P is present in a small quantity, comprising from 3 to 9% of the total acid-soluble seed phosphorus (Dmitrieva and Sobolev, 1984). During seed germination the phosphorus store in phytin is mobilized and utilized by the developing seedling.

On a $\mu g.g^{-1}$ dry weight basis, the phosphorus concentration of the female gametophyte was not significantly different from the phosphorus concentration of its embryo for the majority of the Pinus species investigated in this study. It was determined that seed weight and size measurements were not correlated with P concentrations of the female gametophytes or embryos. These findings suggest; that the seeds of each species have a specific requirement for phosphorus, that this requirement is similar for the female gametophyte and the embryo of a seed, and that the requirement for phosphorus is not dependent on the weight or size of the seed or individual tissue region.

As expected, on a per tissue basis, larger seeds

contained more P in female gametophyte and embryo tissues than smaller seeds. As the seed size increased from P. banksiana to P. koraiensis, the increase in the amount of P per embryo was closely proportional to the increase in P per female gametophyte.

A number of studies on the phytic acid levels of varieties of oats indicated that total P measurements could be used to estimate phytic acid content (Lolas et al., 1976; Miller et al., 1980). Griffiths and Thomas (1981) found that a strong correlation exists between total phytin concentration and total P concentration in Vicia faba seeds. However, based on large variations in the phytate to total phosphorus ratios between samples, they determined that total P content was not the best determinator of total phytin. Since we have found that larger seeds have higher female gametophyte and embryo P concentrations per tissue, it would appear that these seeds also have higher phytin concentrations.

For a particular Pinus species, female gametophyte and embryo phosphorus concentrations were not significantly different between seeds from different collection sites. This indicates that the environment and growth conditions under which the seed developed did not greatly affect phosphorus levels of the mature seed. A plant will tend to supply its seeds with mineral nutrients and organic matter at the expense of other plant organs (Mengel and Kirkby, 1982). This generally results in only small variations in the mineral

nutrient contents of seeds of a particular species. Lott <u>et al</u>. (1985) determined that pea seeds had the ability to closely regulate mineral uptake even under nutrient deficiency stress. Gayler and Sykes (1985) showed that soybean seed total protein levels were virtually unaffected by different nutrient supplies. Therefore, detected differences in phosphorus concentrations between the eleven species investigated, may largely be attributed to genetic factors for each species rather than environmental conditions.

Chapter 4

MEASUREMENT OF VARIOUS ELEMENTS IN FEMALE GAMETOPHYTE AND EMBRYO TISSUES OF PINUS SEEDS BY NEUTRON ACTIVATION ANALYSIS.

Introduction

Neutrons were discovered in 1932 and within four years the principles of neutron activation analysis (NAA) had been set forth by G. Hevesy and H. Levy (as reviewed by Haskin, 1980). NAA is a method of elemental analysis based upon the properties of the nucleus (Dostal and Elson, 1980). Often the sample to be analyzed is sealed in a polyethylene vial and suspended in the core of a nuclear reactor, which is the best source of high neutron fluxes. There the bombardment of the sample with neutrons induces the formation of radioactive isotopes or radionuclides. The most common nuclear reaction is (n,γ) where the produced isotopes are radioactive and decay with characteristic gamma (γ) energy and half-lives to a stable form (Haskin, 1980).

γ-rays result from the transition of an excited nucleus to a lower energy state (Dostal and Elson, 1980). The energy of each nuclear reaction is emitted as a discrete quantum analogous to the x-rays emitted in orbital electron transitions (Kruger, 1971). Therefore, for a given transition, each γ-ray is emitted with the same energy. This

property makes γ-radiation useful for identifying individual radionuclides and from these, the identities of the parent elements in the sample can be determined. The total amount of induced γ-radiation of a particular energy is used to determine the amount of the isotope present.

As outlined by Haskin (1980), the variables affecting the determination of a particular element are as follows: 1) the neutron flux (bombardment intensity) 2) the cross-section or probability for the parent nucleus to absorb a neutron 3) the duration of the neutron irradiation 4) the efficiency of the radiation detector 5) the nature of the radiations accompanying the decay of daughter isotopes ie. whether they are easily detected and 6) the half-life of the daughter isotope which must not be too long or too short.

NAA is a non-destructive method of analysis (Wang et al., 1975; Amiel, 1981) which allows for the simultaneous determination of trace elements in a matrix. Sample preparation often requires only the reduction of the sample material to a suitable particle size for packaging into vials (Hoffman, 1980). NAA is capable of providing measurements of elemental abundances of the order of 10^{-6} to 10^{-12} g (Rakovic, 1970; Wang et al., 1975). Nearly all the elements in the periodic table can be detected with NAA (Corliss, 1964).

When analyzing sample material using NAA methods, certified reference standards with known concentrations of elements are often irradiated with the sample material so that

all conditions of irradiation and detection cancel and induced radioactivities of samples and standards can be compared. A simple proportionality results between the amounts of the element in the sample and the standard and the number of counts observed for each per unit time on the detector (Dostal and Elson, 1980; Haskin, 1980).

NAA was used to quantitatively determine the presence of various elements in female gametophyte and embryo tissues of the seeds of the <u>Pinus</u> species being investigated in this study. Correlations were then determined for seed weight and size measurements with element concentrations.

Materials and Methods

Sample preparation

In order to prepare samples for NAA the seed coats of 100 seeds of each <u>Pinus</u> species being examined were removed and female gametophyte tissues were separated from embryo tissues using glass knives to prevent possible Fe contamination by razor blades. For each species investigated, the one hundred female gametophytes were pooled and the female gametophytes of the largest seeds were cut up into smaller pieces to ensure that 0.01-0.4 g samples would be a good representation of the stock. One hundred embryos were also pooled for each species. Two aliquots of female gametophyte tissue and two aliquots of embryo tissue were taken from the pooled seed tissues of each pine species. Samples were weighed into small polyethylene vials which had been washed, soaked in 0.01% nitric acid and rinsed with deionized water. The small vials were heat-sealed into larger pre-washed polyethylene vials. These larger polyethylene vials or 'rabbits' were used to transfer the samples to and from the reactor core.

Irradiation of samples for the analysis of short-lived radioisotopes

To analyze for Mg, Na, K, Cl, Ca, Cu, S and Mn each of the samples were irradiated for 120 or 240 s at a thermal flux of 5×10^{12} n/cm^2/s in the McMaster University Nuclear Reactor. Once irradiated, each sample was transferred to a clean,

preweighed, large polyethylene vial during a delay time of 200 s. This transfer was made to eliminate any counts produced by the irradiated vial. Each sample was counted for 900 s with counting geometry fixed at 6 cm from the face of a coaxial hyperpure germanium detector, with an efficiency of 19.8% and a resolution of 1.9 keV at 1332 keV (APTEC Engineering Limited, Downsview, Ontario). The detector was coupled to a PC based Nuclear Data AccuSpec acquisition interface board with 16 K channel memory and a Nuclear Data Model ND581 ADC with ND599 Loss Free Counting Module for pulse height analysis of the gamma ray spectra to quantify the desired elements. After counting, the samples were reweighed to correct for any loss during vial transfer. Vanadium flux monitors were run before and after each batch of irradiations to calibrate the neutron flux. Aliquots of NBS Wheat Flour, SRM 1567a (National Bureau of Standards, Washington, D.C.; renamed National Institute of Standards and Technology, Gaithersburg, MD) were analyzed as unknowns with every batch of irradiated samples.

Irradiation of samples for the analysis of long-lived radioisotopes

After a cooling period of a few weeks, the same samples were re-irradiated with the same thermal flux for 4 or 8 h. The emitted gamma rays produced from Fe and Zn in each sample were counted for 2 h. Often each sample was counted more than once and an average of the counts was calculated.

Cobalt wire monitors were used to calibrate the thermal flux of the system. To reduce background counts for each sample, blank vials were run with each batch. The number of counts produced by the irradiated blanks were subtracted from the total counts of each sample.

Analysis of collected sample spectra

Analysis was based on the following energy intensities (Glascock, 1988):

Isotope	Energy (keV)
23-Na (n,γ) 24-Na	1368.6, 2754.0
26-Mg (n,γ) 27-Mg	1014.4
36-S (n,γ) 37-S	3103.9
37-Cl (n,γ) 38-Cl	1642.7, 2167.7
41-K (n,γ) 42-K	1524.6
48-Ca (n,γ) 49-Ca	3084.5
55-Mn (n,γ) 56-Mn	1810.7
58-Fe (n,γ) 59-Fe	1099.3
64-Zn (n,γ) 65-Zn	1115.6
65-Cu (n,γ) 66-Cu	1039.2

The area under each peak in a sample's spectrum represents the number of counts of a particular element in the sample. Total counts for the measured elements were obtained by integrating peaks at the following window widths: Mg, 1009.54-1016.66 keV; Cu, 1033.28-1041.99 keV; Fe, 1095.51-1101.06 keV; Zn, 1111.76-1117.31 keV; Na, 1364.86-1371.19 keV and 2745.79-2760.03 keV; K, 1518.38-1527.87 keV; Cl, 1634.71-

1647.37 keV and 2157.00-2173.62 keV; Mn, 1804.06-1815.13 keV; Ca, 3075.01-3090.05; S, 3096.38-3107.46 keV. Background counts, which were obtained from regions adjacent to the peaks, were subtracted. The remaining background-subtracted counts were used to calculate concentration values (expressed in μg) for the detected elements in each sample with the aid of element libraries that had previously been created using certified reference materials. Final concentration values (expressed in ppm = μg.g^{-1} dry weight) were computed using moisture corrected sample weights.

Results

Element concentrations (μg.g^{-1} dry weight)

Quantitative values for Mg, Na, Ca, K, Cl, Mn, Cu, S, Zn and Fe within female gametophyte and embryo tissues of the investigated species of <u>Pinus</u> are presented as μg/g dry weight in Table 8 and 9 and as μg/tissue in Table 10 and 11. Of these elements, K was measured in the highest amounts in both female gametophyte and embryo tissues (typically detected in 10000-10500 ppm range). High levels of Mg and S (typically detected in the ranges of 4500-5500 ppm and 2500-5000 ppm, respectively) were also found. Significant levels of Cl (400-1000 ppm range), Ca (100-300 ppm range), Mn (50-200 ppm range), Zn (100-200 ppm range) and Fe (50-150 ppm range) were recorded for both female gametophyte and embryo tissues. In contrast, Na and Cu were detected in only trace, variable amounts (typically 10-20 ppm) and therefore warranted no further discussion. For the eight remaining elements, no significant differences were found between concentrations in the female gametophytes or between concentrations in the embryo tissues of seeds of the same species from different collection sites.

Since K concentrations were the highest element levels detected by NAA, a bar graph (Fig. 8) was created from the K data to illustrate the findings for this element. Potassium concentrations were determined to be not significantly different between the female gametophyte and its embryo for

Figure 8.   **Bar Graph of Mean Potassium Values (Weight).**

Mean potassium concentrations (μg.g^{-1}) were plotted against female gametophyte + embryo weight to illustrate the effects of seed size on potassium levels in female gametophyte (F) and embryo (E) tissues. The numbers along the x-axis correspond with the eleven <u>Pinus</u> species in the order that they appear in Table 1 (Chapter 2).

8

Mean potassium values (weight)

Increasing female gametophyte + embryo weight
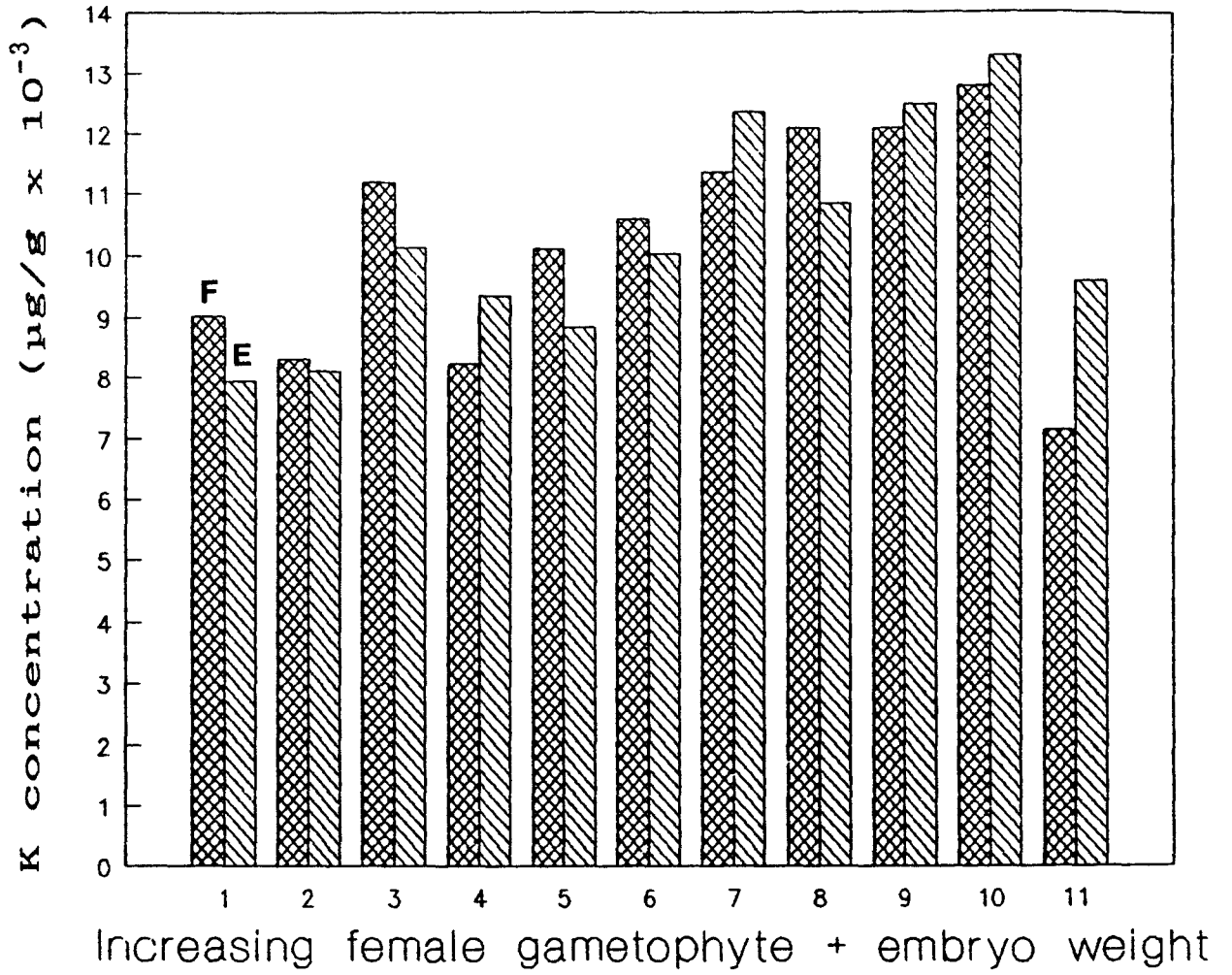
any of the species of <u>Pinus</u> investigated (Fig. 8). In fact, K concentrations were similar for all female gametophyte and embryo tissues, with the exception of the K concentration in the embryo of <u>P</u>. <u>sabiniana</u> which is significantly higher than the K concentration of the female gametophyte of <u>P</u>. <u>koraiensis</u>.

With the exception of <u>P</u>. <u>sabiniana</u>, levels of Mg were not significantly different between the female gametophyte and its embryo. In <u>P</u>. <u>sabiniana</u> the Mg level was approximately two times higher in the female gametophyte tissue than in its embryo.

For the majority of the species investigated in this study, female gametophyte S concentrations were not significantly different from corresponding embryo S concentrations. However, for <u>P</u>. <u>resinosa</u> (A and B) and <u>P</u>. <u>mugo</u> (A and C) sulphur concentrations were significantly higher for the female gametophyte than for its embryo.

The concentrations of Cl in the female gametophytes were significantly higher (2-6 times) than in corresponding embryo tissues except for <u>P</u>. <u>koraiensis</u> where there is no significant difference between Cl levels of the female gametophyte and its embryo.

Calcium levels were found to be 2-3 times higher in the female gametophytes of <u>P</u>. <u>banksiana</u>, <u>P</u>. <u>contorta</u>, <u>P</u>. <u>resinosa</u> A, <u>P</u>. <u>sylvestris</u>, <u>P</u>. <u>mugo</u> (A-C), <u>P</u>. <u>nigra</u> and <u>P</u>. <u>sabiniana</u> than in corresponding embryo tissues of these

species. In the remaining Pinus species, the Ca level of the female gametophyte was not significantly different from that of its embryo.

In P. coulteri and P. sabiniana seeds the concentration of Mn was not significantly different between the female gametophyte and its embryo. In all other species investigated, the concentration of Mn was significantly higher in the female gametophyte than in its embryo.

For nine of the Pinus species investigated there were no significant differences between the Zn concentrations of the female gametophyte and its embryo, but in P. banksiana and P. resinosa A the levels of Zn were significantly higher for the female gametophyte than for its embryo.

Of the 10 elements detected by NAA, Fe was the only element with higher levels in the embryos than in the female gametophytes of some of the Pinus species investigated. Figure 9 illustrates Fe data findings obtained by NAA. In P. banksiana, P. contorta and P. resinosa A the Fe concentrations of the embryo tissues were significantly higher than the Fe concentrations of the female gametophytes. No significant differences were found between the female gametophyte Fe levels and embryo Fe levels of the other Pinus species (Fig. 9).

Female gametophyte + embryo weight was negatively correlated with S, Ca, Zn and Fe (Fig. 9) levels of the female gametophytes but not significantly correlated with K (Fig. 8),

Figure 9.   **Bar Graph of Mean Iron Values (Weight).**

Mean iron concentrations (μg.g^{-1}) were plotted
against female gametophyte + embryo weight to
illustrate the effects of seed size on iron
levels in the female gametophyte (F) and embryo
(E) tissues. The numbers along the x-axis
correspond with the eleven Pinus species in the
order that they appear in Table 1 (Chapter 2).

9

Mean iron values (weight)
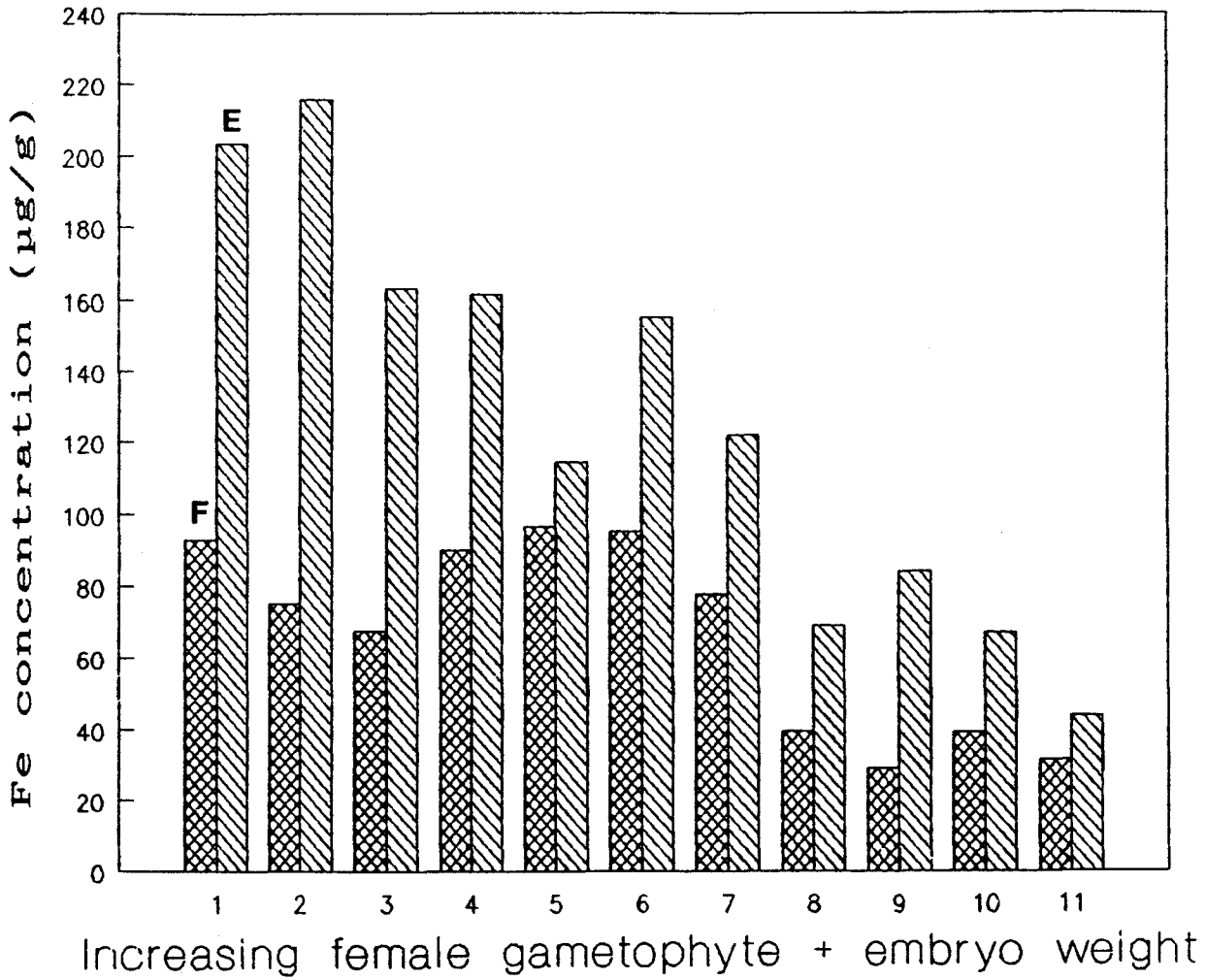
Mg, Cl or Mn (see Appendix A for correlation data). Female gametophyte + embryo weight was negatively correlated with Mn, Zn and Fe levels of the embryo tissues, and positively correlated with Cl concentrations of embryo tissues.

Female gametophyte weight, area and width measurements were negatively correlated with S, Ca, Zn and Fe (Fig. 9) concentrations of female gametophyte tissues. Female gametophyte length, however, was negatively correlated with the female gametophyte levels of S, Zn and Fe, but not Ca. The remaining elements were not significantly correlated with female gametophyte weight or size. For the female gametophyte tissues, positive correlations existed between Mg, K and Cl concentrations, between Ca and Zn levels, between Zn and Fe concentrations and between S and concentrations of Ca, Mn, Zn and Fe.

Embryo weight and size measurements were positively correlated with the concentrations of K (Fig. 8) and Cl in the embryo tissues and negatively correlated with embryo concentrations of Mn and Fe (Fig. 9). In addition, embryo weight and length measurements were negatively correlated with Zn embryo levels. The remaining elements were not significantly correlated with embryo weight or size. For the embryo tissues, positive correlations existed between Mg and Ca concentrations, between K and Cl concentrations, between Zn and Fe concentrations and between Mn and the levels of S and Fe. Negative correlations existed between K and Fe levels and

between Cl and levels of Mn and Fe.

Tissue concentrations (μg per tissue)

Figure 10 illustrates the μg/tissue data findings for K. On a per tissue basis, the K concentration of the female gametophyte was determined to be highly, positively correlated with the K concentration of its embryo (Appendix A). Similar correlations were obtained for the other analyzed elements. Female gametophyte + embryo weight was positively correlated with μg/female gametophyte levels of all the analyzed elements and positively correlated with μg/embryo concentrations of all the elements except Mn.

On a per tissue basis, female gametophyte weight and size measurements were positively correlated with concentrations of all the analyzed elements. Similarly, embryo weight and size measurements were positively correlated with concentrations of all the analyzed elements.

<u>Figure 10.</u>   **Bar Graph of Mean Potassium Values (Tissue).**

Mean potassium concentrations (μg per tissue)
were plotted against female gametophyte + embyro
weight to illustrate the effects of seed size on
potassium levels in whole female gametophyte (F)
and whole embryo (E) tissues. The numbers along
the x-axis correspond with the eleven <u>Pinus</u>
species in the order that they appear in Table
1 (Chapter 2).

10

Mean potassium values (tissue)
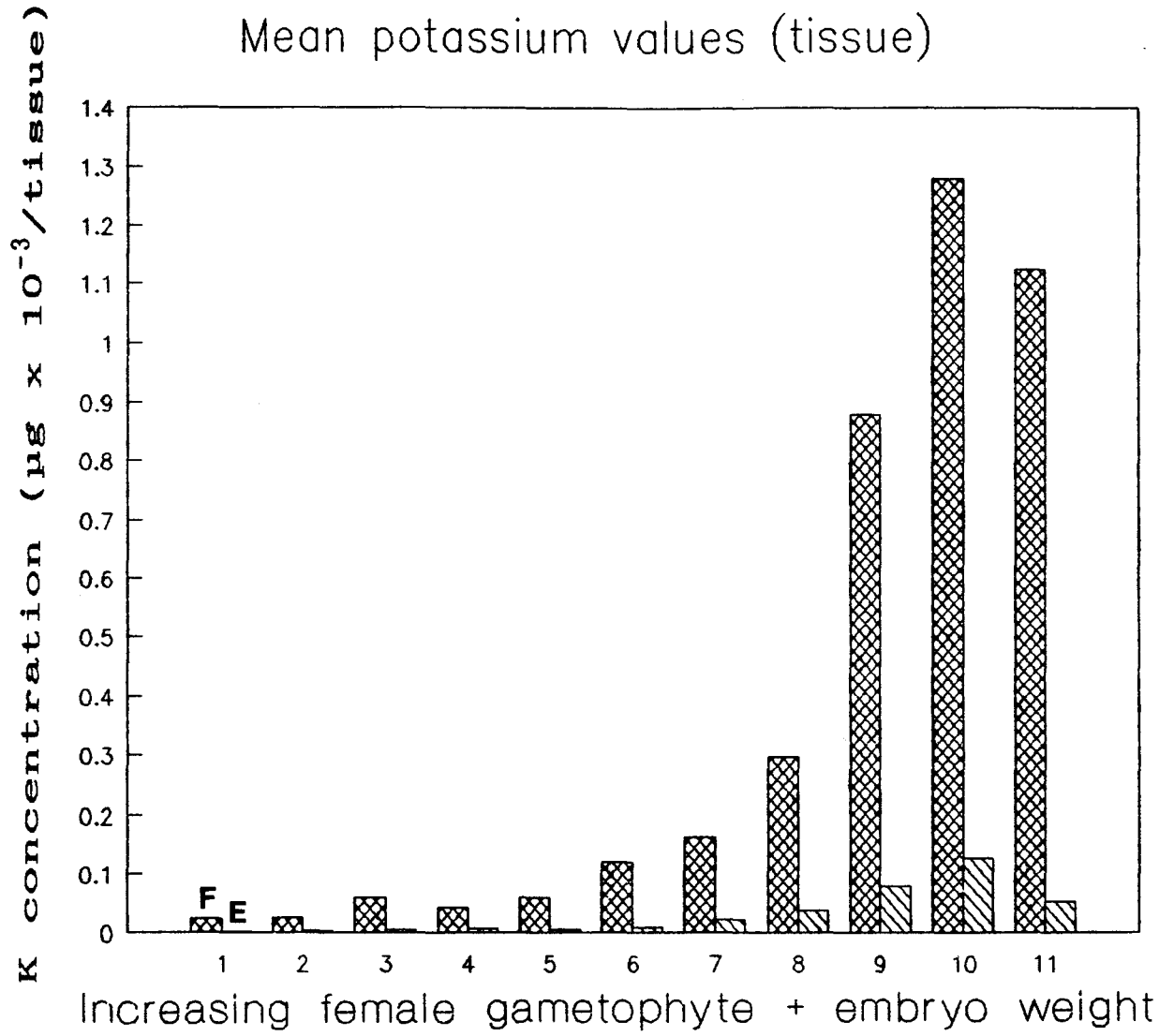
Table 8. Element concentration values (±SE) of Mg, Ca, Na, K and Cl for one gram samples of female gametophyte and embryo tissues of the seeds of various _Pinus_ species based on NAA.

Pinus species	Tissue type	Element concentrations (μg.g^{-1})				
		Mg	Ca	Na	K	Cl
P. banksiana	female gametophyte	5330 ± 202abcde	325 ± 45abc	24.3 ± 2.9abc	9013 ± 495ab	759.4 ± 60.6efgh
	embryo	4413 ± 157bcde	139 ± 23fghi	9.9 ± 2.2defg	7939 ± 409ab	229.1 ± 24.1lm
P. contorta	female gametophyte	4740 ± 187bcde	295 ± 44bcd	36.1 ± 2.6a	8308 ± 441ab	712.9 ± 59.5fghi
	embryo	4522 ± 128bcde	151 ± 15fghi	7.7 ± 1.1defg	8116 ± 310ab	196.6 ± 26.3lm
P. resinosa A	female gametophyte	5550 ± 179abc	303 ± 33bc	3.9 ± 2.6g	11196 ± 502ab	1105.6 ± 45.3b
	embryo	4916 ± 166bcde	174 ± 12defghi	10.6 ± 2.9defg	10107 ± 363ab	191.6 ± 32.6lm
P. resinosa B	female gametophyte	6296 ± 173abc	282 ± 20bcde	4.6 ± 3.4g	10980 ± 451ab	1075.6 ± 34.2bcd
	embryo	5334 ± 150abcde	191 ± 15cdefghi	5.4 ± 2.2fg	9584 ± 334ab	180.3 ± 41.9m
P. sylvestris	female gametophyte	4771 ± 183bcde	291 ± 41bcde	25.5 ± 2.1ab	8232 ± 437ab	835.4 ± 59.7defg
	embryo	4792 ± 158bcde	134 ± 9fghi	17.9 ± 3.0bcdef	9334 ± 327ab	218.4 ± 32.6lm
P. mugo A	female gametophyte	5800 ± 139abc	392 ± 52ab	18.8 ± 1.1bcd	10089 ± 313ab	844.3 ± 168.3def
	embryo	4284 ± 134bcde	175 ± 14defghi	17.7 ± 1.0bcdef	8829 ± 283ab	209.2 ± 27.6lm
P. mugo B	female gametophyte	5506 ± 141abcd	363 ± 10ab	5.6 ± 1.1fg	9467 ± 223ab	719.8 ± 40.3fghi
	embryo	4566 ± 125bcde	149 ± 12fghi	14.7 ± 1.4bcdefg	8921 ± 257ab	201.5 ± 26.1lm
P. mugo C	female gametophyte	6700 ± 172ab	435 ± 8a	7.5 ± 0.7defg	11423 ± 245ab	786.7 ± 32.9efgh
	embryo	4727 ± 133bcde	158 ± 11efghi	6.9 ± 1.5defg	8570 ± 239ab	163.7 ± 43.3m
P. strobus A	female gametophyte	4016 ± 124bcde	151 ± 11fghi	13.0 ± 0.4cdefg	10578 ± 296ab	637.9 ± 18.5ghij
	embryo	4157 ± 136bcde	74 ± 3i	7.6 ± 1.3defg	10010 ± 304ab	345.9 ± 30.2lm
P. strobus B	female gametophyte	4888 ± 135bcde	210 ± 7cdefghi	3.5 ± 1.6g	10417 ± 281ab	741.8 ± 39.7efgh
	embryo	4231 ± 114bcde	77 ± 5hi	7.5 ± 1.1defg	10135 ± 265ab	459.4 ± 33.3ijkl
P. nigra	female gametophyte	5693 ± 152abc	284 ± 41bcde	12.9 ± 0.9cdefg	11367 ± 326ab	1164.1 ± 136.4b
	embryo	5688 ± 111abc	152 ± 44fghi	18.7 ± 0.4bcde	12354 ± 231ab	351.9 ± 167.5lm

P. ponderosa	female gametophyte	4704 ± 165bcde	211 ± 17cdefgh	6.5 ± 0.3efg	12081 ± 319ab	1084.3 ± 11.3bc
	embryo	4209 ± 131bcde	133 ± 2ghi	5.6 ± 1.3fg	10837 ± 291ab	438.3 ± 31.6jkl
P. coulteri	female gametophyte	5465 ± 183abcd	219 ± 15cdefg	3.4 ± 0.0g	12076 ± 306ab	997.5 ± 13.3bcde
	embryo	6147 ± 138abc	212 ± 54cdefg	2.4 ± 1.1g	12474 ± 319ab	596.7 ± 170.3hijk
P. sabiniana	female gametophyte	7720 ± 135a	241 ± 47cdef	4.7 ± 0.6g	12769 ± 234ab	1934.0 ± 181.0a
	embryo	3904 ± 94cde	95 ± 54ghi	2.8 ± 1.2g	13283 ± 323a	851.3 ± 168.9cdef
P. koraiensis	female gametophyte	2225 ± 86e	110 ± 13ghi	2.5 ± 0.2g	7127 ± 172b	391.2 ± 18.3klm
	embryo	2881 ± 77de	88 ± 48ghi	2.5 ± 1.1g	9566 ± 299ab	419.5 ± 170.9kl

Note: Values within the same column that are followed by the same letter are not significantly different at P>0.05.

Table 9. Element concentration values (± SE) of Mn, Cu, S, Zn and Fe for one gram samples of female gametophyte and embryo tissues of the seeds of various _Pinus_ species based on NAA.

Pinus species	Tissue type	Element concentrations ($\mu g.g^{-1}$)				
		Mn	Cu	S	Zn	Fe
P. banksiana	female gametophyte	221.5 ± 5.9cde	18.1 ± 2.7cdefg	5400 ± 1000abcdef	231.3 ± 3.0a	92.7 ± 2.8bcdefgh
	embryo	98.2 ± 2.3ghijk	18.2 ± 3.2cdefg	3200 ± 800cdef	130.5 ± 2.8bcdef	203.4 ± 20.8a
P. contorta	female gametophyte	158.4 ± 4.7efg	17.7 ± 2.5cdefg	5900 ± 900abcdef	215.5 ± 2.7ab	75.2 ± 1.9efgh
	embryo	73.3 ± 1.5ijkl	20.4 ± 2.7bcdefg	2600 ± 800def	159.9 ± 2.1abcd	215.5 ± 4.6a
P. resinosa A	female gametophyte	605.5 ± 13.3a	31.2 ± 3.1abc	7300 ± 900ab	180.6 ± 2.2abc	67.7 ± 1.5efgh
	embryo	105.9 ± 2.0ghij	20.7 ± 2.8bcdefg	2900 ± 500cdef	72.5 ± 2.0def	163.0 ± 1.8abc
P. resinosa B	female gametophyte	608.1 ± 12.2a	35.3 ± 2.4ab	8900 ± 1100a	155.9 ± 2.4abcd	94.1 ± 25.3bcdefgh
	embryo	141.7 ± 2.6fgh	31.6 ± 2.1abc	2600 ± 1000cdef	91.2 ± 2.9def	167.8 ± 16.9ab
P. sylvestris	female gametophyte	233.6 ± 6.1cde	24.8 ± 2.2abcdef	6500 ± 800abcde	185.0 ± 2.3abc	89.8 ± 2.9cdefgh
	embryo	89.3 ± 1.9ghijk	23.0 ± 2.7abcdefg	2900 ± 700cdef	106.6 ± 2.3cdef	161.4 ± 0.5abc
P. mugo A	female gametophyte	148.0 ± 2.5fgh	24.5 ± 1.3abcdefg	6800 ± 500abc	154.5 ± 4.4abcd	96.5 ± 15.9bcdefgh
	embryo	37.5 ± 0.9jklmn	27.5 ± 2.0abcde	2200 ± 700ef	116.9 ± 1.3cdef	114.3 ± 3.0bcdef
P. mugo B	female gametophyte	119.3 ± 2.0fghi	21.2 ± 0.9bcdefg	6800 ± 600abcd	137.8 ± 3.7bcde	78.6 ± 27.6defgh
	embryo	40.1 ± 1.0jklmn	24.9 ± 1.6abcdef	3800 ± 900bcdef	116.5 ± 3.6cdef	107.5 ± 4.4bcdefg
P. mugo C	female gametophyte	187.9 ± 3.6def	25.8 ± 0.8abcdef	8100 ± 700ab	105.8 ± 5.2cdef	89.5 ± 18.8cdefgh
	embryo	41.4 ± 0.4jklmn	26.9 ± 1.4abcdef	2800 ± 800cdef	111.0 ± 4.2cdef	110.3 ± 7.6bcdef

P. strobus A	female gametophyte	263.1 ± 5.4bc	20.9 ± 1.5bcdefg	4100 ± 500bcdef	150.1 ± 0.5abcd	95.0 ± 4.9bcdefgh
	embryo	25.9 ± 0.5klmn	19.4 ± 1.7bcdefg	1600 ± 400f	79.4 ± 1.8def	154.9 ± 10.8abcd
P. strobus B	female gametophyte	310.1 ± 5.9b	24.7 ± 1.2abcdefg	5400 ± 700abcdef	158.0 ± 2.3abcd	106.8 ± 25.1bcdefg
	embryo	35.5 ± 0.6jklmn	18.9 ± 1.4bcdefg	1500 ± 800f	75.6 ± 2.0def	161.9 ± 25.8abc
P. nigra	female gametophyte	254.4 ± 4.9bcd	28.2 ± 1.4abcd	5000 ± 600abcdef	134.7 ± 3.0bcdef	77.6 ± 6.3efgh
	embryo	69.4 ± 1.5ijklm	36.6 ± 1.1a	2900 ± 300cdef	132.7 ± 2.6bcdef	121.8 ± 12.3bcde
P. ponderosa	female gametophyte	105.0 ± 2.1ghij	15.8 ± 1.5defg	4300 ± 600abcdef	123.2 ± 0.8cdef	39.2 ± 0.3fgh
	embryo	32.5 ± 0.5klmn	17.7 ± 1.3cdefg	2200 ± 300ef	91.1 ± 1.5def	68.9 ± 6.9efgh
P. coulteri	female gametophyte	65.3 ± 1.2ijklmn	12.0 ± 1.3efg	3000 ± 500cdef	121.4 ± 1.7cdef	29.0 ± 18.0h
	embryo	21.9 ± 2.2lmn	12.7 ± 1.0efg	2500 ± 400ef	84.5 ± 3.5def	83.7 ± 12.6defgh
P. sabiniana	female gametophyte	71.6 ± 1.5ijklm	8.5 ± 0.8g	3500 ± 300cdef	93.0 ± 1.3def	39.1 ± 2.3fgh
	embryo	15.8 ± 2.3mn	16.5 ± 1.0defg	2300 ± 400ef	57.0 ± 3.3ef	66.9 ± 1.3efgh
P. koraiensis	female gametophyte	80.8 ± 1.7hijkl	10.1 ± 1.2fg	1600 ± 400f	52.1 ± 0.8ef	31.1 ± 2.9gh
	embryo	12.2 ± 2.3n	20.6 ± 1.0bcdefg	2000 ± 400f	50.3 ± 3.1f	43.5 ± 0.7fgh

Note: Values within the same column that are followed by the same letter are not significantly different at P>0.05.

Table 10. Element concentration values (±SE) of Mg, Ca, Na, K and Cl in the female gametophyte
and embryo tissues of the seeds of various Pinus species based on NAA.

Pinus species	Tissue type	Element concentrations (μg/tissue)				
		Mg	Ca	Na	K	Cl
P. banksiana	female gametophyte	14.4 ± 2.2	0.9 ± 0.2	0.1 ± 0.0	24.3 ± 3.8	2.1 ± 0.3
	embryo	1.3 ± 0.4	0.0 ± 0.0	0.0 ± 0.0	2.4 ± 0.8	0.1 ± 0.0
P. contorta	female gametophyte	14.7 ± 2.4	0.9 ± 0.2	0.1 ± 0.0	25.8 ± 4.4	2.2 ± 0.4
	embryo	2.3 ± 0.5	0.1 ± 0.0	0.0 ± 0.0	4.1 ± 0.8	0.1 ± 0.0
P. resinosa A	female gametophyte	29.4 ± 5.6	1.6 ± 0.3	0.2 ± 0.1	59.3 ± 11.5	5.9 ± 1.1
	embryo	2.9 ± 0.5	0.1 ± 0.0	0.0 ± 0.0	6.1 ± 1.0	0.1 ± 0.0
P. resinosa B	female gametophyte	33.4 ± 6.4	1.5 ± 0.3	0.0 ± 0.0	58.1 ± 11.2	5.7 ± 1.1
	embryo	3.2 ± 0.5	0.1 ± 0.0	0.0 ± 0.0	5.8 ± 1.0	0.1 ± 0.0
P. sylvestris	female gametophyte	24.8 ± 5.8	1.5 ± 0.4	0.1 ± 0.0	42.8 ± 10.1	4.3 ± 1.0
	embryo	3.4 ± 0.5	0.1 ± 0.0	0.0 ± 0.0	6.5 ± 1.0	0.2 ± 0.0
P. mugo A	female gametophyte	34.2 ± 9.3	2.3 ± 0.7	0.1 ± 0.0	59.5 ± 16.2	5.0 ± 1.7
	embryo	2.6 ± 0.4	0.1 ± 0.0	0.0 ± 0.0	5.3 ± 0.9	0.1 ± 0.0
P. mugo B	female gametophyte	32.5 ± 8.8	2.1 ± 0.6	0.0 ± 0.0	55.9 ± 15.2	4.2 ± 1.2
	embryo	2.7 ± 0.5	0.1 ± 0.0	0.0 ± 0.0	5.4 ± 0.9	0.1 ± 0.0
P. mugo C	female gametophyte	39.5 ± 10.8	2.6 ± 0.7	0.0 ± 0.0	67.4 ± 18.3	4.6 ± 1.3
	embryo	2.8 ± 0.5	0.1 ± 0.0	0.0 ± 0.0	5.1 ± 0.9	0.1 ± 0.0
P. strobus A	female gametophyte	45.3 ± 11.3	1.7 ± 0.4	0.1 ± 0.0	119.5 ± 29.8	7.2 ± 1.8
	embryo	3.7 ± 0.8	0.1 ± 0.0	0.0 ± 0.0	9.0 ± 2.0	0.3 ± 0.1
P. strobus B	female gametophyte	55.2 ± 13.8	2.4 ± 0.6	0.0 ± 0.0	117.7 ± 29.3	8.4 ± 2.1
	embryo	3.8 ± 0.9	0.1 ± 0.0	0.0 ± 0.0	9.1 ± 2.0	0.4 ± 0.1
P. nigra	female gametophyte	81.4 ± 20.0	4.1 ± 1.2	0.2 ± 0.0	162.5 ± 40.1	16.6 ± 4.5
	embryo	10.2 ± 1.2	0.3 ± 0.1	0.0 ± 0.0	22.2 ± 2.5	0.6 ± 0.3

P. ponderosa	female gametophyte	115.3 ± 30.4	5.2 ± 1.4	0.2 ± 0.0	296.0 ± 77.7	26.6 ± 6.9
	embryo	14.3 ± 2.6	0.5 ± 0.1	0.0 ± 0.0	36.8 ± 6.6	1.5 ± 0.3
P. coulteri	female gametophyte	397.3 ± 104.7	15.9 ± 4.3	0.2 ± 0.1	877.9 ± 230.5	72.5 ± 19.0
	embryo	39.3 ± 19.1	1.4 ± 0.7	0.0 ± 0.0	79.8 ± 38.7	3.8 ± 2.1
P. sabiniana	female gametophyte	773.5 ± 217.4	24.1 ± 8.2	0.5 ± 0.1	1279.5 ± 359.6	193.8 ± 57.3
	embryo	37.1 ± 16.4	0.9 ± 0.6	0.0 ± 0.0	126.2 ± 55.9	8.1 ± 3.9
P. koraiensis	female gametophyte	350.9 ± 86.3	17.3 ± 4.7	0.4 ± 0.1	1123.9 274.3	61.7 ± 15.3
	embryo	15.8 ± 3.8	0.5 ± 0.3	0.0 ± 0.0	52.6 ± 12.5	2.3 ± 1.1

Table 11. Element concentration values (± SE) of Mn, Cu, S, Zn and Fe in female gametophyte and embryo tissues of the seeds of various Pinus species based on NAA.

Pinus species	Tissue type	Element concentrations (μg/tissue)				
		Mn	Cu	S	Zn	Fe
P. banksiana	female gametophyte	0.6 ± 0.1	0.0 ± 0.0	14.6 ± 3.5	0.6 ± 0.1	0.3 ± 0.0
	embryo	0.0 ± 0.0	0.0 ± 0.0	1.0 ± 0.4	0.0 ± 0.0	0.1 ± 0.0
P. contorta	female gametophyte	0.5 ± 0.1	0.1 ± 0.0	18.3 ± 4.1	0.7 ± 0.1	0.2 ± 0.0
	embryo	0.0 ± 0.0	0.0 ± 0.0	1.1 ± 0.5	0.1 ± 0.0	0.1 ± 0.0
P. resinosa A	female gametophyte	3.2 ± 0.6	0.2 ± 0.0	38.7 ± 8.7	1.0 ± 0.2	0.4 ± 0.1
	embryo	0.1 ± 0.0	0.1 ± 0.0	1.7 ± 0.4	0.0 ± 0.0	0.1 ± 0.0
P. resinosa B	female gametophyte	3.2 ± 0.6	0.2 ± 0.0	47.2 ± 10.6	0.8 ± 0.2	0.5 ± 0.2
	embryo	0.1 ± 0.0	0.0 ± 0.0	1.6 ± 0.7	0.1 ± 0.0	0.1 ± 0.0
P. sylvestris	female gametophyte	1.2 ± 0.3	0.1 ± 0.0	33.8 ± 8.8	1.0 ± 0.2	0.5 ± 0.1
	embryo	0.1 ± 0.0	0.0 ± 0.0	2.3 ± 0.6	0.1 ± 0.0	0.1 ± 0.0
P. mugo A	female gametophyte	0.9 ± 0.2	0.1 ± 0.0	40.1 ± 10.9	0.9 ± 0.2	0.6 ± 0.2
	embryo	0.0 ± 0.0	0.0 ± 0.0	1.3 ± 0.5	0.1 ± 0.0	0.1 ± 0.0
P. mugo B	female gametophyte	0.7 ± 0.2	0.1 ± 0.0	40.1 ± 11.4	0.8 ± 0.2	0.5 ± 0.2
	embryo	0.0 ± 0.0	0.0 ± 0.0	2.3 ± 0.7	0.1 ± 0.0	0.1 ± 0.0
P. mugo C	female gametophyte	1.1 ± 0.3	0.2 ± 0.0	47.8 ± 13.6	0.6 ± 0.2	0.5 ± 0.2
	embryo	0.0 ± 0.0	0.0 ± 0.0	1.7 ± 0.6	0.1 ± 0.0	0.1 ± 0.0
P. strobus A	female gametophyte	3.0 ± 0.7	0.2 ± 0.1	46.3 ± 12.8	1.7 ± 0.4	1.1 ± 0.3
	embryo	0.0 ± 0.0	0.1 ± 0.0	1.4 ± 0.5	0.1 ± 0.0	0.1 ± 0.0
P. strobus B	female gametophyte	3.5 ± 0.9	0.3 ± 0.1	61.0 ± 17.1	1.8 ± 0.4	1.2 ± 0.4
	embryo	0.0 ± 0.0	0.0 ± 0.0	1.4 ± 0.8	0.1 ± 0.0	0.1 ± 0.0

P. nigra	female gametophyte	3.6 ± 0.9	0.4 ± 0.1	71.5 ± 19.5	1.9 ± 0.5	1.1 ± 0.3
	embryo	0.1 ± 0.0	0.1 ± 0.0	5.2 ± 0.8	0.2 ± 0.0	0.2 ± 0.0
P. ponderosa	female gametophyte	2.6 ± 0.7	0.4 ± 0.1	105.4 ± 31.2	3.0 ± 0.8	1.0 ± 0.3
	embryo	0.1 ± 0.0	0.1 ± 0.0	7.5 ± 1.7	0.3 ± 0.1	0.2 ± 0.0
P. coulteri	female gametophyte	4.7 ± 1.2	0.9 ± 0.2	218.1 ± 67.6	8.8 ± 2.3	2.1 ± 1.4
	embryo	0.1 ± 0.1	0.1 ± 0.0	16.0 ± 8.2	0.5 ± 0.3	0.5 ± 0.3
P. sabiniana	female gametophyte	7.2 ± 2.0	0.9 ± 0.3	350.7 ± 102.8	9.3 ± 2.6	3.9 ± 1.1
	embryo	0.2 ± 0.1	0.2 ± 0.1	21.9 ± 10.4	0.5 ± 0.2	0.6 ± 0.3
P. koraiensis	female gametophyte	12.7 ± 3.1	1.6 ± 0.4	252.3 ± 87.9	8.2 ± 2.0	4.9 ± 1.3
	embryo	0.1 ± 0.0	0.1 ± 0.0	11.0 ± 3.4	0.3 ± 0.1	0.2 ± 0.1

Discussion

It is remarkable that seeds can contain very different concentrations of elements from those found in most vegetative tissues of the parent plant. Relatively little research has been conducted on the processes controlling the movement and deposition of inorganic ions in seeds. Since phloem is the major vascular tissue linking the parent plant to the developing seed, nutrient mobility in phloem fluid is an important factor in embryo nutrition (Tinker and Läuchli, 1986). There are no vascular or symplastic connections between a developing embryo, endosperm, or female gametophyte and surrounding seed coat layers. Therefore, embryo solutes and ions must be absorbed from the surrounding cells. Likewise, female gametophyte or endosperm solutes must be absorbed from surrounding tissue layers (Tinker and Läuchli, 1986).

The ten elements detected by NAA in this study of mature pine seeds are essential elements required by higher plants (Mengel and Kirkby, 1982). High levels of K, Mg and S were detected in female gametophytes and embryos of all eleven pine species investigated. K and Mg are the principal cations found in salts of phytic acid and are present in significant amounts in globoid crystals of seed protein bodies. Potassium is required by a number of plant enzymes such as pyruvate kinase and is involved in cell turgor, cell expansion, anion neutralization and assimilate conduction (Clarkson and Hanson,

1980; Mengel and Kirkby, 1982). Magnesium acts as a co-factor for many plant enzymes including phosphatases and is an essential component of the chlorophyll molecule (Clarkson and Hanson, 1980; Mengel and Kirkby, 1982; Glass, 1989). Like other divalent ions, Mg is capable of forming complexes with nucleic acids (Shkolnik, 1984). Sulphur, as part of the amino acids cysteine and methionine, is a major constituent of proteins and is involved in polypeptide stabilization by formation of disulphide bonds between amino acids. Ribonuclease and Coenzyme A are sulphur-containing enzymes (Glass, 1989). Sulphur is often detected in the protein bodies of seeds.

Significant levels of Cl, Ca, Mn, Zn and Fe were detected in embryo and female gametophyte tissues of the species investigated in this study. Chlorine is essential in nitrogen and energy metabolism and photosynthesis (Shkolnik, 1984). It has been speculated that Cl^- is required in significant quantities to act as a counter-ion to K^+ (Glass, 1989). Commonly Ca is present in seeds as a cation found in salts of phytic acid (Mengel and Kirkby, 1982). In cell walls, Ca is associated in the middle lamella with free carboxyl groups of pectins (Mengel and Kirkby, 1982). Calcium also functions in maintaining membrane integrity and is involved in cell division and the assembly of microtubules (Glass, 1989). Manganese participates in a number of cellular activities including the photolysis of water in photosystem II

and may be the activator of IAA oxidase (Shkolnik, 1984; Glass, 1989). Zinc can form complexes with various substances such as proteins, nucleic acids, ATP, ADP, sugars, metalloenzymes, amino acids and organic acids (Shkolnik, 1984; Glass, 1984). Zinc has a very high binding affinity for phytic acid. Iron is a constituent of various reductases and hydrogenases. The Fe-containing proteins ferredoxin, cytochrome and peroxidase play important roles in cellular metabolism (Shkolnik, 1984; Glass, 1989). In plants, iron is stored in plastids as a non-toxic protein complex called phytoferritin (Gunning and Steer, 1975).

The element concentrations measured for P. koraiensis tended to be different from measured element concentrations for the remaining Pinus species examined in this study. For example, female gametophyte Mg levels were 2-3 times higher in ten of the Pinus species investigated than in P. koraiensis. Unfortunately the original source of the P. koraiensis seeds used in this study is unknown but may account for some of the nutrient level differences observed. As indicated in Chapter 1, based on morphological characteristics, P. koraiensis was classified into a separate subsection (Cembrae) from the other species that were investigated. This may also contribute to the observed differences. Whole seed morphology and examination of the ultra-structure of P. koraiensis (Chapter 2) did not indicate that the seeds of P. koraiensis were less mature than the seeds of the other species studied. Seed

tissue ultra-structure was determined to be quite comparable between all eleven species.

As previously determined for phosphorus concentrations in Chapter 3, environment and growth conditions of the developing seeds did not greatly affect mineral nutrient levels of the mature seed. For a particular <u>Pinus</u> species, neither female gametophyte potassium levels nor embryo potassium levels were significantly different between seed batches from different collection sites. Likewise, for a particular <u>Pinus</u> species, neither female gametophyte nor embryo levels of the remaining elements measured by NAA were significantly different between seed batches collected from different locations.

Phosphorus levels in the female gametophyte and embryos of the eleven pine species investigated were spectrophotometrically determined (see Chapter 3) rather than determined by using NAA. ^{31}P and ^{27}Al can not be measured in samples known to contain ^{28}Si because all three elements produce the same radionuclide ^{28}Al when bombarded by neutrons. In samples known not to contain silicon, the parts of phosphorus and aluminum in the ^{28}Al activity could be separated mathematically after the sample had been irradiated twice. However, due to the expense of a double irradiation and the fact that the detection sensitivity for phosphorus still remains low after double irradiation, concentrations for this element were determined by a different method.

On a $\mu g.g^{-1}$ dry weight basis, female gametophyte concentrations of K, Mg, S, Zn and Fe were not significantly different from corresponding embryo concentrations. Female gametophyte Cl, Mn and Ca levels were significantly higher than corresponding embryo levels. The female gametophyte concentrations of S, Ca, Zn and Fe were determined to be highest in the smaller seeds and decreased with increasing female gametophyte + embryo weight and/or female gametophyte weight and size measurements. Likewise, embryo Mn, Zn and Fe levels were highest in the smaller seeds and decreased with increasing female gametophyte+embryo weight and/or embryo weight and size measurements. These correlation results obtained for S, Ca, Mn, Zn and Fe may reflect the effect of sampling seeds of different sizes. Assuming that a large seed has the same amount of mineral nutrients as a small seed, one gram of ground tissue from large seeds would inevitably contain more lipids, cell wall components, etc., and therefore less mineral nutrient reserves than one gram of tissue from small seeds. In fact, on a per tissue basis, the bigger seeds with larger female gametophytes and embryos contained sizably larger nutrient stores than smaller seeds. In contrast, embryo K and Cl levels increased with increasing embryo weight and size measurements. The observation that Cl levels increased with K levels conforms with the theory proposed by Glass (1989) that Cl^- acts as a counter-ion to K^+.

Chapter 5

MEASUREMENT OF VARIOUS ELEMENTS IN FEMALE GAMETOPHYTE AND EMBRYO TISSUES OF <u>PINUS</u> SEEDS BY ENERGY DISPERSIVE X-RAY ANALYSIS.

Introduction

The electrons of an atom occur in orbits or shells with discrete energies. When high energy beam electrons of an electron microscope interact with an atom of a specimen, an inner shell electron may be ejected from its orbit. The removal of this electron temporarily ionizes the atom until an outer shell electron drops into the vacancy to stabilize the atom, releasing energy as it falls. This energy is equal to the difference in energy between the two shells and may be released in the form of an x-ray.

X-rays that are produced by electron bombardment have energies that are characteristic of and unique to the electron energy transitions of the atoms giving rise to them (Chandler, 1972). These x-ray energies may be plotted as discrete peaks. Since each element will produce a unique set of peaks, the generated spectrum can be used to identify which elements are present in the excited portion of the specimen.

The number of x-rays in a peak is proportional to the mass of atoms of that element in the excited volume of the

sample (Chandler, 1972). However, the total x-ray counts in a spectral peak includes background which is not uniform for all energies, and is produced primarily by continuum or bremsstrahlung x-rays (Barbi, 1979). Continuum x-rays are created by the deceleration of beam electrons within the coulombic field of atomic nuclei (Bozzola and Russell, 1992). The energy of a continuum x-ray depends on the proximity of the beam electron to the nucleus of an atom. The closer the electron passes by the nucleus, the greater it will be decelerated and the release of x-ray energy will be higher (Bozzola and Russell, 1992). Background x-ray counts must be subtracted from the total counts within a peak to obtain the net counts for a particular element, the parameter which is related to concentration (Barbi, 1979).

A scanning transmission electron microscope (STEM) equipped with an x-ray detector provides TEM resolution and enables a fine probe of high energy electrons to be positioned and rastered over small areas (often as small as part of one cell) of a thin specimen for subcellular element analysis. In order to study the distribution of mineral nutrients in specific tissues with STEM, the sample tissue often must be fixed, dehydrated, embedded and then sectioned. In fact, seeds with a high oil content (typically 45-60% for pine seeds) generally cannot be analyzed without fixation, defatting or freezing (Ockenden and Lott, 1991). However, care must be taken to avoid any loss or redistribution of

elements during these steps. Significant losses can also occur during sectioning of resin-embedded tissue if a water-filled boat is used to float the tissue sections on as they come off the knife edge (Skilnyk, 1990). The use of low-water-content fixation procedures (Lott et al., 1984) and dry-knife sectioning of tissue blocks ensures the retention of water-soluble phytates.

Since globoid crystals are naturally electron dense, they are easy to locate in a tissue section and make good subjects for EDX analysis because they are fairly stable in the electron beam. Previous studies of globoid crystals in various seeds have revealed that they commonly contain P, Mg and K and occasionally other minor elements such as Ca, Na, Mn, Zn, Fe, Ba and S (Lott, 1984; Lott et al., 1979; Lott and Vollmer, 1979; Stewart et al., 1988; Ockenden and Lott, 1990; West and Lott, 1991). The distribution of elements within globoid crystals has been found to vary from species to species, from organ to organ and from tissue to tissue (Lott, 1984).

EDX analysis has been used in this study to investigate the composition and distribution patterns of mineral nutrient stores in the seeds of various Pinus species.

Materials and Methods

EDX analysis

In preparation for fixation, the seed coats of five seeds from each pine species were removed and the embryos were separated from the female gametophyte tissues. Embryo and female gametophyte tissues were routinely cut into small blocks of approximately 1 mm^3 to improve fixative and resin infiltration. Large embryos were divided into cotyledon, hypocotyl and radicle portions to facilitate resin infiltration and tissue region recognition during sectioning. To prevent the extraction of water-soluble phytate, the low-water-content procedures of Lott et al. (1984) were employed. Embryo and female gametophyte tissue pieces were fixed with 5% glutaraldehyde in 80% EtOH for 24 h, dehydrated in 100% EtOH (24 h) and 100% propylene oxide (24 h) and embedded in Spurr's resin following a propylene oxide:Spurr's resin series (3:1, 2:1, 1:1, 1:2, 1:3, 0:1, 0:1) for 24 h periods. Thick (1-1.5 μm) sections were cut with dry glass knives on a Reichert OM U2 ultramicrotome and transferred to formvar-coated copper grids using an eyelash. Most sections were flattened onto the surface of the grid by the addition of a drop of 100% EtOH.

Using the scanning mode of a JEOL-1200 EX-2 TEMSCAN microscope, EDX analysis was carried out at 80 kV for 60 s using a PGT model IMIX-II microanalysis system (Princeton Gamma Tech., Princeton, NJ) with detector distance, aperture, spot size and tilt kept the same for all analyses. Three

seeds from each of the eleven species of <u>Pinus</u> were analyzed. Five globoid crystals and/or electron-dense particles were analyzed from different cells of the female gametophyte and from various embryo tissues including; the shoot apex, the root apex, and the protoderm, ground meristem and provascular tissues of the cotyledons, cotyledon tips and hypocotyl-root axes. Areas of cell walls, lipid vesicles and seed coats were analyzed as controls.

X-ray counts for the measured elements were obtained by integrating peaks at the following window widths: Mg, 1146-1358 eV; P, 1899-2125 eV; S, 2190-2422 eV; K, 3187-3437 eV; Ca, 3562-3818 eV; Mn, 5750-6038 eV; Fe, 6251-6545 eV; Zn, 8468-8792 eV. The background was subtracted from each peak using a computer program that joins specified points along the energy axis. The points were selected to produce an adequate fit of the background. The total number of counts in each element window before and after background subtraction were used to calculate peak-to-background (P/B) ratios (Stewart <u>et al</u>., 1988).

The calcium K_α peak is overlapped by the K_β peak of potassium. In order to calculate the counts for calcium a correction factor of 9.17% of the total x-ray counts in the potassium K_α peak was subtracted from the total counts collected in the Ca_β window. Similarly, the Fe K_α peak is overlapped by the K_β peak of Mn, therefore total Fe counts were corrected by subtracting 11.65% of the total x-ray counts

for Mn.   These correction factors were derived from the analysis of potassium and manganese salts by Wada (personal communication, 1990).

Results

Two types of mineral nutrient-rich stores were observed and analyzed in female gametophyte and embryo tissues; globoid crystals, commonly in the size range of $\geq$ 0.33 μm, within protein bodies, and other naturally, electron-dense particles that were smaller than globoid crystals ($\leq$ 0.33 μm) and never appeared to be contained within the proteinaceous matrix of protein bodies. The results from analysis of the two different mineral storage structures will be presented separately.

Globoid crystals ($\geq$ 0.33 μm)

As indicated in Chapter 2, protein bodies were observed in the cells of female gametophytes and embryo tissues of all eleven <u>Pinus</u> species investigated. Globoid crystals were commonly observed within protein bodies of female gametophytes, root apices and ground meristem tissues of embryos, while protein bodies of the shoot apices, protoderm and provascular tissues of embryos rarely contained globoid crystals. Significant levels of P, Mg and K were detected in varying amounts in all globoid crystals analyzed, as well as trace amounts of Ca and/or Fe (Figs. 11, 12, 13).

High P, Mg and K peak-to-background (P/B) ratios were detected in globoid crystals throughout the seed tissues (Tables 12a-22a). These ratios routinely did not vary significantly from tissue to tissue for globoid crystals in a particular species. When small tissue variations did occur,

Figs. 11 to 16. **EDX Analysis Spectra of Globoid Crystals and Electron-dense Particles in Pinus Seed Tissues.**

The energy lines for each element analyzed are as follows: Mg = 1.2 keV, P = 2.0 keV, S = 2.3 keV, K = 3.3 keV, Ca = 3.7 keV, Fe = 6.3 keV. Copper peaks at 8.0 keV were considered to result from x-rays produced by contamination by the copper grids that were used.

Figure 11.   EDX analysis spectrum of a globoid crystal in the cotyledon ground meristem tissue of the embryo of a P. mugo seed.

Figure 12.   EDX analysis spectrum of a globoid crystal in the hypocotyl ground meristem tissue of the embryo of a P. strobus seed.

Figure 13.   EDX analysis spectrum of a globoid crystal in the female gametophyte of a P. banksiana seed.

Figure 14.   EDX analysis spectrum of an electron-dense particle in the cotyledon ground meristem tissue of a P. mugo seed.

Figure 15.   EDX analysis spectrum of an electron-dense particle in the hypocotyl ground meristem tissue of the embryo of a P. strobus seed.

Figure 16.   EDX analysis spectrum of an electron-dense particle in the female gametophyte of a P. banksiana seed.
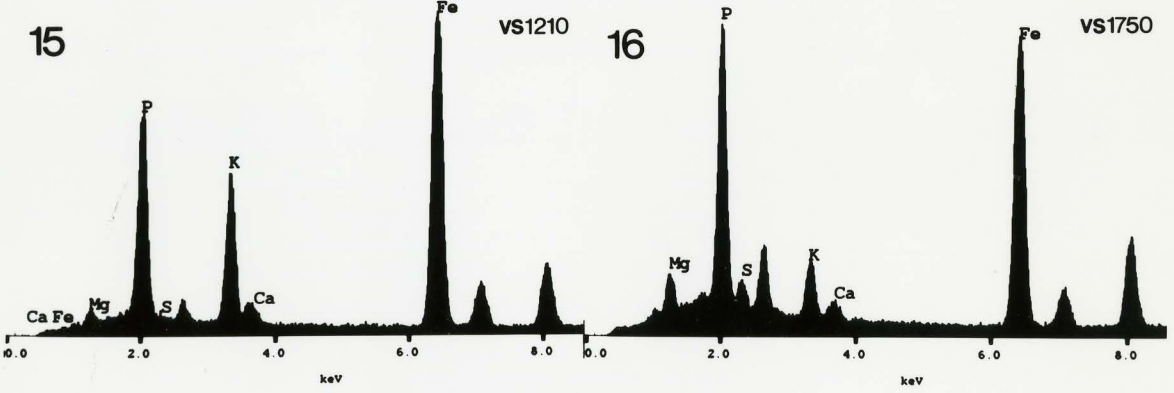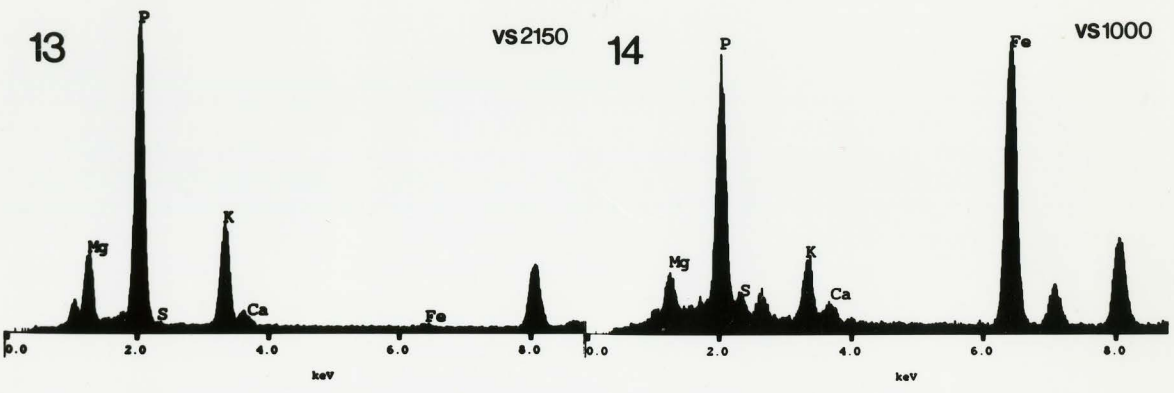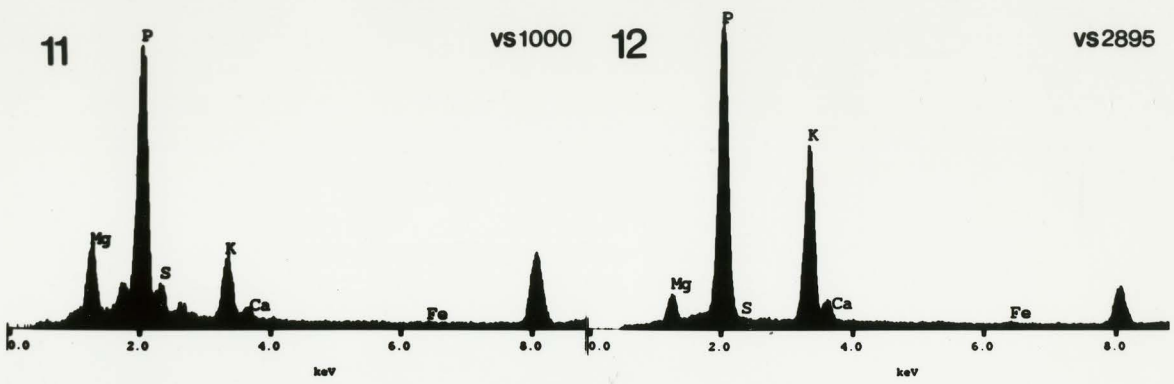
then P, Mg and K appeared to vary proportionally with each other, ie. if the P P/B ratio was slightly lower for a particular tissue region then Mg P/B and K P/B ratios tended to be lower for the same tissue region. Peak-to-background ratios were always higher for P than for Mg, K, Ca or Fe in globoid crystals of all tissue regions. Ca P/B ratios were zero or near zero, while Fe P/B ratios were low and routinely did not vary significantly from tissue to tissue for any <u>Pinus</u> species studied. The results of analyses of cell walls, lipid vesicles and seed coats for all eleven species are presented in Appendix B. Levels of P, Mg and K were higher in globoid crystals than in other seed tissue constituents. Total count rates were also higher for the globoid crystals.

Female gametophyte + embryo weight was negatively correlated with P P/B ratios of globoid crystals in the female gametophyte and ground meristem tissues of the cotyledon and hypocotyl (Appendix C). Mg P/B ratios of globoid crystals in the ground meristem tissue of the hypocotyl were also negatively correlated with female gametophyte + embryo weight.

The weight and size measurements of both female gametophytes and embryos were determined to be negatively correlated with P P/B and Mg P/B ratios of globoid crystals in the female gametophyte, root apex and ground meristem tissues of the cotyledon and hypocotyl. Potassium P/B ratios of globoid crystals in the ground meristem tissue of the cotyledon tip were positively correlated with weight and size

measurements of female gametophytes and embryos.

From P/B ratios, ratios of Mg to P (Mg/P), K to P (K/P), Ca to P (Ca/P), and Fe to P (Fe/P) were generated (Tables 12b-22b). Mg/P ratios of the globoid crystals varied little from 0.3 between the species or between tissue regions within in each species. K/P ratios were higher than Mg/P ratios for globoid crystals of all tissue regions analyzed. It was determined that embryo weight and size measurements were positively correlated with K/P ratios in globoid crystals of the root apex and ground meristem tissues of the embryo. Ca/P and Fe/P ratios were zero or near zero for globoid crystals of all tissue regions of the eleven <u>Pinus</u> species investigated.

Ratios of (Mg+K) to P, (Mg+Ca)/K, (Mg+Ca+Fe)/K, and (Mg+Ca+Fe+K)/P were created from peak-to-background ratios of individual elements (Tables 12c-22c). (Mg+K)/P and (Mg+Ca+Fe+K)/P ratios were fairly consistent between species. Female gametophyte + embryo weight was positively correlated with both of these ratios for globoid crystals of the ground meristem tissues of the embryo and with (Mg+K)/P ratios for globoid crystals of the root apex. Embryo weight and size measurements were positively correlated with (Mg+K)/P ratios for globoid crystals of the root apex and ground meristem tissues of the embryo. (Mg+Ca)/K and (Mg+Ca+Fe)/K ratios were more variable between species. Female gametophyte + embryo weight and embryo weight and size measurements were negatively

correlated with (Mg+Ca)/K and (Mg+Ca+Fe)/K ratios of globoid crystals of the ground meristem tissues of the cotyledon tip and hypocotyl.

Electron-dense particles ($\leq$ 0.33 μm)

Throughout the tissues of the embryo and the female gametophyte, small electron-dense particles were observed (see Chapter 2 for more details). High levels of Fe, varying amounts of P, Mg and K, and traces of Ca were detected in these particles (Figs. 14, 15, 16). Peak-to-background ratios (Tables 12a-22a) were always higher for Fe than for P, Mg, K or Ca in electron-dense particles of all tissue regions. Fe P/B ratios were lower in electron-dense particles of the female gametophytes than in particles of the tissues of the embryo. Within an embryo, Fe P/B ratios were especially high in particles of the protoderm, ground meristem and procambium tissues while slightly lower in particles of the shoot apex. P P/B and Mg P/B ratios of electron-dense particles tended not to vary considerably between tissue regions in a species, while K P/B ratios of the particles were more variable and commonly higher in embryo procambium tissues of a number of the species investigated. Ca P/B ratios were routinely higher in particles of the protoderm and provascular tissues of embryos of most of the species studied.

Analyses of control areas (Appendix B) indicated that high Fe levels were restricted to the electron-dense particles. With the exception of globoid crystals in protein

bodies, P, Mg and K levels were higher in the electron-dense particles than in other seed tissue constituents. Sulphur was not detected within the matrix of the structures surrounding electron-dense particles (data not presented). Significant amounts of sulphur were commonly detected when analyzing the proteinaceous matrix of typical protein bodies.

Female gametophyte + embryo weight was negatively correlated with P P/B and Mg P/B ratios in electron-dense particles of the ground meristem tissue of the cotyledon tip, and negatively correlated with P P/B ratios in particles of the ground meristem tissue of the hypocotyl. Fe P/B ratios in particles of the root apex, protoderm, provascular and ground meristem tissues of the embryo were also negatively correlated with female gametophyte + embryo weight.

Female gametophyte weight and size measurements were negatively correlated with P P/B and Mg P/B ratios in particles of the ground meristem tissue of the cotyledon tip, with P P/B ratios in particles of the ground meristem tissue of the hypocotyl, and with Ca P/B ratios in particles of the root apex, provascular tissue of the cotyledon tip and protoderm tissue of the cotyledon. Fe P/B ratios in particles of the root apex, protoderm, ground meristem and provascular tissues of the embryo were also negatively correlated with female gametophyte weight and size measurements.

Embryo weight and size measurements were negatively correlated with P P/B and Mg P/B ratios in electron-dense

particles of the ground meristem tissues of the cotyledon tip and hypocotyl, with P P/B ratios in particles of the shoot apex, and with Ca P/B ratios in particles of the ground meristem tissue of the hypocotyl, provascular tissue of the cotyledon tip and protoderm tissue of the cotyledon. Fe P/B ratios in particles of the ground meristem and provascular tissues of the embryo, and in particles of the protoderm tissues of the cotyledon tip and cotyledon were also negatively correlated with embryo weight and size measurements.

Mg/P ratios (Tables 12b-22b) of the electron-dense particles varied little from 0.2 between species or between tissue regions within each species examined. K/P ratios were higher than Mg/P ratios in particles of all tissue regions. Embryo weight and size measurements were positively correlated with K/P ratios of particles in the root apex, protoderm and ground meristem tissues of the embryo, and in the provascular tissues of the cotyledon tip and cotyledon. Ca/P ratios of electron-dense particles were zero or near zero, while the Fe/P ratios ranged from 2-4.5 and were higher than K/P ratios for all the tissue regions analyzed. Embryo weight and size measurements were negatively correlated with Fe/P ratios of particles in the protoderm tissue of the cotyledon tip, and in the provascular tissues of the cotyledon tip and cotyledon.

Female gametophyte + embryo weight and embryo weight and size measurements were positively correlated with (Mg+K)/P

ratios (Tables 12c-22c) of electron-dense particles of the root apex, protoderm and provascular tissues of the embryo, and ground meristem tissues of the cotyledon tip and hypocotyl. These measurements were negatively correlated with (Mg+Ca+Fe+K)/P ratios of the particles within provascular tissues of the embryo and with (Mg+Ca+Fe)/K ratios of particles within the root apex and provascular tissue of the embryo, protoderm tissues of the cotyledon tip and hypocotyl, and ground meristem tissues of the cotyledon and cotyledon tip. Female gametophyte + embryo weight and embryo weight and size measurements were negatively correlated with (Mg+Ca)/K ratios of particles within the provascular tissue of the cotyledon tip. Embryo weight and size measurements were also negatively correlated with (Mg+Ca)/K ratios of particles within the ground meristem tissues of the cotyledon and hypocotyl.

Table 12a. Mean (± SD) peak-to-background ratios of elements in globoid crystals (≥ 0.33μm)

or electron-dense particles (≤ 0.33 μm) of various tissues of P. banksiana seeds.

Organ	Region analyzed N=15	Particle size	P	Mg	K	Ca	Fe
female gametophyte		≥ 0.33 μm	10.1 ± 1.3a	2.8 ± 0.3a	4.5 ± 0.6a	0.0 ± 0.1e	0.5 ± 0.4d
female gametophyte		≤ 0.33 μm	3.5 ± 0.9c	0.8 ± 0.4c	2.2 ± 0.8efg	0.2 ± 0.3de	11.8 ± 4.7c
cotyledon tip	protoderm	≤ 0.33 μm	4.7 ± 0.9bc	0.9 ± 0.4bc	1.8 ± 0.4fg	1.0 ± 0.3ab	17.9 ± 3.0ab
cotyledon tip	ground meristem	≥ 0.33 μm	9.2 ± 1.1a	2.9 ± 0.2a	3.5 ± 0.4bc	0.2 ± 0.1de	0.8 ± 0.3d
cotyledon tip	ground meristem	≤ 0.33 μm	4.7 ± 0.9bc	1.1 ± 0.3bc	2.0 ± 0.5efg	0.7 ± 0.3abc	18.6 ± 4.5a
cotyledon tip	procambium	≤ 0.33 μm	4.0 ± 0.9bc	0.8 ± 0.3c	2.5 ± 0.5defg	0.2 ± 0.2de	15.6 ± 3.8abc
cotyledon	protoderm	≤ 0.33 μm	4.1 ± 0.5bc	0.8 ± 0.3c	1.6 ± 0.3g	0.5 ± 0.5cd	14.8 ± 4.5abc
cotyledon	ground meristem	≥ 0.33 μm	10.0 ± 1.6a	2.9 ± 0.5a	3.9 ± 0.5ab	-0.1 ± 0.2e	0.5 ± 0.2d
cotyledon	ground meristem	≤ 0.33 μm	3.7 ± 1.5c	0.7 ± 0.3c	1.7 ± 0.6g	0.2 ± 0.3de	17.0 ± 5.2abc
cotyledon	procambium	≤ 0.33 μm	5.7 ± 2.5b	1.3 ± 0.8b	2.8 ± 0.7cde	0.0 ± 0.2e	16.4 ± 8.3abc
shoot apex		≤ 0.33 μm	3.6 ± 0.9c	0.8 ± 0.3c	1.6 ± 0.5g	0.2 ± 0.1de	12.4 ± 3.3bc
hypocotyl	protoderm	≤ 0.33 μm	4.2 ± 1.3bc	0.8 ± 0.3c	1.6 ± 0.4g	1.1 ± 0.7a	13.7 ± 4.9abc
hypocotyl	ground meristem	≥ 0.33 μm	10.3 ± 1.1a	2.9 ± 0.5a	4.0 ± 0.7ab	-0.1 ± 0.1e	0.9 ± 1.4d
hypocotyl	ground meristem	≤ 0.33 μm	4.7 ± 1.9bc	1.1 ± 0.4bc	2.7 ± 0.6cdef	0.2 ± 0.2de	18.6 ± 7.0a
hypocotyl	procambium	≤ 0.33 μm	4.0 ± 1.7bc	0.8 ± 0.4c	1.9 ± 1.1efg	0.6 ± 0.6bcd	17.1 ± 6.4abc
root apex		≥ 0.33 μm	9.7 ± 1.1a	2.7 ± 0.4a	3.4 ± 1.0bcd	0.2 ± 0.5de	0.3 ± 0.3d
root apex		≤ 0.33 μm	4.3 ± 1.2bc	1.0 ± 0.4bc	2.5 ± 1.5defg	0.3 ± 0.6cde	13.2 ± 5.0abc

Note: Values within the same column that ere followed by the same letter are not

significantly different at P>0.05

Table 12b. Ratios (± SD) of Mg to P, K to P, Ca to P, and Fe to P derived from P/B ratios that were generated by EDX analysis of globoid crystals (≥ 0.33 μm) or electron-dense particles (≤ 0.33 μm) in P. banksiana seed tissues.

Organ	Region analyzed N=15	Particle size	Mg/P	K/P	Ca/P	Fe/P
female gametophyte		≥ 0.33 μm	0.3 ± 0.0a	0.4 ± 0.1a	0.0 ± 0.0c	0.1 ± 0.0b
female gametophyte		≤ 0.33 μm	0.2 ± 0.1a	0.7 ± 0.2a	0.1 ± 0.1bc	3.5 ± 1.3a
cotyledon tip	protoderm	≤ 0.33 μm	0.2 ± 0.1a	0.4 ± 0.1a	0.2 ± 0.1ab	3.9 ± 0.7a
cotyledon tip	ground meristem	≥ 0.33 μm	0.3 ± 0.0a	0.4 ± 0.1a	0.0 ± 0.0c	0.1 ± 0.0b
cotyledon tip	ground meristem	≤ 0.33 μm	0.2 ± 0.1a	0.4 ± 0.1a	0.2 ± 0.1ab	4.1 ± 1.3a
cotyledon tip	procambium	≤ 0.33 μm	0.2 ± 0.1a	0.6 ± 0.1a	0.0 ± 0.1c	4.0 ± 1.3a
cotyledon	protoderm	≤ 0.33 μm	0.2 ± 0.1a	0.4 ± 0.1a	0.1 ± 0.1bc	3.7 ± 1.1a
cotyledon	ground meristem	≥ 0.33 μm	0.3 ± 0.0a	0.4 ± 0.0a	0.0 ± 0.0c	0.0 ± 0.0b
cotyledon	ground meristem	≤ 0.33 μm	0.2 ± 0.1a	0.5 ± 0.1a	0.1 ± 0.1bc	5.0 ± 4.4a
cotyledon	procambium	≤ 0.33 μm	0.2 ± 0.0a	0.5 ± 0.2a	0.0 ± 0.0c	3.1 ± 2.0a
shoot apex		≤ 0.33 μm	0.2 ± 0.1a	0.4 ± 0.1a	0.0 ± 0.0c	3.5 ± 1.0a
hypocotyl	protoderm	≤ 0.33 μm	0.2 ± 0.1a	0.4 ± 0.2a	0.3 ± 0.2a	3.2 ± 0.5a
hypocotyl	ground meristem	≥ 0.33 μm	0.3 ± 0.0a	0.4 ± 0.0a	0.0 ± 0.0c	0.1 ± 0.1b
hypocotyl	ground meristem	≤ 0.33 μm	0.2 ± 0.2a	0.6 ± 0.1a	0.0 ± 0.2c	3.6 ± 1.0a
hypocotyl	procambium	≤ 0.33 μm	0.2 ± 0.1a	0.5 ± 0.2a	0.2 ± 0.2ab	4.2 ± 2.0a
root apex		≥ 0.33 μm	0.3 ± 0.0a	0.4 ± 0.1a	0.0 ± 0.1c	0.0 ± 0.0b
root apex		≤ 0.33 μm	0.2 ± 0.1a	0.6 ± 0.3a	0.1 ± 0.1bc	3.0 ± 0.6a

Note: Values within the same column that are followed by the same letter are not significantly different at P>0.05.

Table 12c. Mean element (± SD) ratios derived from P/B ratios that were generated by EDX analysis of globoid crystals (≥ 0.33 μm) or electron-dense particles (≤ 0.33 μm) in P. banksiana seed tissues.

Organ	Region analyzed N=15	Particle size	$\dfrac{Mg+K}{P}$	$\dfrac{Mg+Ca}{K}$	$\dfrac{Mg+Ca+Fe}{K}$	$\dfrac{Mg+Ca+Fe+K}{P}$
female gametophyte		≥ 0.33 μm	0.7 ± 0.1bc	0.6 ± 0.1bc	0.8 ± 0.2e	0.8 ± 0.1b
female gametophyte		≤ 0.33 μm	0.9 ± 0.2a	0.5 ± 0.3bc	6.3 ± 1.7d	4.7 ± 1.0a
cotyledon tip	protoderm	≤ 0.33 μm	0.6 ± 0.1c	1.2 ± 0.3a	11.6 ± 2.6a	4.7 ± 0.8a
cotyledon tip	ground meristem	≥ 0.33 μm	0.7 ± 0.1bc	0.9 ± 0.1ab	1.1 ± 0.2e	0.8 ± 0.1b
cotyledon tip	ground meristem	≤ 0.33 μm	0.6 ± 0.1c	0.9 ± 0.3ab	11.0 ± 2.8a	4.9 ± 1.4a
cotyledon tip	procambium	≤ 0.33 μm	0.8 ± 0.1ab	0.4 ± 0.2c	6.7 ± 1.6cd	4.9 ± 1.4a
cotyledon	protoderm	≤ 0.33 μm	0.6 ± 0.1c	0.9 ± 0.3ab	10.2 ± 3.5ab	4.4 ± 1.1a
cotyledon	ground meristem	≥ 0.33 μm	0.7 ± 0.1bc	0.7 ± 0.2bc	0.9 ± 0.2e	0.7 ± 0.1b
cotyledon	ground meristem	≤ 0.33 μm	0.7 ± 0.1bc	0.6 ± 0.2bc	9.9 ± 2.9ab	4.7 ± 1.5a
cotyledon	procambium	≤ 0.33 μm	0.7 ± 0.2bc	0.6 ± 0.3bc	6.1 ± 3.0d	3.8 ± 2.1a
shoot apex		≤ 0.33 μm	0.7 ± 0.1bc	0.6 ± 0.2bc	8.8 ± 3.1abcd	4.2 ± 1.0a
hypocotyl	protoderm	≤ 0.33 μm	0.6 ± 0.2c	1.2 ± 0.2a	9.9 ± 2.8ab	4.1 ± 0.7a
hypocotyl	ground meristem	≥ 0.33 μm	0.7 ± 0.1bc	0.7 ± 0.1bc	0.9 ± 0.4e	0.8 ± 0.1b
hypocotyl	ground meristem	≤ 0.33 μm	0.8 ± 0.1ab	0.5 ± 0.1bc	7.3 ± 2.1bcd	4.4 ± 1.0a
hypocotyl	procambium	≤ 0.33 μm	0.7 ± 0.3bc	1.3 ± 0.5a	9.4 ± 3.3abc	4.1 ± 0.6a
root apex		≥ 0.33 μm	0.6 ± 0.1c	0.9 ± 0.4ab	1.0 ± 0.4e	0.7 ± 0.1b
root apex		≤ 0.33 μm	0.8 ± 0.3ab	0.7 ± 0.5bc	7.4 ± 3.9bcd	3.9 ± 0.6a

Note: Values within the same column that are followed by the same letter are not significantly different at P>0.05.

Table 13a. Mean (± SD) peak-to-background ratios of elements in globoid crystals (≥ 0.33 μm)

or electron-dense particles (≤ 0.33μm) of various tissues of P. contorta seeds.

Organ	Region analyzed N=15	Particle size	P	Mg	K	Ca	Fe
female gametophyte		≥ 0.33 μm	6.5 ± 1.9b	1.0 ± 0.2b	2.5 ± 0.3b	-0.1 ± 0.1b	0.1 ± 0.1d
female gametophyte		≤ 0.33 μm	3.8 ± 1.3c	0.7 ± 0.3b	1.8 ± 0.7b	-0.1 ± 0.1b	9.1 ± 7.0bc
cotyledon tip	protoderm	≤ 0.33 μm	4.3 ± 0.9c	0.8 ± 0.2b	1.7 ± 0.3b	0.1 ± 0.2ab	13.5 ± 3.5abc
cotyledon tip	ground meristem	≥ 0.33 μm	9.4 ± 0.9a	2.3 ± 0.9a	3.7 ± 0.4a	0.0 ± 0.2ab	0.8 ± 0.4d
cotyledon tip	ground meristem	≤ 0.33 μm	4.9 ± 1.3c	0.9 ± 0.3b	1.8 ± 0.5b	0.0 ± 0.1ab	17.4 ± 4.4a
cotyledon tip	procambium	≤ 0.33 μm	5.1 ± 1.0bc	0.9 ± 0.4b	2.2 ± 0.7b	0.1 ± 0.4ab	18.3 ± 4.1a
cotyledon	protoderm	≤ 0.33 μm	4.8 ± 0.9c	0.9 ± 0.3b	2.1 ± 0.8b	0.3 ± 0.5a	16.5 ± 4.3a
cotyledon	ground meristem	≥ 0.33 μm	8.9 ± 1.0a	2.2 ± 0.8a	3.8 ± 1.1a	-0.1 ± 0.1b	0.3 ± 0.2d
cotyledon	ground meristem	≤ 0.33 μm	4.6 ± 0.9c	1.0 ± 0.4b	2.1 ± 0.6b	0.0 ± 0.2ab	14.0 ± 4.5ab
cotyledon	procambium	≤ 0.33 μm	4.8 ± 0.6c	0.9 ± 0.3b	2.4 ± 0.6b	-0.1 ± 0.1b	16.5 ± 3.0a
shoot apex		≤ 0.33 μm	5.2 ± 1.7bc	1.2 ± 0.6b	2.5 ± 0.9b	-0.1 ± 0.2b	9.0 ± 7.2c
hypocotyl	protoderm	≤ 0.33 μm	5.0 ± 1.2c	0.8 ± 0.2b	1.8 ± 0.5b	0.1 ± 0.2ab	14.9 ± 5.0a
hypocotyl	ground meristem	≥ 0.33 μm	9.5 ± 0.7a	2.3 ± 0.8a	4.1 ± 0.6a	-0.2 ± 0.1b	0.3 ± 0.1d
hypocotyl	ground meristem	≤ 0.33 μm	4.6 ± 1.4c	0.8 ± 0.2b	2.2 ± 0.6b	0.1 ± 0.1ab	15.3 ± 4.4a
hypocotyl	procambium	≤ 0.33 μm	4.4 ± 0.8c	0.9 ± 0.3b	2.3 ± 0.5b	-0.1 ± 0.1b	14.7 ± 3.7a
root apex		≥ 0.33 μm	8.6 ± 1.3a	2.4 ± 0.5a	4.1 ± 1.0a	-0.2 ± 0.2b	0.4 ± 0.3d
root apex		≤ 0.33 μm	4.1 ± 0.8c	0.9 ± 0.2b	1.9 ± 0.6b	0.1 ± 0.4ab	13.6 ± 3.2abc

Note: Values within the same column that are followed by the same letter are not significantly

different at P>0.05.

Table 13b. Ratios (± SD) of Mg to P, K to P, Ca to P, and Fe to P derived from P/B ratios
that were generated by EDX analysis of globoid crystals (≥ 0.33 μm) or electron-
dense particles (≤ 0.33 μm) in P. contorta seed tissues.

Organ	Region analyzed N=15	Particle size	Mg/P	K/P	Ca/P	Fe/P
female gametophyte		≥ 0.33 μm	0.2 ± 0.0b	0.4 ± 0.1a	0.0 ± 0.0b	0.0 ± 0.0c
female gametophyte		≤ 0.33 μm	0.2 ± 0.0b	0.5 ± 0.1a	0.0 ± 0.0b	2.6 ± 1.8ab
cotyledon tip	protoderm	≤ 0.33 μm	0.2 ± 0.1b	0.4 ± 0.1a	0.0 ± 0.1b	3.1 ± 0.4ab
cotyledon tip	ground meristem	≥ 0.33 μm	0.2 ± 0.1b	0.4 ± 0.0a	0.0 ± 0.0b	0.1 ± 0.0c
cotyledon tip	ground meristem	≤ 0.33 μm	0.2 ± 0.1b	0.4 ± 0.1a	0.0 ± 0.0b	3.2 ± 0.4a
cotyledon tip	procambium	≤ 0.33 μm	0.2 ± 0.1b	0.4 ± 0.1a	0.0 ± 0.1b	3.6 ± 0.5a
cotyledon	protoderm	≤ 0.33 μm	0.2 ± 0.0b	0.4 ± 0.1a	0.1 ± 0.1a	3.4 ± 0.6a
cotyledon	ground meristem	≥ 0.33 μm	0.2 ± 0.1b	0.4 ± 0.1a	0.0 ± 0.0b	0.0 ± 0.0c
cotyledon	ground meristem	≤ 0.33 μm	0.2 ± 0.1b	0.4 ± 0.1a	0.0 ± 0.0b	3.0 ± 0.7ab
cotyledon	procambium	≤ 0.33 μm	0.2 ± 0.1b	0.5 ± 0.1a	0.0 ± 0.0b	3.5 ± 0.8a
shoot apex		≤ 0.33 μm	0.2 ± 0.1b	0.5 ± 0.1a	0.0 ± 0.0b	2.1 ± 1.7b
hypocotyl	protoderm	≤ 0.33 μm	0.2 ± 0.0b	0.4 ± 0.1a	0.0 ± 0.0b	2.9 ± 0.5ab
hypocotyl	ground meristem	≥ 0.33 μm	0.2 ± 0.1b	0.4 ± 0.1a	0.0 ± 0.0b	0.0 ± 0.0c
hypocotyl	ground meristem	≤ 0.33 μm	0.2 ± 0.1b	0.5 ± 0.1a	0.0 ± 0.0b	3.1 ± 0.8ab
hypocotyl	procambium	≤ 0.33 μm	0.2 ± 0.1b	0.5 ± 0.1a	0.0 ± 0.0b	3.3 ± 0.6a
root apex		≥ 0.33 μm	0.3 ± 0.0a	0.5 ± 0.1a	0.0 ± 0.0b	0.0 ± 0.0c
root apex		≤ 0.33 μm	0.2 ± 0.1b	0.5 ± 0.1a	0.0 ± 0.1b	3.5 ± 1.6a

Note: Values within the same column that are followed by the same letter are not significantly
different at P>0.05.

Table 13c. Mean element (± SD) ratios derived from P/B ratios that were generated by EDX analysis of globoid crystals (≥ 0.33 μm) or electron-dense particles (≤ 0.33 μm) in P. contorta seed tissues.

Organ	Region analyzed N=15	Particle size	Mg+K / P	Mg+Ca / K	Mg+Ca+Fe / K	Mg+Ca+Fe+K / P
female gametophyte		≥ 0.33 μm	0.6 ± 0.1bc	0.4 ± 0.1bc	0.4 ± 0.1e	0.6 ± 0.1d
female gametophyte		≤ 0.33 μm	0.6 ± 0.1bc	0.3 ± 0.1c	5.6 ± 3.6cd	3.2 ± 1.8bc
cotyledon tip	protoderm	≤ 0.33 μm	0.6 ± 0.1bc	0.5 ± 0.2abc	8.6 ± 2.0ab	3.7 ± 0.5abc
cotyledon tip	ground meristem	≥ 0.33 μm	0.6 ± 0.1bc	0.6 ± 0.2ab	0.8 ± 0.3e	0.7 ± 0.1d
cotyledon tip	ground meristem	≤ 0.33 μm	0.6 ± 0.1bc	0.5 ± 0.2abc	9.3 ± 1.2a	3.7 ± 0.5abc
cotyledon tip	procambium	≤ 0.33 μm	0.6 ± 0.1bc	0.5 ± 0.3abc	8.9 ± 1.5ab	4.2 ± 0.5a
cotyledon	protoderm	≤ 0.33 μm	0.6 ± 0.1bc	0.7 ± 0.4a	9.0 ± 3.0ab	4.1 ± 0.7ab
cotyledon	ground meristem	≥ 0.33 μm	0.7 ± 0.2ab	0.6 ± 0.2ab	0.6 ± 0.2e	0.7 ± 0.2d
cotyledon	ground meristem	≤ 0.33 μm	0.7 ± 0.1ab	0.5 ± 0.1abc	7.1 ± 1.1abcd	3.6 ± 0.7abc
cotyledon	procambium	≤ 0.33 μn	0.7 ± 0.1ab	0.3 ± 0.1c	7.4 ± 1.7abc	4.2 ± 0.8a
shoot apex		≤ 0.33 μm	0.7 ± 0.1ab	0.5 ± 0.2abc	4.8 ± 3.3c	2.8 ± 1.7c
hypocotyl	protoderm	≤ 0.33 μm	0.5 ± 0.1c	0.6 ± 0.2ab	8.9 ± 2.9ab	3.5 ± 0.5abc
hypocotyl	ground meristem	≥ 0.33 μm	0.7 ± 0.1ab	0.5 ± 0.2abc	0.6 ± 0.2e	0.7 ± 0.1d
hypocotyl	ground meristem	≤ 0.33 μm	0.6 ± 0.1bc	0.3 ± 0.1c	7.0 ± 1.2abcd	3.6 ± 0.8abc
hypocotyl	procambium	≤ 0.33 μm	0.7 ± 0.1ab	0.3 ± 0.1c	6.8 ± 1.1bcd	4.0 ± 0.6ab
root apex		≥ 0.33 μm	0.8 ± 0.1a	0.6 ± 0.2ab	0.7 ± 0.3e	0.8 ± 0.1d
root apex		≤ 0.33 μm	0.7 ± 0.1ab	0.6 ± 0.5ab	7.7 ± 2.0abc	3.9 ± 0.5ab

Note: Values within the same column that are followed by the same letter are not significantly different at P>0.05.

Table 14a. Mean (±SD) peak-to-background ratios of several elements in globoid crystals (≥ 0.33 μm)
or electron-dense particles (≤ 0.33 μm) of various tissues of P. resinosa seeds.

Organ	Region analyzed N=15	Particle size (μm)	P	Mg	K	Ca	Fe
female gametophyte		≥ 0.33	7.8 ± 2.5c	2.5 ± 0.7ab	5.0 ± 1.6a	-0.1 ± 0.1bcd	0.5 ± 0.4f
female gametophyte		≤ 0.33	5.3 ± 2.3d	1.2 ± 1.1c	3.8 ± 1.5bcd	0.0 ± 0.3bcd	8.7 ± 6.1e
cotyledon tip	protoderm	≤ 0.33	5.7 ± 0.7d	1.1 ± 0.2c	3.0 ± 0.4cde	0.5 ± 0.3a	22.4 ± 4.3abc
cotyledon tip	ground meristem	≥ 0.33	10.0 ± 1.1a	2.8 ± 0.4a	4.4 ± 1.3ab	0.2 ± 0.2b	0.1 ± 0.1f
cotyledon tip	ground meristem	≤ 0.33	5.7 ± 0.6d	1.0 ± 0.3c	3.1 ± 0.6cde	0.2 ± 0.2b	22.1 ± 4.7abc
cotyledon tip	procambium	≤ 0.33	5.7 ± 0.8d	1.0 ± 0.3c	3.4 ± 0.5bcde	0.2 ± 0.3b	24.0 ± 5.5a
cotyledon	protoderm	≤ 0.33	5.0 ± 0.4d	0.8 ± 0.1c	3.1 ± 0.7cde	0.2 ± 0.1b	19.2 ± 4.2bcd
cotyledon	ground meristem	≥ 0.33	7.9 ± 3.2bc	2.0 ± 0.9b	3.9 ± 1.4abc	0.1 ± 0.4bc	0.1 ± 0.1f
cotyledon	ground meristem	≤ 0.33	4.6 ± 1.8d	0.9 ± 0.3c	2.5 ± 0.8e	0.1 ± 0.2bc	17.0 ± 3.4d
cotyledon	procambium	≤ 0.33	4.5 ± 1.4d	0.9 ± 0.2c	3.1 ± 0.5cde	0.0 ± 0.1bcd	19.8 ± 3.7abcd
shoot apex		≤ 0.33	5.5 ± 0.7d	1.0 ± 0.3c	3.4 ± 0.4bcde	0.1 ± 0.2bc	23.4 ± 3.8ab
hypocotyl	protoderm	≤ 0.33	4.8 ± 1.4d	0.8 ± 0.2c	2.5 ± 0.5e	0.5 ± 0.2a	19.6 ± 3.3abcd
hypocotyl	ground meristem	≥ 0.33	9.8 ± 1.3ab	2.5 ± 0.6ab	4.3 ± 0.6ab	-0.1 ± 0.1cd	0.1 ± 0.1f
hypocotyl	ground meristem	≤ 0.33	5.1 ± 0.9d	1.0 ± 0.3c	3.1 ± 0.7cde	0.0 ± 0.2bcd	18.5 ± 3.3cd
hypocotyl	procambium	≤ 0.33	4.6 ± 0.9d	0.8 ± 0.2c	3.8 ± 0.7bcd	-0.2 ± 0.1d	18.0 ± 3.5cd
root apex		≥ 0.33	9.2 ± 1.8abc	2.8 ± 0.8a	4.4 ± 1.0ab	-0.2 ± 0.1d	0.1 ± 0.1f
root apex		≤ 0.33	5.1 ± 1.2d	1.0 ± 0.4c	2.7 ± 0.7de	0.0 ± 0.1bcd	16.6 ± 5.1d

Note: Values within the same column that are followed by the same letter are not significantly
different at P>0.05.

Table 14b. Ratios (± SD) of Mg to P, K to P, Ca to P, and Fe to P derived from P/B

ratios that were generated by EDX analysis of globoid crystals (≥ 0.33 μm)

or electron-dense particles (≤ 0.33 μm) in P. resinosa seed tissues.

Organ	Region analyzed	Particle size	Mg/P	K/P	Ca/P	Fe/P
female gametophyte		≥ 0.33 μm	0.3 ± 0.1a	0.6 ± 0.2bc	0.0 ± 0.0b	0.0 ± 0.0d
female gametophyte		≤ 0.33 μm	0.2 ± 0.1b	0.7 ± 0.2ab	0.0 ± 0.1b	2.1 ± 1.4c
cotyledon tip	protoderm	≤ 0.33 μm	0.2 ± 0.0b	0.5 ± 0.1cd	0.1 ± 0.0a	3.9 ± 0.6ab
cotyledon tip	ground meristem	≥ 0.33 μm	0.3 ± 0.0a	0.5 ± 0.2cd	0.0 ± 0.0b	0.0 ± 0.0d
cotyledon tip	ground meristem	≤ 0.33 μm	0.2 ± 0.0b	0.6 ± 0.1bc	0.0 ± 0.0b	3.9 ± 0.8ab
cotyledon tip	procambium	≤ 0.33 μm	0.2 ± 0.0b	0.6 ± 0.1bc	0.0 ± 0.0b	4.2 ± 0.9a
cotyledon	protoderm	≤ 0.33 μm	0.2 ± 0.0b	0.6 ± 0.1bc	0.0 ± 0.0b	3.8 ± 0.7ab
cotyledon	ground meristem	≥ 0.33 μm	0.3 ± 0.0a	0.5 ± 0.1cd	0.0 ± 0.1b	0.0 ± 0.0d
cotyledon	ground meristem	≤ 0.33 μm	0.2 ± 0.0b	0.6 ± 0.1bc	0.0 ± 0.0b	4.3 ± 1.7a
cotyledon	procambium	≤ 0.33 μm	0.2 ± 0.0b	0.7 ± 0.1ab	0.0 ± 0.0b	4.3 ± 1.0a
shoot apex		≤ 0.33 μm	0.2 ± 0.0b	0.6 ± 0.1bc	0.0 ± 0.0b	4.3 ± 1.0a
hypocotyl	protoderm	≤ 0.33 μm	0.2 ± 0.0b	0.5 ± 0.1cd	0.1 ± 0.2a	4.0 ± 0.5ab
hypocotyl	ground meristem	≥ 0.33 μm	0.3 ± 0.0a	0.4 ± 0.1d	0.0 ± 0.0b	0.0 ± 0.0d
hypocotyl	ground meristem	≤ 0.33 μm	0.2 ± 0.0b	0.6 ± 0.1bc	0.0 ± 0.0b	3.6 ± 0.4ab
hypocotyl	procambium	≤ 0.33 μm	0.2 ± 0.0b	0.8 ± 0.2a	0.0 ± 0.0b	3.9 ± 0.5ab
root apex		≥ 0.33 μm	0.3 ± 0.1a	0.5 ± 0.1cd	0.0 ± 0.0b	0.0 ± 0.0d
root apex		≤ 0.33 μm	0.2 ± 0.0b	0.5 ± 0.1cd	0.0 ± 0.0b	3.2 ± 0.5b

Note: Values within   the same column that are followed by the same letter are not

significantly different at P>0.05.

Table 14c. Mean element (± SD) ratios derived from P/B ratios that were generated by EDX analysis of globoid crystals (≥ 0.33 μm) or electron-dense particles (≤ 0.33 μm) in P. resinosa seed tissues.

Organ	Region analyzed N=15	Particle size	Mg+K	Mg+Ca	Mg+Ca+Fe	Mg+Ca+Fe+K
			P	K	K	P
female gametophyte		≥ 0.33 μm	0.9 ± 0.2ab	0.5 ± 0.2bc	0.5 ± 0.2f	0.9 ± 0.2d
female gametophyte		≤ 0.33 μn	0.9 ± 0.2ab	0.3 ± 0.2de	3.3 ± 2.1e	3.1 ± 1.3c
cotyledon tip	protoderm	≤ 0.33 μn.	0.7 ± 0.1c	0.5 ± 0.1bc	7.9 ± 1.4ab	4.7 ± 0.6ab
cotyledon tip	ground meristem	≥ 0.33 μm	0.7 ± 0.2c	0.7 ± 0.2a	0.8 ± 0.2f	0.8 ± 0.2d
cotyledon tip	ground meristem	≤ 0.33 μm	0.7 ± 0.1c	0.4 ± 0.2cd	7.7 ± 2.3abc	4.7 ± 0.9ab
cotyledon tip	procambium	≤ 0.33 μm	0.8 ± 0.1bc	0.4 ± 0.1cd	7.5 ± 1.0abc	5.0 ± 0.9a
cotyledon	protoderm	≤ 0.33 μm	0.8 ± 0.1bc	0.3 ± 0.1de	6.8 ± 1.3bc	4.7 ± 0.8ab
cotyledon	ground meristem	≥ 0.33 μm	0.8 ± 0.2bc	0.5 ± 0.2bc	0.5 ± 0.2f	0.8 ± 0.1d
cotyledon	ground meristem	≤ 0.33 μm	0.8 ± 0.1bc	0.4 ± 0.1cd	7.8 ± 2.1ab	5.0 ± 1.8a
cotyledon	procambium	≤ 0.33 μm	0.9 ± 0.1ab	0.3 ± 0.1de	6.6 ± 1.2bc	5.2 ± 1.0a
shoot apex		≤ 0.33 μm	0.8 ± 0.1bc	0.3 ± 0.1de	7.2 ± 0.7abc	5.1 ± 1.1a
hypocotyl	protoderm	≤ 0.33 μm	0.7 ± 0.1c	0.5 ± 0.1bc	8.4 ± 1.2a	4.8 ± 0.7ab
hypocotyl	ground meristem	≥ 0.33 μm	0.7 ± 0.1c	0.6 ± 0.2ab	0.6 ± 0.2f	0.7 ± 0.1d
hypocotyl	ground meristem	≤ 0.33 μm	0.8 ± 0.1bc	0.3 ± 0.1de	6.3 ± 1.1cd	4.4 ± 0.5ab
hypocotyl	procambium	≤ 0.33 μm	1.0 ± 0.2a	0.2 ± 0.1e	4.9 ± 1.0d	4.9 ± 0.6ab
root apex		≥ 0.33 μm	0.8 ± 0.1bc	0.6 ± 0.1ab	0.6 ± 0.1f	0.8 ± 0.1d
root apex		≤ 0.33 μm	0.7 ± 0.1c	0.4 ± 0.1cd	6.5 ± 1.0bc	4.0 ± 0.5bc

Note: Values within the same column that are followed by the same letter are not significantly different at P>0.05.

Table 15a. Mean (± SD) peak-to-background ratios of several elements in globoid crystals (≥ 0.33 μm) or electron-dense particles (≤ 0.33 μm) of various tissues of P. sylvestris seeds.

Organ	Region analyzed N=15	Particle size	P	Mg	K	Ca	Fe
female gametophyte		≥ 0.33 μm	7.5 ± 1.7b	2.3 ± 0.5ab	4.2 ± 0.8a	0.1 ± 0.1defg	0.2 ± 0.1d
female gametophyte		≤ 0.33 μm	3.5 ± 1.3d	0.8 ± 0.4c	2.3 ± 0.8cdefg	0.0 ± 0.1efg	10.9 ± 4.9c
cotyledon tip	protoderm	≤ 0.33 μm	4.9 ± 1.2cd	0.9 ± 0.3c	1.7 ± 0.6efg	0.8 ± 0.1a	17.4 ± 4.2ab
cotyledon tip	ground meristem	≥ 0.33 μm	8.5 ± 1.7ab	2.6 ± 0.6a	2.9 ± 0.6cd	0.0 ± 0.1efg	0.1 ± 0.1d
cotyledon tip	ground meristem	≤ 0.33 μm	5.1 ± 0.7c	1.0 ± 0.2c	2.0 ± 0.5defg	0.5 ± 0.2abc	19.4 ± 3.1a
cotyledon tip	procambium	≤ 0.33 μm	5.1 ± 0.5c	0.9 ± 0.2c	2.3 ± 0.6cdefg	0.3 ± 0.4bcde	19.4 ± 2.8a
cotyledon	protoderm	≤ 0.33 μm	4.3 ± 0.6cd	0.7 ± 0.2c	1.4 ± 0.3g	0.8 ± 0.4a	17.4 ± 3.4ab
cotyledon	ground meristem	≥ 0.33 μm	7.5 ± 1.7b	2.1 ± 0.5b	3.0 ± 0.8bc	0.0 ± 0.1efg	0.5 ± 0.3d
cotyledon	ground meristem	≤ 0.33 μm	5.0 ± 0.8c	0.9 ± 0.2c	1.7 ± 0.5efg	0.3 ± 0.2bcde	17.0 ± 2.9ab
cotyledon	procambium	≤ 0.33 μm	4.4 ± 0.7cd	0.9 ± 0.3c	1.7 ± 0.7efg	0.4 ± 0.3bcd	16.0 ± 4.5ab
shoot apex		≤ 0.33 μm	4.1 ± 1.1cd	0.8 ± 0.3c	1.8 ± 0.6defg	0.4 ± 0.4bcd	15.5 ± 8.2abc
hypocotyl	protoderm	≤ 0.33 μm	4.3 ± 1.0cd	0.7 ± 0.2c	1.5 ± 0.5fg	0.6 ± 0.2ab	13.9 ± 3.0bc
hypocotyl	ground meristem	≥ 0.33 μm	9.1 ± 0.6a	2.5 ± 0.5ab	3.9 ± 0.8ab	-0.2 ± 0.1g	0.2 ± 0.2d
hypocotyl	ground meristem	≤ 0.33 μm	4.9 ± 1.1cd	0.9 ± 0.3c	2.4 ± 0.8cdef	0.2 ± 0.4cdef	18.6 ± 5.5ab
hypocotyl	procambium	≤ 0.33 μm	4.6 ± 1.0cd	0.9 ± 0.3c	2.5 ± 0.7cde	-0.1 ± 0.1fg	16.4 ± 5.2ab
root apex		≥ 0.33 μm	7.6 ± 1.8b	2.4 ± 0.5ab	3.2 ± 0.9bc	0.0 ± 0.3efg	0.2 ± 0.1d
root apex		≤ 0.33 μm	4.2 ± 0.6cd	0.8 ± 0.2c	2.6 ± 1.5cde	0.4 ± 0.5bcd	16.8 ± 3.6ab

Note: Values within the same column that are followed by the same letter are not significantly different at P>0.05.

Table 15b. Ratios (± SD) of Mg to P, K to P, Ca to P, and Fe to P derived from P/B ratios that were generated by EDX analysis of globoid crystals (≥ 0.33 μm) or electron-dense particles (≤ 0.33 μm) in P. sylvestris seed tissues.

Organ	Region analyzed N=15	Particle size	Mg/P	K/P	Ca/P	Fe/P
female gametophyte		≥ 0.33 μm	0.3 ± 0.0a	0.6 ± 0.1ab	0.0 ± 0.0c	0.0 ± 0.0c
female gametophyte		≤ 0.33 μm	0.2 ± 0.1b	0.7 ± 0.2a	0.0 ± 0.0c	3.3 ± 1.2ab
cotyledon tip	protoderm	≤ 0.33 μm	0.2 ± 0.0b	0.3 ± 0.1d	0.2 ± 0.1a	3.6 ± 0.6ab
cotyledon tip	ground meristem	≥ 0.33 μm	0.3 ± 0.0a	0.3 ± 0.1d	0.0 ± 0.0c	0.0 ± 0.0c
cotyledon tip	ground meristem	≤ 0.33 μm	0.2 ± 0.0b	0.4 ± 0.1cd	0.1 ± 0.0b	3.8 ± 0.5ab
cotyledon tip	procambium	≤ 0.33 μm	0.2 ± 0.0b	0.5 ± 0.1bc	0.1 ± 0.1b	3.9 ± 0.6ab
cotyledon	protoderm	≤ 0.33 μm	0.2 ± 0.0b	0.3 ± 0.1d	0.2 ± 0.1a	4.0 ± 0.5ab
cotyledon	ground meristem	≥ 0.33 μm	0.3 ± 0.0a	0.4 ± 0.1cd	0.0 ± 0.0c	0.0 ± 0.0c
cotyledon	ground meristem	≤ 0.33 μm	0.2 ± 0.0b	0.4 ± 0.1cd	0.1 ± 0.0b	3.4 ± 0.7ab
cotyledon	procambium	≤ 0.33 μm	0.2 ± 0.1b	0.4 ± 0.1cd	0.1 ± 0.1b	4.1 ± 0.4a
shoot apex		≤ 0.33 μm	0.2 ± 0.1b	0.4 ± 0.1cd	0.1 ± 0.1b	3.8 ± 1.4ab
hypocotyl	protoderm	≤ 0.33 μm	0.2 ± 0.0b	0.4 ± 0.1cd	0.2 ± 0.1a	3.3 ± 0.6b
hypocotyl	ground meristem	≥ 0.33 μm	0.3 ± 0.0a	0.4 ± 0.1cd	0.0 ± 0.0c	0.0 ± 0.0c
hypocotyl	ground meristem	≤ 0.33 μm	0.2 ± 0.0b	0.5 ± 0.1bc	0.1 ± 0.1b	3.8 ± 0.5ab
hypocotyl	procambium	≤ 0.33 μm	0.2 ± 0.0b	0.5 ± 0.1bc	0.0 ± 0.0c	3.6 ± 0.7ab
root apex		≥ 0.33 μm	0.3 ± 0.0a	0.4 ± 0.1cd	0.0 ± 0.0c	0.0 ± 0.0c
root apex		≤ 0.33 μm	0.2 ± 0.0b	0.6 ± 0.3ab	0.1 ± 0.1b	4.0 ± 0.5ab

Note: Values within the same column that are followed by the same letter are not significantly different at P>0.05.

Table 15c. Mean element (± SD) ratios derived from P/B ratios that were generated by EDX

   analysis of globoid crystals (≥ 0.33 μm) or electron-dense particles (≤ 0.33 μm)

   in P. sylvestris seed tissues.

Organ	Region analyzed N=15	Particle size	Mg+K P	Mg+Ca K	Mg+Ca+Fe K	Mg+Ca+Fe+K P
female gametophyte		≥ 0.33 μm	0.9 ± 0.1a	0.6 ± 0.2cde	0.6 ± 0.2f	0.9 ± 0.1b
female gametophyte		≤ 0.33 μm	0.9 ± 0.2a	0.4 ± 0.2ef	5.6 ± 1.4e	4.3 ± 1.1a
cotyledon tip	protoderm	≤ 0.33 μm	0.5 ± 0.1d	1.1 ± 0.3a	12.3 ± 3.5ab	4.3 ± 0.6a
cotyledon tip	ground meristem	≥ 0.33 μm	0.6 ± 0.1cd	0.9 ± 0.2ab	1.0 ± 0.2f	0.7 ± 0.1b
cotyledon tip	ground meristem	≤ 0.33 μm	0.6 ± 0.1cd	0.8 ± 0.2bc	11.0 ± 1.9abc	4.5 ± 0.5a
cotyledon tip	procambium	≤ 0.33 μm	0.6 ± 0.1cd	0.6 ± 0.2cde	9.4 ± 2.8bcd	4.6 ± 0.7a
cotyledon	protoderm	≤ 0.33 μm	0.5 ± 0.1d	1.1 ± 0.2a	13.8 ± 2.8a	4.7 ± 0.5a
cotyledon	ground meristem	≥ 0.33 μm	0.7 ± 0.1bc	0.7 ± 0.2bcd	0.8 ± 0.2f	0.7 ± 0.1b
cotyledon	ground meristem	≤ 0.33 μm	0.5 ± 0.1d	0.7 ± 0.2bcd	10.8 ± 3.2bc	4.0 ± 0.6a
cotyledon	procambium	≤ 0.33 μm	0.6 ± 0.2cd	0.7 ± 0.3bcd	11.9 ± 3.8ab	4.7 ± 0.3a
shoot apex		≤ 0.33 μm	0.6 ± 0.1cd	0.7 ± 0.3bcd	9.9 ± 3.5bcd	4.4 ± 1.5a
hypocotyl	protoderm	≤ 0.33 μm	0.5 ± 0.1d	0.9 ± 0.2ab	10.4 ± 2.2bc	4.0 ± 0.7a
hypocotyl	ground meristem	≥ 0.33 μm	0.7 ± 0.1bc	0.6 ± 0.2cde	0.7 ± 0.2f	0.7 ± 0.1b
hypocotyl	ground meristem	≤ 0.33 μm	0.7 ± 0.1bc	0.5 ± 0.3ef	8.4 ± 1.6cde	4.5 ± 0.5a
hypocotyl	procambium	≤ 0.33 μm	0.7 ± 0.1bc	0.3 ± 0.1f	7.0 ± 2.0de	4.3 ± 0.7a
root apex		≥ 0.33 μm	0.7 ± 0.1bc	0.8 ± 0.2bc	0.8 ± 0.3f	0.8 ± 0.1b
root apex		≤ 0.33 μm	0.8 ± 0.3ab	0.7 ± 0.4bcd	8.7 ± 3.7cd	4.9 ± 0.6a

Note: Values within the same column that are followed by the same letter are not significantly

   different at P>0.05.

Table 16a. Mean (± SD) peak-to-background ratios of several elements in globoid crystals (≥ 0.33 μm) or electron-dense particles (≤ 0.33 μm) of various tissues of P. mugo seeds.

Organ	Region analyzed N=15	Particle size	P	Mg	K	Ca	Fe
female gametophyte		≥ 0.33 μm	9.1 ± 1.0ab	3.1 ± 0.4a	5.0 ± 0.5a	0.1 ± 0.2cd	0.4 ± 0.3c
female gametophyte		≤ 0.33 μm	4.1 ± 1.3ef	0.8 ± 0.3d	2.2 ± 0.7de	0.0 ± 0.1cd	14.1 ± 6.0b
cotyledon tip	protoderm	≤ 0.33 μm	3.8 ± 1.5f	0.7 ± 0.4d	2.0 ± 0.9e	0.2 ± 0.2bc	15.2 ± 4.8ab
cotyledon tip	ground meristem	≥ 0.33 μm	7.1 ± 3.0bcd	1.9 ± 0.8c	3.2 ± 1.2bcde	-0.1 ± 0.1d	0.3 ± 0.4c
cotyledon tip	ground meristem	≤ 0.33 μm	4.6 ± 2.1ef	1.0 ± 0.5d	2.5 ± 0.9de	0.1 ± 0.1cd	18.2 ± 6.5ab
cotyledon tip	procambium	≤ 0.33 μm	4.8 ± 2.1ef	0.9 ± 0.4d	3.0 ± 1.6bcde	0.0 ± 0.2cd	20.1 ± 6.4a
cotyledon	protoderm	≤ 0.33 μm	4.8 ± 0.9ef	1.0 ± 0.2d	2.4 ± 0.7de	0.4 ± 0.1ab	15.5 ± 3.4ab
cotyledon	ground meristem	≥ 0.33 μm	9.2 ± 0.7a	2.7 ± 0.5ab	4.2 ± 0.6ab	0.0 ± 0.3cd	0.1 ± 0.1c
cotyledon	ground meristem	≤ 0.33 μm	5.2 ± 0.9def	0.8 ± 0.1d	3.1 ± 1.0bcde	0.1 ± 0.2cd	17.9 ± 3.9ab
cotyledon	procambium	≤ 0.33 μm	4.8 ± 0.8ef	1.0 ± 0.2d	3.4 ± 0.6bcd	0.0 ± 0.1cd	17.8 ± 3.5ab
shoot apex		≤ 0.33 μm	5.4 ± 0.8def	1.0 ± 0.2d	3.8 ± 0.5abc	0.0 ± 0.1cd	20.0 ± 5.6a
hypocotyl	protoderm	≤ 0.33 μm	4.2 ± 0.8ef	0.7 ± 0.1d	2.0 ± 0.5e	0.5 ± 0.1a	16.3 ± 3.8ab
hypocotyl	ground meristem	≥ 0.33 μm	7.8 ± 2.3abc	2.3 ± 0.7bc	4.0 ± 1.3abc	-0.1 ± 0.2d	0.3 ± 0.3c
hypocotyl	ground meristem	≤ 0.33 μm	5.2 ± 0.9def	0.8 ± 0.3d	3.1 ± 0.9bcde	0.1 ± 0.1cd	19.2 ± 5.4ab
hypocotyl	procambium	≤ 0.33 μm	5.3 ± 1.3def	0.9 ± 0.3d	3.3 ± 1.0bcd	-0.1 ± 0.1d	20.2 ± 7.2a
root apex		≥ 0.33 μm	5.9 ± 2.7cde	1.9 ± 1.1c	3.2 ± 1.7bcde	0.0 ± 0.3cd	0.2 ± 0.1c
root apex		≤ 0.33 μm	5.5 ± 0.8def	0.8 ± 0.3d	2.8 ± 0.6cde	0.1 ± 0.3cd	19.7 ± 3.9a

Note: Values within the same column that are followed by the same letter are not significantly different at P>0.05.

Table 16b. Ratios (± SD) of Mg to P, K to P, Ca to P, and Fe to P derived from P/B ratios

that were generated by EDX analysis of globoid crystals (≥ 0.33 μm) or electron-

dense particles (≤ 0.33 μm) in P. mugo seed tissues.

Organ	Region analyzed N=15	Particle size	Mg/P	K/P	Ca/P	Fe/P
female gametophyte		≥ 0.33 μn.	0.3 ± 0.0a	0.5 ± 0.1bc	0.0 ± 0.0b	0.1 ± 0.0c
female gametophyte		≤ 0.33 μm	0.2 ± 0.0b	0.5 ± 0.1bc	0.0 ± 0.0b	3.3 ± 0.7b
cotyledon tip	protoderm	≤ 0.33 μm	0.2 ± 0.0b	0.5 ± 0.1bc	0.0 ± 0.1b	4.3 ± 1.0ab
cotyledon tip	ground meristem	≥ 0.33 μm	0.3 ± 0.0a	0.5 ± 0.1bc	0.0 ± 0.0b	0.0 ± 0.0c
cotyledon tip	ground meristem	≤ 0.33 μm	0.2 ± 0.0b	0.6 ± 0.1ab	0.0 ± 0.0b	4.3 ± 1.3ab
cotyledon tip	procambium	≤ 0.33 μm	0.2 ± 0.0b	0.6 ± 0.1ab	0.0 ± 0.1b	4.7 ± 1.2a
cotyledon	protoderm	≤ 0.33 μm	0.2 ± 0.1b	0.5 ± 0.2bc	0.0 ± 0.0b	3.4 ± 0.3ab
cotyledon	ground meristem	≥ 0.33 μm	0.2 ± 0.0b	0.4 ± 0.1c	0.0 ± 0.0b	0.0 ± 0.0c
cotyledon	ground meristem	≤ 0.33 μm	0.2 ± 0.0b	0.6 ± 0.2ab	0.0 ± 0.0b	3.4 ± 0.3ab
cotyledon	procambium	≤ 0.33 μm	0.2 ± 0.0b	0.7 ± 0.1a	0.0 ± 0.0b	3.7 ± 0.6ab
shoot apex		≤ 0.33 μm	0.2 ± 0.0b	0.7 ± 0.2a	0.0 ± 0.0b	3.6 ± 0.7ab
hypocotyl	protoderm	≤ 0.33 μm	0.2 ± 0.0b	0.5 ± 0.1bc	0.1 ± 0.0a	3.9 ± 0.5ab
hypocotyl	ground meristem	≥ 0.33 μm	0.3 ± 0.1a	0.5 ± 0.1bc	0.0 ± 0.0b	0.0 ± 0.0c
hypocotyl	ground meristem	≤ 0.33 μm	0.1 ± 0.0c	0.6 ± 0.1ab	0.0 ± 0.0b	3.7 ± 0.6ab
hypocotyl	procambium	≤ 0.33 μm	0.2 ± 0.0b	0.6 ± 0.1ab	0.0 ± 0.0b	3.7 ± 0.7ab
root apex		≥ 0.33 μm	0.3 ± 0.1a	0.5 ± 0.1bc	0.0 ± 0.1b	0.0 ± 0.0c
root apex		≤ 0.33 μm	0.1 ± 0.1c	0.5 ± 0.1bc	0.0 ± 0.1b	3.6 ± 0.4ab

Note: Values within the same column that are followed by the same letter are not significantly

different at P>0.05.

Table 16c. Mean element (± SD) ratios derived from P/B ratios that were generated by EDX analysis of globoid crystals (≥ 0.33 μm) or electron-dense particles (≤ 0.33 μm) in P. mugo seed tissues.

Organ	Region analyzed N=15	Particle size	Mg+K / P	Mg+Ca / K	Mg+Ca+Fe / K	Mg+Ca+Fe+K / P
female gametophyte		≥ 0.33 μm	0.9 ± 0.2a	0.8 ± 0.2a	0.7 ± 0.2e	0.9 ± 0.3d
female gametophyte		≤ 0.33 μm	0.9 ± 0.1a	0.4 ± 0.2cd	6.5 ± 1.4cd	4.1 ± 0.7c
cotyledon tip	protoderm	≤ 0.33 μm	0.7 ± 0.1bc	0.4 ± 0.2cd	8.5 ± 2.0ab	5.1 ± 1.0ab
cotyledon tip	ground meristem	≥ 0.33 μm	0.8 ± 0.1ab	0.5 ± 0.1bcd	0.6 ± 0.2e	0.8 ± 0.1d
cotyledon tip	ground meristem	≤ 0.33 μm	0.8 ± 0.1ab	0.3 ± 0.1cd	7.9 ± 1.4abc	5.1 ± 1.4ab
cotyledon tip	procambium	≤ 0.33 μm	0.8 ± 0.1ab	0.4 ± 0.2cd	8.2 ± 2.6abc	5.5 ± 1.3a
cotyledon	protoderm	≤ 0.33 μm	0.7 ± 0.2bc	0.5 ± 0.2bcd	7.2 ± 2.0abcd	4.2 ± 0.4bc
cotyledon	ground meristem	≥ 0.33 μm	0.7 ± 0.1bc	0.6 ± 0.1abc	0.6 ± 0.1e	0.7 ± 0.1d
cotyledon	ground meristem	≤ 0.33 μm	0.8 ± 0.2ab	0.3 ± 0.1d	6.5 ± 1.8cd	4.2 ± 0.4bc
cotyledon	procambium	≤ 0.33 μm	0.9 ± 0.1a	0.3 ± 0.1d	5.8 ± 1.2d	4.6 ± 0.6abc
shoot apex		≤ 0.33 μm	0.9 ± 0.2a	0.3 ± 0.1d	5.7 ± 2.0d	4.5 ± 0.6bc
hypocotyl	protoderm	≤ 0.33 μm	0.6 ± 0.1c	0.6 ± 0.1abc	9.0 ± 1.0a	4.6 ± 0.6abc
hypocotyl	ground meristem	≥ 0.33 μm	0.8 ± 0.1ab	0.5 ± 0.2bcd	0.5 ± 0.2e	0.8 ± 0.1d
hypocotyl	ground meristem	≤ 0.33 μm	0.7 ± 0.1bc	0.3 ± 0.1d	6.6 ± 1.3bcd	4.4 ± 0.6bc
hypocotyl	procambium	≤ 0.33 μm	0.8 ± 0.1ab	0.3 ± 0.1d	6.3 ± 1.1cd	4.5 ± 0.7bc
root apex		≥ 0.33 μm	0.8 ± 0.2ab	0.7 ± 0.3ab	0.8 ± 0.4e	0.9 ± 0.1d
root apex		≤ 0.33 μm	0.7 ± 0.1bc	0.4 ± 0.2cd	7.5 ± 0.9abcd	4.3 ± 0.4bc

Note: Values within the same column that are followed by the same letter are not significantly different at P>0.05.

Table 17a. Mean (± SD) peak-to-background ratios of several elements in globoid crystals (≥ 0.33 μm)

or electron-dense particles (≤ 0.33 μm) of various tissues of P. strobus seeds.

Organ	Region analyzed N=15	Particle size	P	Mg	K	Ca	Fe
female gametophyte		≥ 0.33 μm	9.2 ± 1.7b	2.3 ± 0.5bc	4.9 ± 1.0a	0.0 ± 0.2a	0.4 ± 0.2f
female gametophyte		≤ 0.33 μm	5.5 ± 0.7f	0.9 ± 0.2e	3.4 ± 0.8de	-0.2 ± 0.1bc	13.6 ± 3.7e
cotyledon tip	protoderm	≤ 0.33 μm	6.0 ± 0.6ef	1.2 ± 0.2de	3.0 ± 0.5e	0.0 ± 0.2a	17.0 ± 3.3cde
cotyledon tip	ground meristem	≥ 0.33 μm	8.8 ± 1.1b	2.7 ± 0.3a	4.6 ± 0.9ab	-0.1 ± 0.1ab	0.4 ± 0.2f
cotyledon tip	ground meristem	≤ 0.33 μm	6.2 ± 0.8ef	1.2 ± 0.2de	3.3 ± 0.4de	-0.1 ± 0.1ab	17.6 ± 3.1bcd
cotyledon tip	procambium	≤ 0.33 μm	6.8 ± 1.1def	1.2 ± 0.2de	3.2 ± 0.5de	-0.1 ± 0.1ab	18.8 ± 3.5abcd
cotyledon	protoderm	≤ 0.33 μm	6.5 ± 0.6def	1.2 ± 0.2de	3.2 ± 0.6de	0.0 ± 0.3a	18.3 ± 2.0abcd
cotyledon	ground meristem	≥ 0.33 μm	10.6 ± 1.2a	2.6 ± 0.3ab	4.3 ± 1.0abc	-0.1 ± 0.1ab	0.2 ± 0.1f
cotyledon	ground meristem	≤ 0.33 μm	7.5 ± 0.7cd	1.4 ± 0.1d	3.9 ± 0.7bcd	-0.1 ± 0.1ab	21.8 ± 2.2a
cotyledon	procambium	≤ 0.33 μm	6.7 ± 0.9def	1.3 ± 0.2d	3.6 ± 0.6cde	-0.1 ± 0.1ab	19.8 ± 3.8abc
shoot apex		≤ 0.33 μm	6.1 ± 0.8ef	1.2 ± 0.2de	3.6 ± 0.4cde	-0.2 ± 0.1bc	15.7 ± 3.0de
hypocotyl	protoderm	≤ 0.33 μm	5.9 ± 0.7ef	1.1 ± 0.2de	3.1 ± 0.5de	-0.1 ± 0.1ab	16.2 ± 2.0de
hypocotyl	ground meristem	≥ 0.33 μm	8.8 ± 1.4b	2.0 ± 0.5c	4.5 ± 0.8ab	-0.2 ± 0.1bc	0.5 ± 0.7f
hypocotyl	ground meristem	≤ 0.33 μm	6.2 ± 1.2ef	1.1 ± 0.4de	3.5 ± 0.8cde	-0.1 ± 0.1ab	18.8 ± 6.0abcd
hypocotyl	procambium	≤ 0.33 μm	6.3 ± 0.9def	1.2 ± 0.3de	3.8 ± 0.4bcde	-0.1 ± 0.2ab	17.6 ± 3.0bcd
root apex		≥ 0.33 μm	8.7 ± 1.1bc	2.5 ± 0.5ab	4.5 ± 0.8ab	-0.3 ± 0.1c	0.1 ± 0.1f
root apex		≤ 0.33 μm	6.9 ± 0.7de	1.4 ± 0.3d	3.3 ± 0.4de	-0.1 ± 0.2ab	20.8 ± 2.7ab

Note: Values within the same column that are followed by the same letter are not significantly

different at P>0.05.

Table 17b. Ratios (± SD) of Mg to P, K to P, Ca to P, and Fe to P derived from P/B ratios that were generated by EDX analysis of globoid crystals (≥ 0.33 μm) or electron-dense particles (≤ 0.33 μm) in P. strobus seed tissues.

Organ	Region analyzed N=15	Particle size	Mg/P	K/P	Ca/P	Fe/P
female gametophyte		≥ 0.33 μm	0.3 ± 0.0a	0.5 ± 0.1ab	0.0 ± 0.0a	0.0 ± 0.0c
female gametophyte		≤ 0.33 μm	0.2 ± 0.0b	0.6 ± 0.1a	0.0 ± 0.0a	2.5 ± 0.5b
cotyledon tip	protoderm	≤ 0.33 μm	0.2 ± 0.0b	0.5 ± 0.1ab	0.0 ± 0.0a	2.8 ± 0.4ab
cotyledon tip	ground meristem	≥ 0.33 μm	0.3 ± 0.0a	0.5 ± 0.1ab	0.0 ± 0.0a	0.0 ± 0.0c
cotyledon tip	ground meristem	≤ 0.33 μm	0.2 ± 0.0b	0.5 ± 0.1ab	0.0 ± 0.0a	2.8 ± 0.3ab
cotyledon tip	procambium	≤ 0.33 μm	0.2 ± 0.0b	0.5 ± 0.1ab	0.0 ± 0.0a	2.8 ± 0.4ab
cotyledon	protoderm	≤ 0.33 μm	0.2 ± 0.0b	0.5 ± 0.1ab	0.0 ± 0.0a	2.8 ± 0.4ab
cotyledon	ground meristem	≥ 0.33 μm	0.2 ± 0.0b	0.4 ± 0.1b	0.0 ± 0.0a	0.0 ± 0.0c
cotyledon	ground meristem	≤ 0.33 μm	0.2 ± 0.0b	0.5 ± 0.1ab	0.0 ± 0.0a	2.9 ± 0.3ab
cotyledon	procambium	≤ 0.33 μm	0.2 ± 0.0b	0.5 ± 0.1ab	0.0 ± 0.0a	2.9 ± 0.3ab
shoot apex		≤ 0.33 μm	0.2 ± 0.0b	0.6 ± 0.1a	0.0 ± 0.0a	2.6 ± 0.3b
hypocotyl	protoderm	≤ 0.33 μm	0.2 ± 0.0b	0.5 ± 0.1ab	0.0 ± 0.0a	2.8 ± 0.4ab
hypocotyl	ground meristem	≥ 0.33 μm	0.2 ± 0.1b	0.5 ± 0.1ab	0.0 ± 0.0a	0.1 ± 0.1c
hypocotyl	ground meristem	≤ 0.33 μm	0.2 ± 0.0b	0.6 ± 0.1a	0.0 ± 0.0a	2.8 ± 0.4ab
hypocotyl	procambium	≤ 0.33 μm	0.2 ± 0.1b	0.6 ± 0.1a	0.0 ± 0.0a	2.8 ± 0.5ab
root apex		≥ 0.33 μm	0.3 ± 0.0a	0.5 ± 0.1ab	0.0 ± 0.0a	0.0 ± 0.0c
root apex		≤ 0.33 μm	0.2 ± 0.0b	0.5 ± 0.1ab	0.0 ± 0.0a	3.1 ± 0.4a

Note: Values within the same column that are followed by the same letter are not significantly different at P>0.05.

Table 17c. Mean element (± SD) ratios derived from P/B ratios that were generated by EDX analysis of globoid crystals (≥ 0.33 μm) or electron-dense particles (≤ 0.33 μm) in P. strobus seed tissues.

Organ	Region analyzed N=15	Particle size	Mg+K / P	Mg+Ca / K	Mg+Ca+Fe / K	Mg+Ca+Fe+K / P
female gametophyte		≥ 0.33 μm	0.8 ± 0.1a	0.5 ± 0.2ab	0.6 ± 0.2g	0.8 ± 0.1c
female gametophyte		≤ 0.33 μm	0.8 ± 0.1a	0.2 ± 0.1d	4.3 ± 0.8f	3.2 ± 0.5b
cotyledon tip	protoderm	≤ 0.33 μm	0.7 ± 0.1ab	0.4 ± 0.1bc	6.1 ± 0.8abc	3.5 ± 0.5ab
cotyledon tip	ground meristem	≥ 0.33 μm	0.8 ± 0.1a	0.6 ± 0.1a	0.7 ± 0.2g	0.9 ± 0.1c
cotyledon tip	ground meristem	≤ 0.33 μm	0.7 ± 0.1ab	0.3 ± 0.1cd	5.7 ± 1.2bcd	3.6 ± 0.3ab
cotyledon tip	procambium	≤ 0.33 μm	0.7 ± 0.1ab	0.3 ± 0.1cd	6.3 ± 1.3abc	3.4 ± 0.4ab
cotyledon	protoderm	≤ 0.33 μm	0.7 ± 0.1ab	0.4 ± 0.1bc	6.4 ± 1.9ab	3.5 ± 0.4ab
cotyledon	ground meristem	≥ 0.33 μm	0.6 ± 0.1b	0.6 ± 0.1a	0.6 ± 0.1g	0.6 ± 0.1c
cotyledon	ground meristem	≤ 0.33 μm	0.7 ± 0.1ab	0.3 ± 0.1cd	5.8 ± 0.8bcd	3.6 ± 0.3ab
cotyledon	procambium	≤ 0.33 μm	0.7 ± 0.1ab	0.3 ± 0.1cd	5.9 ± 0.8abc	3.7 ± 0.4a
shoot apex		≤ 0.33 μm	0.8 ± 0.1a	0.3 ± 0.0cd	4.7 ± 0.8ef	3.3 ± 0.3ab
hypocotyl	protoderm	≤ 0.33 μm	0.7 ± 0.1ab	0.3 ± 0.1cd	5.6 ± 1.0bcde	3.5 ± 0.5ab
hypocotyl	ground meristem	≥ 0.33 μm	0.7 ± 0.2ab	0.4 ± 0.1bc	0.5 ± 0.2g	0.8 ± 0.2c
hypocotyl	ground meristem	≤ 0.33 μm	0.7 ± 0.1ab	0.3 ± 0.1cd	5.3 ± 1.0cde	3.6 ± 0.5ab
hypocotyl	procambium	≤ 0.33 μm	0.8 ± 0.1a	0.3 ± 0.1cd	4.9 ± 0.9def	3.6 ± 0.6ab
root apex		≥ 0.33 μm	0.8 ± 0.1a	0.5 ± 0.2ab	0.5 ± 0.2g	0.8 ± 0.1c
root apex		≤ 0.33 μm	0.7 ± 0.1ab	0.4 ± 0.1bc	6.8 ± 1.0a	3.7 ± 0.4a

Note: Values within the same column that are followed by the same letter are not significantly different at P>0.05.

Table 18a. Mean (± SD) peak-to-background ratios of elements in globoid crystals (≥ 0.33 μm) or electron-dense particles (≤ 0.33 μm) of various tissues of P. nigra seeds.

Organ	Region analyzed N=15	Particle size	P	Mg	K	Ca	Fe
female gametophyte		≥ 0.33 μm	8.4 ± 1.4ab	2.3 ± 0.6a	4.4 ± 1.1ab	-0.1 ± 0.1cd	0.8 ± 0.8d
female gametophyte		≤ 0.33 μm	4.1 ± 0.9e	0.8 ± 0.2b	2.6 ± 0.7e	0.0 ± 0.1bc	11.6 ± 2.5c
cotyledon tip	protoderm	≤ 0.33 μm	5.2 ± 1.4cde	0.9 ± 0.4a	2.9 ± 0.9de	0.2 ± 0.2ab	12.8 ± 4.7bc
cotyledon tip	ground meristem	≥ 0.33 μm	9.2 ± 1.2a	2.4 ± 0.7a	4.7 ± 0.6ab	-0.3 ± 0.1d	0.6 ± 0.5d
cotyledon tip	ground meristem	≤ 0.33 μm	5.6 ± 1.6cde	1.0 ± 0.5b	3.3 ± 0.9cde	0.0 ± 0.2bc	13.8 ± 6.9bc
cotyledon tip	procambium	≤ 0.33 μm	6.1 ± 1.2cd	1.1 ± 0.2b	3.7 ± 0.8bcd	-0.1 ± 0.1cd	17.7 ± 4.3ab
cotyledon	protoderm	≤ 0.33 μm	5.8 ± 1.1cde	1.0 ± 0.2b	3.3 ± 0.6cde	0.3 ± 0.3a	16.3 ± 3.9abc
cotyledon	ground meristem	≥ 0.33 μm	9.3 ± 1.8a	2.4 ± 0.4a	4.2 ± 0.8abc	-0.3 ± 0.1d	0.6 ± 0.4d
cotyledon	ground meristem	≤ 0.33 μm	5.7 ± 1.2cde	1.2 ± 0.3b	3.8 ± 0.6bcd	-0.1 ± 0.1cd	18.0 ± 5.2ab
cotyledon	procambium	≤ 0.33 μm	6.2 ± 1.1cd	1.2 ± 0.4b	4.0 ± 0.5bc	-0.1 ± 0.1cd	22.0 ± 9.1a
shoot apex		≤ 0.33 μm	6.0 ± 0.8cd	0.9 ± 0.2a	4.2 ± 0.7abc	-0.1 ± 0.1cd	17.9 ± 4.7ab
hypocotyl	protoderm	≤ 0.33 μm	6.1 ± 1.0cd	1.1 ± 0.3b	3.8 ± 0.7bcd	0.3 ± 0.3a	17.8 ± 3.7ab
hypocotyl	ground meristem	≥ 0.33 μm	9.5 ± 1.1a	2.5 ± 0.4b	5.1 ± 1.4a	-0.3 ± 0.1d	0.3 ± 0.2d
hypocotyl	ground meristem	≤ 0.33 μm	5.8 ± 1.2cde	1.1 ± 0.2b	4.1 ± 1.1abc	-0.1 ± 0.2cd	17.0 ± 5.0ab
hypocotyl	procambium	≤ 0.33 μm	5.1 ± 1.0de	0.8 ± 0.2b	4.4 ± 0.9ab	-0.2 ± 0.1cd	18.3 ± 5.4abc
root apex		≥ 0.33 μm	7.0 ± 3.3bc	2.2 ± 0.8a	4.1 ± 1.2abc	0.0 ± 0.2bc	0.3 ± 0.2d
root apex		≤ 0.33 μm	4.9 ± 0.9de	1.1 ± 0.3b	3.7 ± 0.8bcd	0.0 ± 0.1bc	14.5 ± 5.3bc

Note: Values within the same column that are followed by the same letter are not significantly different at P>0.05.

Table 18b. Ratios (± SD) of Mg to P, K to P, Ca to P, and Fe to P derived from P/B

ratios that were generated by EDX analysis of globoid crystals (≥ 0.33 μm)

or electron-dense particles (≤ 0.33 μm) in P. nigra seed tissues.

Organ	Region analyzed N=15	Particle size	Mg/P	K/P	Ca/P	Fe/P
female gametophyte		≥ 0.33 μm	0.3 ± 0.1a	0.5 ± 0.1d	0.0 ± 0.0d	0.1 ± 0.1c
female gametophyte		≤ 0.33 μm	0.2 ± 0.0b	0.6 ± 0.1cd	0.0 ± 0.0cd	2.8 ± 0.4ab
cotyledon tip	protoderm	≤ 0.33 μm	0.2 ± 0.0b	0.6 ± 0.1cd	0.0 ± 0.0abc	2.4 ± 0.6b
cotyledon tip	ground meristem	≥ 0.33 μm	0.3 ± 0.1a	0.5 ± 0.1d	0.0 ± 0.0d	0.1 ± 0.1c
cotyledon tip	ground meristem	≤ 0.33 μm	0.2 ± 0.1b	0.6 ± 0.1cd	0.0 ± 0.0bcd	2.4 ± 0.8b
cotyledon tip	procambium	≤ 0.33 μm	0.2 ± 0.0b	0.6 ± 0.1cd	0.0 ± 0.0d	2.9 ± 0.5ab
cotyledon	protoderm	≤ 0.33 μm	0.2 ± 0.0b	0.6 ± 0.1cd	0.1 ± 0.1ab	2.9 ± 0.4ab
cotyledon	ground meristem	≥ 0.33 μm	0.3 ± 0.1a	0.5 ± 0.2d	0.0 ± 0.0d	0.1 ± 0.0c
cotyledon	ground meristem	≤ 0.33 μm	0.2 ± 0.0b	0.7 ± 0.1bc	0.0 ± 0.0d	3.1 ± 0.5ab
cotyledon	procambium	≤ 0.33 μm	0.2 ± 0.0b	0.7 ± 0.1bc	0.0 ± 0.0d	3.5 ± 1.1a
shoot apex		≤ 0.33 μm	0.2 ± 0.0b	0.7 ± 0.1bc	0.0 ± 0.0d	3.0 ± 0.8ab
hypocotyl	protoderm	≤ 0.33 μm	0.2 ± 0.0b	0.6 ± 0.0cd	0.1 ± 0.1a	2.9 ± 0.4ab
hypocotyl	ground meristem	≥ 0.33 μm	0.3 ± 0.0a	0.5 ± 0.2d	0.0 ± 0.0d	0.0 ± 0.0c
hypocotyl	ground meristem	≤ 0.33 μm	0.2 ± 0.0b	0.7 ± 0.1bc	0.0 ± 0.0d	3.1 ± 0.8ab
hypocotyl	procambium	≤ 0.33 μm	0.1 ± 0.0c	0.9 ± 0.1a	0.0 ± 0.0d	3.4 ± 0.5a
root apex		≥ 0.33 μm	0.3 ± 0.1a	0.7 ± 0.3bc	0.0 ± 0.0bcd	0.1 ± 0.0c
root apex		≤ 0.33 μm	0.2 ± 0.0b	0.8 ± 0.2ab	0.0 ± 0.0cd	3.1 ± 1.1ab

Note: Values within the same column that are followed by the same letter are not significantly

different at P>0.05.

Table 18c. Mean element (± SD) ratios derived from P/B ratios that were generated by EDX analysis of globoid crystals (≥ 0.33 μm) or electron-dense particles (≤ 0.33 μm) in P. nigra seed tissues.

Organ	Region analyzed N=15	Particle size	Mg+K P	Mg+Ca K	Mg+Ca+Fe K	Mg+Ca+Fe+K P
female gametophyte		≥ 0.33 μm	0.8 ± 0.1bc	0.5 ± 0.1a	0.7 ± 0.2e	0.9 ± 0.2c
female gametophyte		≤ 0.33 μm	0.8 ± 0.1bc	0.3 ± 0.1bc	5.0 ± 0.9abcd	3.6 ± 0.4ab
cotyledon tip	protoderm	≤ 0.33 μm	0.7 ± 0.1c	0.4 ± 0.1ab	4.8 ± 1.2abcd	3.2 ± 0.7b
cotyledon tip	ground meristem	≥ 0.33 μm	0.8 ± 0.1bc	0.5 ± 0.2a	0.6 ± 0.2e	0.8 ± 0.1c
cotyledon tip	ground meristem	≤ 0.33 μm	0.8 ± 0.1bc	0.3 ± 0.1bc	4.5 ± 1.5cd	3.2 ± 0.7b
cotyledon tip	procambium	≤ 0.33 μm	0.8 ± 0.1bc	0.3 ± 0.1bc	5.1 ± 0.7abc	3.7 ± 0.6ab
cotyledon	protoderm	≤ 0.33 μm	0.8 ± 0.1bc	0.4 ± 0.1ab	5.6 ± 1.0ab	3.7 ± 0.4ab
cotyledon	ground meristem	≥ 0.33 μm	0.8 ± 0.2bc	0.5 ± 0.2a	0.7 ± 0.3e	0.8 ± 0.2c
cotyledon	ground meristem	≤ 0.33 μm	0.9 ± 0.1ab	0.3 ± 0.1bc	5.0 ± 1.0abcd	4.0 ± 0.5ab
cotyledon	procambium	≤ 0.33 μm	0.8 ± 0.1bc	0.3 ± 0.1bc	5.7 ± 1.9a	4.3 ± 1.1a
shoot apex		≤ 0.33 μm	0.9 ± 0.1ab	0.2 ± 0.1cd	4.4 ± 0.9cd	3.8 ± 0.8ab
hypocotyl	protoderm	≤ 0.33 μm	0.8 ± 0.1bc	0.4 ± 0.1ab	5.1 ± 0.8abc	3.8 ± 0.4ab
hypocotyl	ground meristem	≥ 0.33 μm	0.8 ± 0.2bc	0.5 ± 0.2a	0.5 ± 0.2e	0.8 ± 0.2c
hypocotyl	ground meristem	≤ 0.33 μm	0.9 ± 0.2ab	0.3 ± 0.1bc	4.7 ± 0.8bcd	4.0 ± 0.8ab
hypocotyl	procambium	≤ 0.33 μm	1.0 ± 0.1a	0.1 ± 0.0d	4.1 ± 0.7d	4.3 ± 0.4a
root apex		≥ 0.33 μm	1.0 ± 0.3a	0.5 ± 0.1a	0.6 ± 0.1e	1.1 ± 0.3c
root apex		≤ 0.33 μm	1.0 ± 0.2a	0.3 ± 0.1bc	4.4 ± 0.5cd	4.1 ± 1.3ab

Note: Values within the same column that are followed by the same letter are not significantly different at P>0.05.

Table 19a. Mean (± SD) peak-to-background ratios of elements in globoid crystals (≥ 0.33 μm) or

electron-dense particles (≤ 0.33 μm) of various tissues of P. ponderosa seeds.

Organ	Region analyzed N=15	Particle size	P	Mg	K	Ca	Fe
female gametophyte		≥ 0.33 μm	7.0 ± 2.8c	1.9 ± 0.9bc	4.5 ± 1.9ab	-0.2 ± 0.2bc	0.2 ± 0.2e
female gametophyte		≤ 0.33 μm	3.2 ± 1.8g	0.9 ± 0.5d	2.4 ± 0.9def	0.1 ± 0.3bc	5.3 ± 3.8cd
cotyledon tip	protoderm	≤ 0.33 μm	5.2 ± 0.9de	1.1 ± 0.2d	3.3 ± 0.6cd	0.0 ± 0.2bc	15.6 ± 3.3a
cotyledon tip	ground meristem	≥ 0.33 μm	9.1 ± 0.9a	2.6 ± 0.4a	4.7 ± 0.9ab	-0.1 ± 0.3bc	0.2 ± 0.2e
cotyledon tip	ground meristem	≤ 0.33 μm	5.1 ± 0.8def	1.1 ± 0.2d	3.1 ± 0.7cdef	-0.1 ± 0.1bc	14.9 ± 2.3a
cotyledon tip	procambium	≤ 0.33 μm	4.7 ± 1.0efg	0.9 ± 0.3d	3.2 ± 0.5cde	0.0 ± 0.1bc	15.3 ± 4.4a
cotyledon	protoderm	≤ 0.33 μm	3.4 ± 0.8fg	0.7 ± 0.1d	2.2 ± 0.7def	0.0 ± 0.1bc	11.8 ± 2.5ab
cotyledon	ground meristem	≥ 0.33 μm	7.2 ± 2.6bc	2.1 ± 0.8abc	4.5 ± 1.3ab	-0.2 ± 0.1bc	0.1 ± 0.1e
cotyledon	ground meristem	≤ 0.33 μm	4.0 ± 1.1efg	1.0 ± 0.3d	2.7 ± 0.6cdef	-0.1 ± 0.0bc	13.5 ± 3.2ab
cotyledon	procambium	≤ 0.33 μm	5.0 ± 1.0de	1.1 ± 0.3d	3.1 ± 0.4cdef	0.0 ± 0.1bc	14.9 ± 4.3a
shoot apex		≤ 0.33 μm	3.6 ± 1.6efg	0.8 ± 0.5d	2.1 ± 0.9ef	0.1 ± 0.2bc	5.1 ± 5.2cd
hypocotyl	protoderm	≤ 0.33 μm	4.1 ± 0.7efg	1.0 ± 0.3d	2.0 ± 0.4f	0.2 ± 0.2b	9.5 ± 3.0bc
hypocotyl	ground meristem	≥ 0.33 μm	8.8 ± 0.9ab	2.4 ± 0.4ab	5.0 ± 0.7a	-0.3 ± 0.1c	0.2 ± 0.1e
hypocotyl	ground meristem	≤ 0.33 μm	4.6 ± 0.7efg	1.0 ± 0.2d	2.4 ± 0.5def	-0.1 ± 0.1bc	10.6 ± 4.1b
hypocotyl	procambium	≤ 0.33 μm	3.8 ± 0.9efg	0.9 ± 0.3d	2.3 ± 0.6def	0.0 ± 0.1bc	9.5 ± 3.9bc
root apex		≥ 0.33 μm	6.7 ± 1.9cd	1.8 ± 0.5c	3.7 ± 1.6bc	0.7 ± 1.4a	0.1 ± 0.1e
root apex		≤ 0.33 μm	3.4 ± 1.0efg	0.7 ± 0.2d	2.1 ± 0.7ef	0.0 ± 0.2bc	9.2 ± 3.9cd

Note: Values within the same column that are followed by the same letter are not significantly

different at P>0.05.

Table 19b. Ratios (± SD) of Mg to P, K to P, Ca to P, and Fe to P derived from P/B ratios that were generated by EDX analysis of globoid crystals (≥ 0.33 μm) or electron-dense particles (≤ 0.33 μm) in P. ponderosa seed tissues.

Organ	Region analyzed N=15	Particle size	Mg/P	K/P	Ca/P	Fe/P
female gametophyte		≥ 0.33 μm	0.3 ± 0.1a	0.7 ± 0.2a	0.0 ± 0.0b	0.1 ± 0.1e
female gametophyte		≤ 0.33 μm	0.2 ± 0.1b	0.6 ± 0.3a	0.0 ± 0.1b	1.5 ± 1.9d
cotyledon tip	protoderm	≤ 0.33 μm	0.2 ± 0.0b	0.7 ± 0.2a	0.0 ± 0.0b	3.1 ± 0.6ab
cotyledon tip	ground meristem	≥ 0.33 μm	0.3 ± 0.0a	0.5 ± 0.1a	0.0 ± 0.0b	0.0 ± 0.0e
cotyledon tip	ground meristem	≤ 0.33 μm	0.2 ± 0.0b	0.6 ± 0.1a	0.0 ± 0.0b	3.0 ± 0.5ab
cotyledon tip	procambium	≤ 0.33 μm	0.2 ± 0.1b	0.7 ± 0.1a	0.0 ± 0.0b	3.2 ± 0.8ab
cotyledon	protoderm	≤ 0.33 μm	0.2 ± 0.0b	0.7 ± 0.2a	0.0 ± 0.0b	3.5 ± 0.7a
cotyledon	ground meristem	≥ 0.33 μm	0.3 ± 0.0a	0.6 ± 0.1a	0.0 ± 0.0b	0.0 ± 0.0e
cotyledon	ground meristem	≤ 0.33 μm	0.2 ± 0.0b	0.7 ± 0.1a	0.0 ± 0.0b	3.5 ± 0.9a
cotyledon	procambium	≤ 0.33 μm	0.2 ± 0.0b	0.6 ± 0.1a	0.0 ± 0.0b	3.0 ± 0.6ab
shoot apex		≤ 0.33 μm	0.2 ± 0.1b	0.6 ± 0.2a	0.0 ± 0.1b	1.7 ± 1.3cd
hypocotyl	protoderm	≤ 0.33 μm	0.2 ± 0.1b	0.5 ± 0.1a	0.1 ± 0.0a	2.4 ± 0.7bcd
hypocotyl	ground meristem	≥ 0.33 μm	0.3 ± 0.0a	0.6 ± 0.1a	0.0 ± 0.0b	0.0 ± 0.0e
hypocotyl	ground meristem	≤ 0.33 μm	0.2 ± 0.0b	0.5 ± 0.1a	0.0 ± 0.0b	2.3 ± 0.9bcd
hypocotyl	procambium	≤ 0.33 μm	0.2 ± 0.1b	0.6 ± 0.2a	0.0 ± 0.0b	2.5 ± 0.7bc
root apex		≥ 0.33 μm	0.3 ± 0.1a	0.5 ± 0.2a	0.1 ± 0.3a	0.0 ± 0.0e
root apex		≤ 0.33 μm	0.2 ± 0.0b	0.6 ± 0.1a	0.0 ± 0.0b	2.8 ± 1.3ab

Note: Values within the same column that are followed by the same letter are not significantly different at P>0.05.

Table 19c. Mean element (± SD) ratios derived from P/B ratios that were generated by EDX analysis of globoid crystals (≥ 0.33 μm) or electron-dense particles (≤ 0.33 μm) in P. ponderosa seed tissues.

Organ	Region analyzed N=15	Particle size	Mg+K / P	Mg+Ca / K	Mg+Ca+Fe / K	Mg+Ca+Fe+K / P
female gametophyte		≥ 0.33 μm	1.0 ± 0.3a	0.3 ± 0.2b	0.4 ± 0.1d	1.1 ± 0.3fg
female gametophyte		≤ 0.33 μm	1.0 ± 0.3a	0.4 ± 0.3b	1.7 ± 1.9d	2.0 ± 1.8ef
cotyledon tip	protoderm	≤ 0.33 μm	0.9 ± 0.2ab	0.4 ± 0.1b	5.2 ± 1.0ab	3.9 ± 0.7abc
cotyledon tip	ground meristem	≥ 0.33 μm	0.8 ± 0.1bc	0.6 ± 0.2b	0.6 ± 0.2d	0.8 ± 0.1g
cotyledon tip	ground meristem	≤ 0.33 μm	0.8 ± 0.1bc	0.4 ± 0.1b	5.3 ± 1.3ab	3.8 ± 0.6abc
cotyledon tip	procambium	≤ 0.33 μm	0.9 ± 0.1ab	0.3 ± 0.1b	5.0 ± 1.1ab	4.1 ± 0.8ab
cotyledon	protoderm	≤ 0.33 μm	0.9 ± 0.2ab	0.3 ± 0.2b	6.0 ± 1.5a	4.4 ± 0.8a
cotyledon	ground meristem	≥ 0.33 μm	0.9 ± 0.1ab	0.4 ± 0.1b	0.4 ± 0.1d	0.9 ± 0.1g
cotyledon	ground meristem	≤ 0.33 μm	0.9 ± 0.1ab	0.3 ± 0.1b	5.5 ± 1.2ab	4.4 ± 1.0a
cotyledon	procambium	≤ 0.33 μm	0.9 ± 0.1ab	0.3 ± 0.1b	5.2 ± 1.4ab	3.9 ± 0.7abc
shoot apex		≤ 0.33 μm	0.8 ± 0.2bc	0.5 ± 0.2b	3.2 ± 2.1c	2.6 ± 1.4de
hypocotyl	protoderm	≤ 0.33 μm	0.7 ± 0.1c	0.6 ± 0.2b	5.5 ± 1.2ab	3.2 ± 0.8bcd
hypocotyl	ground meristem	≥ 0.33 μm	0.8 ± 0.1bc	0.4 ± 0.1b	0.5 ± 0.1d	0.8 ± 0.1g
hypocotyl	ground meristem	≤ 0.33 μm	0.8 ± 0.1bc	0.4 ± 0.1b	4.7 ± 1.3ab	3.1 ± 0.9cd
hypocotyl	procambium	≤ 0.33 μm	0.9 ± 0.2ab	0.4 ± 0.2b	4.5 ± 1.6bc	3.3 ± 0.6bcd
root apex		≥ 0.33 μm	0.8 ± 0.2bc	1.1 ± 1.2a	1.1 ± 1.2d	1.0 ± 0.2g
root apex		≤ 0.33 μm	0.8 ± 0.1bc	0.4 ± 0.2b	4.8 ± 1.6ab	3.7 ± 1.4abc

Note: Values within the same column that are followed by the same letter are not significantly different at P>0.05.

Table 20a. Mean (± SD) peak-to-background ratios of elements in globoid crystals (≥ 0.33 μm) or

electron-dense particles (≤ 0.33 μm) of various tissues of P. coulteri seeds.

Organ	Region analyzed N=15	Particle size	P	Mg	K	Ca	Fe
female gametophyte		≥ 0.33 μm	6.2 ± 2.5ab	1.5 ± 0.8ab	3.7 ± 1.0ab	-0.3 ± 0.1cd	0.2 ± 0.1g
female gametophyte		≤ 0.33 μm	4.7 ± 1.3bcd	0.9 ± 0.2cd	3.0 ± 0.8bcde	0.0 ± 0.1ab	16.6 ± 3.7ab
cotyledon tip	protoderm	≤ 0.33 μm	3.1 ± 0.6d	0.6 ± 0.2d	2.1 ± 0.6e	0.0 ± 0.1ab	7.5 ± 4.2f
cotyledon tip	ground meristem	≥ 0.33 μm	7.2 ± 2.3a	1.8 ± 0.7a	4.2 ± 1.3a	-0.2 ± 0.1cd	0.2 ± 0.1g
cotyledon tip	ground meristem	≤ 0.33 μm	3.5 ± 1.8d	0.8 ± 0.4d	2.4 ± 1.0de	-0.1 ± 0.1bc	12.1 ± 3.3bcde
cotyledon tip	procambium	≤ 0.33 μm	3.8 ± 0.8d	0.7 ± 0.3d	2.9 ± 1.0bcde	0.0 ± 0.2ab	9.1 ± 5.0ef
cotyledon	protoderm	≤ 0.33 μm	4.3 ± 1.7cd	0.9 ± 0.4cd	2.7 ± 0.8bcde	0.0 ± 0.2ab	9.8 ± 4.3def
cotyledon	ground meristem	≥ 0.33 μm	5.9 ± 1.5abc	1.4 ± 0.6abc	3.7 ± 1.1ab	-0.1 ± 0.3bc	0.1 ± 0.1g
cotyledon	ground meristem	≤ 0.33 μm	3.8 ± 0.7d	0.6 ± 0.2d	2.5 ± 1.2cde	0.2 ± 0.5a	13.6 ± 3.8abcd
cotyledon	procambium	≤ 0.33 μm	4.3 ± 0.9cd	0.9 ± 0.2cd	3.3 ± 0.6abcd	-0.1 ± 0.1bc	14.6 ± 4.0abc
shoot apex		≤ 0.33 μm	3.3 ± 0.9d	0.8 ± 0.3d	2.3 ± 0.4de	0.0 ± 0.1ab	8.5 ± 3.3ef
hypocotyl	protoderm	≤ 0.33 μm	4.1 ± 1.5cd	0.8 ± 0.5d	2.4 ± 0.8de	0.1 ± 0.1ab	17.2 ± 2.9a
hypocotyl	ground meristem	≥ 0.33 μm	4.6 ± 0.6bcd	1.0 ± 0.1bcd	2.8 ± 0.2bcde	-0.4 ± 0.0d	0.1 ± 0.1g
hypocotyl	ground meristem	≤ 0.33 μm	3.4 ± 1.6d	0.7 ± 0.5d	2.3 ± 0.8de	-0.2 ± 0.1cd	14.1 ± 1.6abc
hypocotyl	procambium	≤ 0.33 μm	4.3 ± 1.0cd	0.9 ± 0.4cd	3.3 ± 0.7abcd	-0.1 ± 0.1bc	12.6 ± 3.9cde
root apex		≥ 0.33 μm	5.8 ± 2.0abc	1.5 ± 0.8ab	3.5 ± 1.1abc	-0.3 ± 0.3cd	0.2 ± 0.2g
root apex		≤ 0.33 μm	3.6 ± 1.4d	1.0 ± 0.4cd	2.4 ± 0.5de	-0.1 ± 0.1bc	11.5 ± 4.1bcde

Note: Values within the same column that are followed by the same letter are not significantly

different at P>0.05.

Table 20b. Ratios (± SD) of Mg to P, K to P, Ca to P, and Fe to P derived from P/B ratios that were generated by EDX analysis of globoid crystals (≥ 0.33 μm) or electron-dense particles (≤ 0.33 μm) in P. coulteri seed tissues.

Organ	Region analyzed N=15	Particle size	Mg/P	K/P	Ca/P	Fe/P
female gametophyte		≥ 0.33 μm	0.2 ± 0.0a	0.6 ± 0.1b	-0.1 ± 0.0b	0.0 ± 0.0d
female gametophyte		≤ 0.33 μm	0.2 ± 0.0a	0.7 ± 0.1ab	0.0 ± 0.0a	3.7 ± 0.8abc
cotyledon tip	protoderm	≤ 0.33 μm	0.2 ± 0.1a	0.7 ± 0.1ab	0.0 ± 0.1a	2.6 ± 1.6c
cotyledon tip	ground meristem	≥ 0.33 μm	0.2 ± 0.0a	0.6 ± 0.1b	0.0 ± 0.0a	0.0 ± 0.0d
cotyledon tip	ground meristem	≤ 0.33 μm	0.2 ± 0.1a	0.7 ± 0.1ab	0.0 ± 0.0a	3.5 ± 1.4bc
cotyledon tip	procambium	≤ 0.33 μm	0.2 ± 0.1a	0.8 ± 0.2a	0.0 ± 0.1a	2.6 ± 1.6c
cotyledon	protoderm	≤ 0.33 μm	0.2 ± 0.0a	0.7 ± 0.2ab	0.0 ± 0.0a	2.6 ± 1.2c
cotyledon	ground meristem	≥ 0.33 μm	0.2 ± 0.0a	0.6 ± 0.1b	0.0 ± 0.0a	0.0 ± 0.0d
cotyledon	ground meristem	≤ 0.33 μm	0.2 ± 0.0a	0.6 ± 0.3b	0.0 ± 0.2a	3.7 ± 1.2abc
cotyledon	procambium	≤ 0.33 μm	0.2 ± 0.0a	0.8 ± 0.1a	0.0 ± 0.0a	3.5 ± 1.0bc
shoot apex		≤ 0.33 μm	0.2 ± 0.1a	0.7 ± 0.1ab	0.0 ± 0.0a	2.8 ± 1.3c
hypocotyl	protoderm	≤ 0.33 μm	0.2 ± 0.1a	0.6 ± 0.1b	0.0 ± 0.0a	4.6 ± 1.3ab
hypocotyl	ground meristem	≥ 0.33 μm	0.2 ± 0.0a	0.6 ± 0.1b	-0.1 ± 0.0b	0.0 ± 0.0d
hypocotyl	ground meristem	≤ 0.33 μm	0.2 ± 0.1a	0.7 ± 0.2ab	0.0 ± 0.0a	5.1 ± 2.6a
hypocotyl	procambium	≤ 0.33 μm	0.2 ± 0.1a	0.8 ± 0.2a	0.0 ± 0.0a	3.0 ± 0.8c
root apex		≥ 0.33 μm	0.2 ± 0.0a	0.6 ± 0.1b	0.0 ± 0.1a	0.0 ± 0.0d
root apex		≤ 0.33 μm	0.2 ± 0.1a	0.7 ± 0.2ab	0.0 ± 0.1a	3.0 ± 0.6c

Note: Values within the same column that are followed by the same letter are not significantly different at $P > 0.05$.

Table 20c. Mean element (± SD) ratios derived from P/B ratios that were generated by EDX analysis of globoid crystals (≥ 0.33 μm) or electron-dense particles (≤ 0.33 μm) in P. coulteri seed tissues.

Organ	Region analyzed N=15	Particle size	Mg+K P	Mg+Ca K	Mg+Ca+Fe K	Mg+Ca+Fe+K P
female gametophyte		≥ 0.33 μm	0.9 ± 0.1a	0.3 ± 0.2a	0.4 ± 0.2e	0.8 ± 0.1d
female gametophyte		≤ 0.33 μm	0.9 ± 0.1a	0.3 ± 0.1a	6.1 ± 1.3bc	4.6 ± 0.9abc
cotyledon tip	protoderm	≤ 0.33 μm	0.9 ± 0.1a	0.3 ± 0.1a	4.5 ± 3.0cd	3.5 ± 1.6c
cotyledon tip	ground meristem	≥ 0.33 μm	0.8 ± 0.1a	0.3 ± 0.1a	0.4 ± 0.1e	0.8 ± 0.1d
cotyledon tip	ground meristem	≤ 0.33 μm	1.1 ± 0.7a	0.3 ± 0.1a	5.3 ± 2.0bcd	4.6 ± 1.5abc
cotyledon tip	procambium	≤ 0.33 μm	1.0 ± 0.2a	0.3 ± 0.2a	3.4 ± 2.1d	3.5 ± 1.5c
cotyledon	protoderm	≤ 0.33 μm	0.9 ± 0.2a	0.4 ± 0.2a	4.3 ± 1.7cd	3.5 ± 1.3c
cotyledon	ground meristem	≥ 0.33 μm	0.9 ± 0.1a	0.3 ± 0.1a	0.4 ± 0.1e	0.8 ± 0.1d
cotyledon	ground meristem	≤ 0.33 μm	0.8 ± 0.3a	0.2 ± 0.1a	4.3 ± 1.4cd	4.6 ± 1.1abc
cotyledon	procambium	≤ 0.33 μm	1.0 ± 0.1a	0.2 ± 0.1a	4.8 ± 1.5cd	4.4 ± 1.0bc
shoot apex		≤ 0.33 μm	0.9 ± 0.1a	0.3 ± 0.1a	4.2 ± 1.7cd	3.7 ± 1.4c
hypocotyl	protoderm	≤ 0.33 μm	0.8 ± 0.1a	0.4 ± 0.2a	8.1 ± 2.9a	5.4 ± 1.4ab
hypocotyl	ground meristem	≥ 0.33 μm	0.8 ± 0.1a	0.2 ± 0.0a	0.3 ± 0.0e	0.8 ± 0.1d
hypocotyl	ground meristem	≤ 0.33 μm	0.9 ± 0.2a	0.2 ± 0.2a	6.8 ± 1.9ab	6.0 ± 2.9a
hypocotyl	procambium	≤ 0.33 μm	1.0 ± 0.2a	0.2 ± 0.1a	4.1 ± 1.0d	3.9 ± 0.9c
root apex		≥ 0.33 μm	0.9 ± 0.1a	0.3 ± 0.2a	0.4 ± 0.2e	0.8 ± 0.1d
root apex		≤ 0.33 μm	0.9 ± 0.2a	0.4 ± 0.3a	5.2 ± 1.9bcd	3.8 ± 0.8c

Note: Values within the same column that are followed by the same letter are not significantly different at P>0.05.

Table 21a. Mean (± SD) peak-to-background ratios of elements in globoid crystals (≥ 0.33 μm) or

electron-dense particles (≤ 0.33 μm) of various tissues of P. sabiniana seeds.

Organ	Region analyzed N=15	Particle size (μm)	P	Mg	K	Ca	Fe
female gametophyte		≥ 0.33	4.9 ± 1.8c	1.2 ± 0.5c	2.9 ± 0.8bcd	-0.3 ± 0.1e	0.1 ± 0.1d
female gametophyte		≤ 0.33	2.5 ± 0.8fg	0.5 ± 0.2ef	1.6 ± 0.5f	-0.1 ± 0.1cd	9.4 ± 3.5bc
cotyledon tip	protoderm	≤ 0.33	3.8 ± 1.3cde	0.7 ± 0.2def	2.6 ± 0.8bcde	0.2 ± 0.2a	9.2 ± 4.0bc
cotyledon tip	ground meristem	≥ 0.33	8.6 ± 0.9a	2.2 ± 0.5a	5.4 ± 0.8a	-0.3 ± 0.1e	0.1 ± 0.1d
cotyledon tip	ground meristem	≤ 0.33	4.1 ± 0.5cd	0.7 ± 0.2def	2.9 ± 0.5bcd	-0.1 ± 0.1cd	10.2 ± 2.7ab
cotyledon tip	procambium	≤ 0.33	4.4 ± 1.3cd	0.8 ± 0.4de	3.2 ± 0.7b	-0.2 ± 0.1de	10.0 ± 3.8ab
cotyledon	protoderm	≤ 0.33	3.2 ± 0.7defg	0.7 ± 0.3def	2.3 ± 0.5cdef	0.0 ± 0.1bc	11.3 ± 4.2ab
cotyledon	ground meristem	≥ 0.33	4.3 ± 0.7cd	0.9 ± 0.1cd	2.5 ± 0.9bcde	-0.1 ± 0.4cd	0.1 ± 0.1d
cotyledon	ground meristem	≤ 0.33	3.4 ± 0.6def	0.6 ± 0.2def	2.3 ± 0.4cdef	-0.2 ± 0.1de	10.9 ± 3.5ab
cotyledon	procambium	≤ 0.33	3.6 ± 1.0def	0.6 ± 0.4def	2.7 ± 0.6bcde	-0.1 ± 0.1cd	5.6 ± 2.3c
shoot apex		≤ 0.33	3.2 ± 1.1defg	0.7 ± 0.2def	2.1 ± 0.8def	0.1 ± 0.1ab	9.8 ± 5.0ab
hypocotyl	protoderm	≤ 0.33	2.8 ± 0.5efg	0.5 ± 0.1ef	1.9 ± 0.4ef	0.1 ± 0.1ab	11.0 ± 3.7ab
hypocotyl	ground meristem	≥ 0.33	4.0 ± 0.6cde	0.8 ± 0.1de	2.6 ± 0.3bcde	-0.2 ± 0.1de	0.1 ± 0.1d
hypocotyl	ground meristem	≤ 0.33	2.0 ± 0.4g	0.4 ± 0.1f	1.5 ± 0.2f	-0.1 ± 0.1cd	8.9 ± 2.6bc
hypocotyl	procambium	≤ 0.33	3.6 ± 0.8def	0.6 ± 0.3def	2.7 ± 0.5bcde	-0.2 ± 0.1de	10.0 ± 5.3ab
root apex		≥ 0.33	6.9 ± 1.5b	1.8 ± 0.4b	5.2 ± 1.2a	-0.2 ± 0.2de	0.1 ± 0.1d
root apex		≤ 0.33	3.9 ± 1.0cde	0.7 ± 0.2def	3.1 ± 0.7bc	-0.1 ± 0.1cd	13.7 ± 4.6a

Note: Values within the same column that are followed by the same letter are not significantly

different at P>0.05.

Table 21b. Ratios (± SD) of Mg to P, K to P, Ca to P, and Fe to P derived from P/B ratios that were generated by EDX analysis of globoid crystals (≥ 0.33 μm) or electron-dense particles (≤ 0.33 μm) in P. sabiniana seed tissues.

Organ	Region analyzed N=15	Particle size	Mg/P	K/P	Ca/P	Fe/P
female gametophyte		≥ 0.33 μm	0.2 ± 0.0b	0.6 ± 0.1b	-0.1 ± 0.0c	0.0 ± 0.0h
female gametophyte		≤ 0.33 μm	0.2 ± 0.1b	0.6 ± 0.1b	0.0 ± 0.0b	3.7 ± 0.7ab
cotyledon tip	protoderm	≤ 0.33 μm	0.2 ± 0.0b	0.7 ± 0.1ab	0.1 ± 0.0a	2.5 ± 0.7efg
cotyledon tip	ground meristem	≥ 0.33 μm	0.3 ± 0.1a	0.6 ± 0.1b	0.0 ± 0.0b	0.0 ± 0.0h
cotyledon tip	ground meristem	≤ 0.33 μm	0.2 ± 0.1b	0.7 ± 0.2ab	0.0 ± 0.0b	2.5 ± 0.8efg
cotyledon tip	procambium	≤ 0.33 μm	0.2 ± 0.0b	0.8 ± 0.1a	0.0 ± 0.0b	2.3 ± 0.5fg
cotyledon	protoderm	≤ 0.33 μm	0.2 ± 0.1b	0.7 ± 0.1ab	0.0 ± 0.0b	3.6 ± 1.4abc
cotyledon	ground meristem	≥ 0.33 μm	0.2 ± 0.0b	0.6 ± 0.2b	0.0 ± 0.1b	0.0 ± 0.0h
cotyledon	ground meristem	≤ 0.33 μm	0.2 ± 0.1b	0.7 ± 0.1ab	-0.1 ± 0.0c	3.4 ± 1.5bcde
cotyledon	procambium	≤ 0.33 μm	0.2 ± 0.1b	0.8 ± 0.2a	0.0 ± 0.0b	1.7 ± 0.8g
shoot apex		≤ 0.33 μm	0.2 ± 0.0b	0.7 ± 0.2ab	0.0 ± 0.0b	2.7 ± 1.0cdef
hypocotyl	protoderm	≤ 0.33 μm	0.2 ± 0.1b	0.7 ± 0.2ab	0.0 ± 0.0b	3.9 ± 1.3ab
hypocotyl	ground meristem	≥ 0.33 μm	0.2 ± 0.0b	0.7 ± 0.1ab	-0.1 ± 0.0c	0.0 ± 0.0h
hypocotyl	ground meristem	≤ 0.33 μm	0.2 ± 0.1b	0.8 ± 0.2a	-0.1 ± 0.0c	4.5 ± 0.9a
hypocotyl	procambium	≤ 0.33 μm	0.2 ± 0.0b	0.7 ± 0.2ab	0.0 ± 0.0b	2.6 ± 0.8defg
root apex		≥ 0.33 μm	0.3 ± 0.1a	0.8 ± 0.1a	0.0 ± 0.0b	0.0 ± 0.0h
root apex		≤ 0.33 μm	0.2 ± 0.1b	0.8 ± 0.2a	0.0 ± 0.0b	3.5 ± 0.5bcd

Note: Values within the same column that are followed by the same letter are not significantly different at P>0.05.

Table 21c. Mean element (± SD) ratios derived from P/B ratios that were generated by EDX analysis of globoid crystals (≥ 0.33 μm) or electron-dense particles (≤ 0.33 μm) in P. sabiniana seed tissues.

Organ	Region analyzed N=15	Particle size	Mg+K / P	Mg+Ca / K	Mg+Ca+Fe / K	Mg+Ca+Fe+K / P
female gametophyte		≥ 0.33 μm	0.9 ± 0.1ab	0.3 ± 0.1a	0.3 ± 0.1f	0.8 ± 0.1g
female gametophyte		≤ 0.33 μm	0.8 ± 0.1b	0.2 ± 0.1a	6.2 ± 1.6a	4.5 ± 0.8abc
cotyledon tip	protoderm	≤ 0.33 μm	0.9 ± 0.1ab	0.4 ± 0.1a	3.9 ± 1.0bc	3.4 ± 0.7def
cotyledon tip	ground meristem	≥ 0.33 μm	0.9 ± 0.1ab	0.2 ± 0.1a	0.4 ± 0.1f	0.9 ± 0.1g
cotyledon tip	ground meristem	≤ 0.33 μm	0.9 ± 0.2ab	0.2 ± 0.1a	4.1 ± 0.6bc	3.4 ± 0.8def
cotyledon tip	procambium	≤ 0.33 μm	0.9 ± 0.1ab	0.2 ± 0.1a	3.2 ± 0.9cd	3.2 ± 0.6ef
cotyledon	protoderm	≤ 0.33 μm	0.9 ± 0.1ab	0.3 ± 0.1a	5.3 ± 1.8ab	4.6 ± 1.5abc
cotyledon	ground meristem	≥ 0.33 μm	0.8 ± 0.2b	0.8 ± 1.9a	0.9 ± 2.0ef	0.8 ± 0.2g
cotyledon	ground meristem	≤ 0.33 μm	0.9 ± 0.2ab	0.2 ± 0.1a	5.0 ± 1.9ab	4.3 ± 1.6bcd
cotyledon	procambium	≤ 0.33 μm	1.0 ± 0.2a	0.2 ± 0.2a	2.3 ± 0.8de	2.7 ± 1.0f
shoot apex		≤ 0.33 μm	0.9 ± 0.2ab	0.3 ± 0.1a	4.4 ± 1.0bc	3.8 ± 1.4cde
hypocotyl	protoderm	≤ 0.33 μm	0.8 ± 0.2b	0.3 ± 0.1a	6.2 ± 2.1a	4.8 ± 1.3ab
hypocotyl	ground meristem	≥ 0.33 μm	0.9 ± 0.1ab	0.2 ± 0.1a	0.3 ± 0.1f	0.8 ± 0.1g
hypocotyl	ground meristem	≤ 0.33 μm	1.0 ± 0.2a	0.1 ± 0.1a	6.0 ± 1.6a	5.4 ± 1.0a
hypocotyl	procambium	≤ 0.33 μm	0.9 ± 0.1ab	0.2 ± 0.1a	3.3 ± 0.9cd	3.4 ± 0.9def
root apex		≥ 0.33 μm	1.0 ± 0.1a	0.3 ± 0.2a	0.4 ± 0.2f	1.0 ± 0.1g
root apex		≤ 0.33 μm	1.0 ± 0.2a	0.2 ± 0.1a	4.8 ± 1.5ab	4.4 ± 0.5bc

Note: Values within the same column that are followed by the same letter are not significantly different at P>0.05.

Table 22a. Mean (± SD) peak-to-background ratios of elements in globoid crystals (≥ 0.33 μm) or

electron-dense particles (≤ 0.33 μm) of various tissues of P. koraiensis seeds.

Organ	Region analyzed N=15	Particle size	P	Mg	K	Ca	Fe
female gametophyte		≥ 0.33 μm	6.1 ± 1.4abc	1.8 ± 0.3bc	4.5 ± 1.1abc	-0.1 ± 0.1ab	0.3 ± 0.4c
female gametophyte		≤ 0.33 μm	4.4 ± 1.8ef	1.1 ± 0.6de	2.9 ± 1.3ef	-0.1 ± 0.1ab	7.1 ± 6.1b
cotyledon tip	protoderm	≤ 0.33 μm	4.3 ± 0.7ef	0.8 ± 0.2e	2.9 ± 0.7ef	-0.1 ± 0.1ab	12.7 ± 3.7a
cotyledon tip	ground meristem	≥ 0.33 μm	7.4 ± 1.0a	2.4 ± 0.3a	4.8 ± 0.6ab	-0.3 ± 0.1c	0.2 ± 0.1c
cotyledon tip	ground meristem	≤ 0.33 μm	4.1 ± 1.0ef	0.9 ± 0.5e	3.1 ± 1.0def	-0.2 ± 0.1bc	10.8 ± 4.8ab
cotyledon tip	procambium	≤ 0.33 μm	4.1 ± 1.1ef	0.8 ± 0.3e	2.9 ± 0.5ef	-0.1 ± 0.1ab	10.4 ± 3.1ab
cotyledon	protoderm	≤ 0.33 μm	4.5 ± 0.7cdef	0.9 ± 0.3e	3.0 ± 0.8def	0.0 ± 0.1a	11.3 ± 3.9ab
cotyledon	ground meristem	≥ 0.33 μm	6.5 ± 2.2ab	2.1 ± 0.7ab	4.3 ± 1.5abcd	-0.2 ± 0.2bc	0.1 ± 0.1c
cotyledon	ground meristem	≤ 0.33 μm	5.6 ± 1.0bcde	1.4 ± 0.5cd	3.8 ± 1.2bcde	-0.2 ± 0.1bc	11.8 ± 7.5ab
cotyledon	procambium	≤ 0.33 μm	4.4 ± 1.1def	1.1 ± 0.3de	3.1 ± 1.0def	-0.2 ± 0.1bc	11.6 ± 4.7ab
shoot apex		≤ 0.33 μm	4.0 ± 0.8ef	1.0 ± 0.4de	2.5 ± 0.5f	-0.1 ± 0.1ab	7.9 ± 5.2ab
hypocotyl	protoderm	≤ 0.33 μm	4.3 ± 1.2def	0.9 ± 0.4e	3.3 ± 1.1cdef	-0.1 ± 0.1ab	7.0 ± 2.7b
hypocotyl	ground meristem	≥ 0.33 μm	7.0 ± 0.6ab	2.0 ± 0.3ab	5.5 ± 0.5a	-0.3 ± 0.1c	0.1 ± 0.1c
hypocotyl	ground meristem	≤ 0.33 μm	4.1 ± 0.9ef	1.0 ± 0.4de	3.1 ± 1.3def	0.0 ± 0.2a	7.8 ± 6.1ab
hypocotyl	procambium	≤ 0.33 μm	4.5 ± 1.6cdef	0.9 ± 0.4e	3.8 ± 1.1bcde	-0.2 ± 0.1bc	9.2 ± 3.0ab
root apex		≥ 0.33 μm	5.9 ± 0.8abcd	2.0 ± 0.3ab	4.4 ± 0.6abc	0.0 ± 0.3a	0.1 ± 0.1c
root apex		≤ 0.33 μm	3.8 ± 1.0f	1.1 ± 0.4de	2.8 ± 1.1ef	-0.1 ± 0.2ab	7.3 ± 3.3b

Note: Values within the same column that are followed by the same letter are not significantly

different at P>0.05.

Table 22b. Ratios (± SD) of Mg to P, K to P, Ca to P, and Fe to P derived from P/B
ratios that were generated by EDX analysis of globoid crystals (≥ 0.33 μm)
or electron-dense particles (≤ 0.33 μm) in P. koraiensis seed tissues.

Organ	Region analyzed N=15	Particle size	Mg/P	K/P	Ca/P	Fe/P
female gametophyte		≥ 0.33 μm	0.3 ± 0.0a	0.7 ± 0.1a	0.0 ± 0.0a	0.1 ± 0.1c
female gametophyte		≤ 0.33 μm	0.3 ± 0.1a	0.7 ± 0.2a	0.0 ± 0.0a	2.1 ± 1.6ab
cotyledon tip	protoderm	≤ 0.33 μm	0.2 ± 0.0b	0.7 ± 0.2a	0.0 ± 0.0a	3.0 ± 0.6a
cotyledon tip	ground meristem	≥ 0.33 μm	0.3 ± 0.0a	0.7 ± 0.1a	0.0 ± 0.0a	0.0 ± 0.0c
cotyledon tip	ground meristem	≤ 0.33 μm	0.2 ± 0.1b	0.8 ± 0.4a	0.0 ± 0.0a	2.3 ± 0.8ab
cotyledon tip	procambium	≤ 0.33 μm	0.2 ± 0.0b	0.7 ± 0.1a	0.0 ± 0.0a	2.5 ± 0.3ab
cotyledon	protoderm	≤ 0.33 μm	0.2 ± 0.0b	0.7 ± 0.1a	0.0 ± 0.0a	2.5 ± 0.6ab
cotyledon	ground meristem	≥ 0.33 μm	0.3 ± 0.1a	0.7 ± 0.2a	0.0 ± 0.0a	0.0 ± 0.0c
cotyledon	ground meristem	≤ 0.33 μm	0.2 ± 0.1b	0.7 ± 0.1a	0.0 ± 0.0a	2.3 ± 1.4ab
cotyledon	procambium	≤ 0.33 μm	0.2 ± 0.1b	0.7 ± 0.1a	0.0 ± 0.0a	2.5 ± 0.6ab
shoot apex		≤ 0.33 μm	0.2 ± 0.1b	0.7 ± 0.2a	0.0 ± 0.0a	2.0 ± 1.1b
hypocotyl	protoderm	≤ 0.33 μm	0.2 ± 0.1b	0.8 ± 0.2a	0.0 ± 0.0a	1.7 ± 0.6b
hypocotyl	ground meristem	≥ 0.33 μm	0.3 ± 0.0a	0.8 ± 0.1a	0.0 ± 0.0a	0.0 ± 0.0c
hypocotyl	ground meristem	≤ 0.33 μm	0.2 ± 0.1b	0.7 ± 0.2a	0.0 ± 0.1a	1.8 ± 1.2b
hypocotyl	procambium	≤ 0.33 μm	0.2 ± 0.1b	0.9 ± 0.3a	0.0 ± 0.0a	2.1 ± 0.5ab
root apex		≥ 0.33 μm	0.3 ± 0.0a	0.8 ± 0.1a	0.0 ± 0.0a	0.0 ± 0.0c
root apex		≤ 0.33 μm	0.3 ± 0.0a	0.7 ± 0.2a	0.0 ± 0.0a	1.9 ± 0.8b

Note: Values within the same column that are followed by the same letter are not
significantly different at P>0.05.

Table 22c. Mean element (± SD) ratios derived from P/B ratios that were generated by EDX analysis
of globoid crystals (≥ 0.33 μm) or electron-dense particles (≤ 0.33 μm) in P. koraiensis
seed tissues.

Organ	Region analyzed N=15	Particle size	Mg+K P	Mg+Ca K	Mg+Ca+Fe K	Mg+Ca+Fe+K P
female gametophyte		≥ 0.33 μm	1.0 ± 0.1a	0.4 ± 0.1ab	0.5 ± 0.1d	1.1 ± 0.2c
female gametophyte		≤ 0.33 μm	1.0 ± 0.2a	0.3 ± 0.2bc	2.7 ± 2.0c	2.8 ± 1.6b
cotyledon tip	protoderm	≤ 0.33 μm	0.9 ± 0.2a	0.3 ± 0.1bc	4.6 ± 0.9a	3.8 ± 0.8a
cotyledon tip	ground meristem	≥ 0.33 μm	1.0 ± 0.1a	0.5 ± 0.1a	0.5 ± 0.1d	1.0 ± 0.1c
cotyledon tip	ground meristem	≤ 0.33 μm	1.0 ± 0.3a	0.3 ± 0.5bc	3.4 ± 1.0abc	3.0 ± 1.0ab
cotyledon tip	procambium	≤ 0.33 μm	0.9 ± 0.1a	0.2 ± 0.1c	3.8 ± 0.7abc	3.4 ± 0.3ab
cotyledon	protoderm	≤ 0.33 μm	0.9 ± 0.1a	0.3 ± 0.1bc	4.2 ± 0.9ab	3.4 ± 0.7ab
cotyledon	ground meristem	≥ 0.33 μm	1.0 ± 0.2a	0.5 ± 0.2a	0.5 ± 0.2d	1.0 ± 0.2c
cotyledon	ground meristem	≤ 0.33 μm	0.9 ± 0.2a	0.3 ± 0.1bc	3.8 ± 1.9abc	3.1 ± 1.4ab
cotyledon	procambium	≤ 0.33 μm	1.0 ± 0.2a	0.3 ± 0.1bc	4.0 ± 1.2abc	3.4 ± 0.6ab
shoot apex		≤ 0.33 μm	0.9 ± 0.2a	0.3 ± 0.2bc	3.6 ± 2.0abc	2.9 ± 1.0ab
hypocotyl	protoderm	≤ 0.33 μm	1.0 ± 0.2a	0.3 ± 0.1bc	2.6 ± 1.0c	2.6 ± 0.6b
hypocotyl	ground meristem	≥ 0.33 μm	1.1 ± 0.1a	0.3 ± 0.1bc	0.4 ± 0.1d	1.1 ± 0.1c
hypocotyl	ground meristem	≤ 0.33 μm	1.0 ± 0.2a	0.4 ± 0.2ab	2.9 ± 1.7bc	2.8 ± 1.2b
hypocotyl	procambium	≤ 0.33 μm	1.1 ± 0.3a	0.2 ± 0.1c	2.7 ± 0.9c	3.2 ± 0.6ab
root apex		≥ 0.33 μm	1.1 ± 0.1a	0.5 ± 0.1a	0.5 ± 0.1d	1.1 ± 0.1c
root apex		≤ 0.33 μm	1.0 ± 0.2a	0.4 ± 0.1ab	3.0 ± 1.0bc	2.9 ± 0.9ab

Note: Values within the same column that are followed by the same letter are not significantly
different at P>0.05.

Discussion

EDX analysis, using a detector fitted with a beryllium window, permits the simultaneous detection of elements of atomic number 11 (Na) and greater in specific cell regions. When using EDX spectra to compare element concentrations, it is necessary to take into consideration that peak heights will not be the same for equal amounts of all of the detected elements. Russ (1972) used standards to calculate P values for a number of elements. The P values indicate the relative intensity of each element from the same concentration. Iron has a P value (for an operating energy of 80 kV) of 0.98. P values of 0.94 and 0.93 for K and Ca respectively, indicate that peak heights would be relatively the same for these two elements if they were present in equal amounts. Phosphorus and Mg, with P values of 0.75 and 0.47 respectively, are underestimated relative to other elements in the spectrum (Russ, 1972).

Phytin is the only compound present in seed tissues known to provide EDX spectra such as those obtained in this study when analyzing globoid crystals. It is useful to present values of K, Mg and Ca in the form of ratios to P as these elements are likely present as counterions to negatively-charged phosphate groups on the phytate molecule (Lott and Ockenden, 1986). Phytic acid always contains six P atoms per molecule and has 12 available binding sites for cations so a number of different mixed salts could be formed

(Ockenden and Lott, 1990; Ockenden and Lott, 1991). When a seed begins to germinate, the cations are released during the enzymatic hydrolysis of phytin and become available to the developing seedling.

Globoid crystals ($\geq$ 0.33 μm)

No major differences were found between the seeds of the eleven <u>Pinus</u> species with regard to the types of elements stored in the globoid crystals or their relative concentrations. Even between tissues of different ploidy levels, differences in element stores were not large. Globoid crystals of the embryo tissues (2N) and female gametophyte (1N) were determined to contain high levels of P, Mg and K, with traces of Ca and/or Fe. P, Mg and K are usually the main EDX analyzable elements present in globoid crystals in seeds of many plants (Lott, 1984). Trace amounts of Ca and Fe have previously been found in globoid crystals of various seeds.

Previous studies of globoid crystals in various seeds have shown a connection between the levels of elements such as Mg and Ca that form divalent ions, with the levels of elements like K that form monovalent ions (Lott <u>et</u> <u>al</u>., 1979; West and Lott, 1991). In those studies Mg P/B and Ca P/B ratios were highest in globoid crystals in the tissue regions where K P/B ratios were the lowest. This trend was not observed for globoid crystals in the <u>Pinus</u> species investigated in this study. In fact, high Mg P/B and K P/B ratios were often recorded within globoid crystals of the same tissue region of

a pine seed.

Phosphorus, Mg and Ca levels in globoid crystals of the eleven species investigated decreased as seed size increased. However, with the exception of the globoid crystals of the cotyledon tips, K levels in globoid crystals were not correlated with seed size. In tissues of the cotyledon tips K levels of the globoid crystals increased with increasing seed size. Pate et al. (1986) found that small-seeded species of Proteaceae commonly contained significantly more concentrated pools of P+K+Mg+Ca than larger-seeded species, a trend which they found generally expressed a higher protein-to-oil ratio. Such a statement on the protein-to-oil ratio for Pinus species cannot not be made since total seed protein and oil contents were not measured in this study.

As mentioned, Ca levels were found to be negatively correlated with seed size. A similar trend was previously observed for Cucurbita seeds. Cucurbita species with small seeds were found to have a more homogeneous and widespread distribution of Ca in globoid crystals than Cucurbita species with larger seeds (Lott and Vollmer, 1979). In fact whole embryos of small-seeded cucurbits contained significantly higher Ca concentrations than whole embryos of the large-seeded cucurbits (Ockenden and Lott, 1988). Therefore it appeared that seed size was related to the distribution of Ca in cucurbit embryos. Ockenden and Lott (1988) hypothesized that the differences in Ca concentrations between seeds of the

Cucurbita species could be related to different growth rates of developing seeds. Large seeds, with higher numbers of cells, have higher growth rates and therefore a faster rate of dry matter increase (Egli et al., 1981). Hocking and Pate (1977) found that Ca accumulation within the embryo tends to be slower than dry matter increase. From their study, Ockenden and Lott (1988) surmised that the higher growth rate in larger seeds would exaggerate the lag in Ca accumulation.

Results showed that ratios of divalent and monovalent ions to P, namely; (Mg+K)/P and (Mg+Ca+Fe+K)/P, were positively correlated with seed size for globoid crystals of the embryo tissues. The near zero Ca and Fe levels of globoid crystals were not sources of the increase in these ratios to P in larger pine seeds. Magnesium levels in globoid crystals decreased with increasing seed size and therefore did not contribute to the increase in the ratios. Globoid crystal K levels were positively correlated with seed size in ground meristem tissue of the cotyledon tips only, an observation which does not explain why the globoid crystal ratios of divalent + monovalent ratios to P are positively correlated with seed size for the remaining tissue of the embryo. Only a consistent decline in P levels within the globoid crystals from the small to larger-sized pine seeds provides a feasible explanation of the positive correlation between the ratios and seed size. This suggests that of all the elements within globoid crystals of pine seeds, it is the level of P that is

most related to seed size.

Electron-dense particles ($\leq$ 0.33 μm)

High levels of Fe and significant levels of P, Mg and K were detected in electron-dense particles throughout the tissues of the embryo and female gametophyte of all eleven species of <u>Pinus</u> studied. Fe has previously been detected in trace amounts in globoid crystals of the seeds of a number of species such as <u>Capsella</u> and <u>Lycopersicon</u> (Spitzer <u>et</u> <u>al.</u>, 1980), <u>Datura</u> (Maldonado and Lott, 1991) and <u>Capsicum</u> (Chen and Lott, 1992). This is the first report of high levels of Fe being present, with other elements commonly detected in globoid crystals, in seed tissues.

Fe levels were found to be higher in electron-dense particles of embryo tissues than in electron-dense particles of female gametophytes of pine seeds. Fe is not easily mobilized in seed tissue (Hocking and Pate, 1977). Therefore, Fe stores in the embryo could be utilized more efficiently by the germinating seed than Fe stores of the female gametophyte. As mentioned in Chapter 4, Fe is an important component of a number of proteins involved in cellular metabolism and is required by the germinating seedling in order to establish photosynthesis and respiration functions.

Fe levels within the electron-dense particles decreased as seed size increased. Hocking and Pate (1977) determined that in various legumes Fe may accumulate significantly and consistently with dry matter increase or

like Ca, Fe accumulation may lag behind dry matter increase. As mentioned earlier, Ca levels within globoid crystals were also negatively correlated with increasing seed size. Perhaps Ockenden and Lott's (1988) hypothesis, that the higher growth rate in larger seeds would exaggerate the lag in Ca accumulation, also holds for the Fe trends observed in this study. In order to confirm this, it would require a study of Fe mobilization in Pinus seeds.

The Fe-rich particles may be molecules of phytoferritin protein which are visible as electron-dense bodies in the electron microscope due to the rich abundance of iron atoms within a proteinaceous shell (Gunning and Steer, 1975). In tissues phytoferritin molecules often aggregate to form closely packed clusters of approximately 0.5 μm in diameter (Seckbach, 1972). Phytoferritin has been found in plastids and chloroplasts (Gunning and Steer, 1975), can be associated with cytoplasmic lipid globules and has been seen in plastids which contain electron-dense granules as the main or sole inclusion. Hyde et al. (1963) analyzed phytoferritin molecules and determined that iron was the only metal present in high concentrations. Other elements (B, Pb, Cu, Ca, Mg, Ba and Si) were present only in minute traces. However, EDX analysis of the electron-dense particles in pine seeds revealed significant amounts of P, Mg and K which are elements common to phytin. Iron is known to form complexes with phytin. In fact, a number of methods for phytic acid analysis

employ ferric chloride to precipitate phytate from plant tissue extracts (Thompson and Erdman, 1982). The presence of significant amounts of other elements in the Fe-rich particles suggests that they are not phytoferritin particles, but rather iron-associated phytin deposits. Although EDX analysis supplies the user with information on elements present within a particular subcellular region, unfortunately this technique does not provide any exact information on the compounds contained within the analyzed region.

Chapter 6

GENERAL DISCUSSION OF KEY FINDINGS.

This study has been the most exhaustive investigation of mineral nutrient storage within mature seeds of one genus in terms of the number of species that were investigated, the number of tissue regions in each seed that were studied, and the total number of elements that were measured quantitatively and semi-quantitatively. Hocking and Pate (1977) presented evidence that showed the selective absorption of minerals by endosperms and embryos of angiosperm seeds. Levels of Cu, Mn, Zn and Fe were very different for endosperm and embryo tissues within a seed. A comparative study of mineral nutrient reserves in haploid female gametophyte versus diploid embryo tissues of gymnosperm seeds has not been the focus of any previous studies of seed mineral storage reserves.

Lipids and proteins were found to be major constituents of the storage reserves of Pinus seeds, the majority of which is stored in the female gametophyte which contributes approximately 90% of the total female gametophyte + embryo weight in all eleven species investigated. Although not measured quantitatively, starch appeared to be only a minor component of mature pine seeds.

Protein crystalloids and globoid crystals were

commonly observed in protein bodies throughout female gametophyte and embryo tissues. Protein crystalloids have been shown to be the major proteins of female gametophyte and embryo tissues of pine seeds (Gifford, 1988). The hydrolysis of protein crystalloids in female gametophyte and embryo tissues of germinating pine seeds begins before radicle emergence (Lammer and Gifford, 1989). Bewley and Black (1985) defined radicle emergence from the seed coat as the completion of the seed germination process. Following radicle emergence, embryo crystalloid proteins were mobilized quickly resulting in a significant increase in free amino acids within this tissue. Female gametophyte crystalloid proteins were mobilized more slowly, without a significant increase in free amino acids within the female gametophyte. It was determined that the free amino acids generated by the hydrolysis of protein crystalloids within the female gametophyte were promptly transferred to the embryo (Lammer and Gifford, 1989). Free amino acids are required by the embryo early during seed germination for the synthesis of enzymes required for protein storage reserve mobilization.

Total mineral nutrient levels of mature pine seeds did not appear to be markedly altered by the environment and growth conditions experienced by the developing seeds. Female gametophyte and embryo tissues of all the pine seeds analyzed were determined to contain high levels of P, K, Mg and S, as well as significant levels of Cl, Ca, Mn, Zn and Fe. The

importance of each of these mineral nutrients was discussed in Chapter 4. During germination, P is transferred from the female gametophyte at an earlier stage than other substances and accumulates temporarily in the hypocotyl of seedlings, so that seedling total phosphorus increases as the phosphorus level of the female gametophyte decreases (Aiba, 1963). Later this phosphorus is mobilized to the cotyledons and epicotyl (Aiba, 1963).

On a $\mu g.g^{-1}$ dry weight basis P, K, Mg, S, Zn and Fe concentrations were not significantly different between the female gametophyte and corresponding embryo tissues of the majority of species investigated in this study. However, Cl, Mn and Ca levels were determined to be significantly higher in female gametophytes than embryos. Concentrations of P and Mg were not correlated with seed size. Sulphur, Ca, Mn, Zn and Fe concentrations of the female gametophyte and/or embryo tissue were negatively correlated with seed size, while K and Cl concentrations were positively correlated with seed size. On a μg per tissue basis, larger seeds were found to contain more mineral nutrients than smaller seeds. Female gametophytes contained higher levels of mineral nutrients than corresponding embryos.

The globoid crystals contained the highest concentrations of reserve P, Mg and K (indicative of phytate presence) of all pine seed tissue constituents, as well as traces of Ca and Fe. Based on previous studies of the

distribution of mineral nutrients within seed tissues, it is believed that the bulk of stored mineral nutrients in many seed tissues is stored within the globoid crystals of protein bodies. However, Mn, Cl, Zn and the majority of Fe did not appear to be associated with the phytate stores in protein bodies. While K levels in globoid crystals were not significantly correlated with seed size, P, Mg and Ca levels in the globoid crystals were negatively correlated with seed size indicating that phytate concentrations within globoid crystals were lower in larger-sized seeds. An accurate measure of total phytin in female gametophyte and embryo tissues of the eleven species would be necessary to confirm whether or not phytate levels in the globoid crystals of pine seeds are related to seed size. The positive correlation between Ca and seed size was previously found for Cucurbita seeds (Lott and Vollmer, 1979) and was also demonstrated by the NAA results of this study.

High Fe levels were recorded for electron-dense particles contained within membrane-bound structures that were observed to be present in all tissues of the embryo and female gametophyte. I believe that the presence of P, Mg and K in significant amounts in these Fe-rich particles identifies these particles as iron associated, phytate-rich particles. Energy dispersive x-ray analysis results showed Fe levels to be higher in electron-dense particles of embryo tissues than in electron-dense particles of the female gametophyte. NAA

results supported this finding. Iron was the only element measured by NAA that yielded higher embryo levels than female gametophyte levels for three of the species studied. The EDX analysis and NAA findings of this study indicated a negative correlation between Fe levels and seed size. Thus not only were Fe-rich particles more numerous in the tissues of small-sized pine seeds (as indicated in Chapter 2), but they also contained higher levels of Fe.

EDX analysis results and ultrastructure observations (Chapter 2) indicated that the Fe-rich particles were not contained within typical protein bodies. In order to determine the nature of the membrane-bound structure surrounding these particles, it would be necessary to study pine seeds at different stages of maturation. Organelle structure within seed tissues is easier to observe prior to the deposition of lipids within the seed. Due to their density within pine seed tissue, lipids impede fixation and infiltration procedures and affect one's ability to distinguish fine detail. A study of pine seed germination may indicate the possible role of the Fe-rich particles and surrounding structures by observing their fates within the developing seedling.

During seed germination, the utilization of lipid reserves within conifer seeds appears to be under embryo influence, while the breakdown of storage proteins appears to be controlled by the female gametophyte (Cyr et al., 1991).

The embryo mobilizes its own reserves initially, then depends on reserves of the female gametophyte (Groome et al., 1991). Lipid and protein reserves of the female gametophyte provide fatty acids and amino acids for the developing seedling after embryo reserves are depleted and before photosynthetic independence is attained (Groome et al., 1991). Simola (1974) observed that protein bodies disappear from pine embryos before the mobilization of the main protein reserves of the female gametophyte.

Female gametophyte reserves are important for the successful establishment of gymnosperm seedlings. During germination and seedling growth a decrease in dry weight of the female gametophyte and an increase in dry weight of the seedling plant occurs (Sasaki and Kozlowski, 1969). Berlyn and Miksche (1965) determined that excised embryos could be cultured in vitro but did not grow as well as embryos which were left in contact with their female gametophytes. The initiation of embryo growth in P. resinosa seeds does not depend on female gametophyte reserves, but over-all growth of the hypocotyl-radicle axis and cotyledons was found to be stimulated by female gametophyte reserves. Removal of the female gametophyte reserves impeded growth of these embryo tissues (Sasaki and Kozlowski, 1969).

This study has shown that lipids and proteins were the main storage reserve constituents of both the haploid female gametophyte and the diploid embryo of a pine seed. On a $\mu g.g^{-1}$

dry weight basis, total mineral nutrient stores did not vary greatly between female gametophytes and corresponding embryos for the eleven Pinus species investigated. Protein body structure and the types of mineral nutrients stored in the globoid crystals of protein bodies was similar for female gametophyte and embryo tissues of mature pine seeds. Phosphorus, Mg and Ca concentrations in globoid crystals and Fe concentrations in electron-dense particles were determined to be related to seed size in pine seeds. The levels of these elements were highest in small-sized species of Pinus and decreased as seed size increased.

References

AIBA, Y. 1963. Movement of phosphorus in pine seedlings. I. Movement of total phosphorus in germination process. J. Japan. Forestry Society **45**: 131-134.

AMIEL, S. 1981. Studies in analytical chemistry. Vol. 3. Non-destructive activation analysis. Elsevier Scientific Publishing Co., Amsterdam.

ASHTON, F. L. 1936. Influence of the temperature of ashing on the accuracy of the determination of phosphorus in grass. J. Soc. Chem. Ind. **55**: 106-108.

ASHTON, F. M. 1976. Mobilization of storage proteins of seeds. Ann. Rev. Plant Physiol. **27**: 95-117.

ASHTON, W. M., and WILLIAMS, P. C. 1958. The phosphorus compounds of oats. I. The content of phytate phosphorus. J. Sci. Food Agric. **9**: 505-511.

BARBI, N. C. 1979. Quantitative methods in biological x-ray microanalysis. Scanning Electron Microsc. **II**: 658-672.

BARONDES, S. H. 1981. Lectins: their multiple endogenous cellular functions. Ann. Rev. Biochem. **50**: 207-231.

BERLYN, G. P., and MIKSCHE, J. P. 1965. Growth of excised pine embryos and the role of the cotyledons during germination in vitro. Am. J. Bot. **52**: 730-736.

BEWLEY, J. D., and BLACK, M. 1985. Seeds: physiology of development and germination. Plenum Press, New York.

BOZZOLA, J. J., and RUSSELL, L. D. 1992. Electron microscopy: principles and techniques for biologists. Jones and Bartlett Publishers, Boston.

BRIGGS, A. P. 1924. Some applications of the colorimetric phosphate method. J. Biol. Chem. **59**: 255-264.

BUCHHOLZ, J. T. 1946. Volumetric studies of seeds, endosperms, and embryos in _Pinus ponderosa_ during embryonic differentiation. Bot. Gaz. **108**: 232-244.

BUCHHOLZ, J. T., and STIEMERT, M. L. 1945. Development of seeds and embryos in Pinus ponderosa, with special reference to seed size. Ill. Acad. Sci. Trans. **38**: 27-50.

CANADA DEPARTMENT OF MINES AND RESOURCES 1939. Native trees of Canada. Bulletin No. 61, Ottawa. pp. 210.

CHANDLER, J. A. 1972. An introduction to analytical electron microscopy. Micron **3**: 85-92.

CHEN, C., CHIANG, Y. P., and POMERANZ, Y. 1989. Image analysis and characterization of cereal grains with a laser range finder and camera contour extractor. Cereal Chem. **66**: 466-470.

CHEN, P., and LOTT, J. N. A. 1992. Studies of Capsicum annuum seeds: structure, storage reserves, and mineral nutrients. Can. J. Bot. **70**: 518-529.

CLARKSON, D. T., and HANSON, J. B. 1980. The mineral nutrition of higher plants. Ann. Rev. Plant Physiol. **31**: 239-298.

CLEGG, M. S., KEEN, C. L., LONNERDAL, B., and HURLEY, L. S. 1981. Influence of ashing techniques on the analysis of trace elements in biological samples. II. Dry ashing. Biol. Trace Element Res. **3**: 237-244.

COPELAND, L. O. 1976. Principles of seed science and technology. Burgess Publishing Co., Minneapolis.

CORLISS, W. R. 1964. Neutron activation analysis. United States Atomic Energy Commission, Division of Technical Information. pp. 2-28.

CRITCHFIELD, W. B., and LITTLE, E. L. 1966. Geographic distribution of the pines of the world. U. S. Dept. Agr. Forest Service, Washington. Misc. Publ. No. 991.

CYR, D. R., WEBSTER, F. B., and ROBERTS, D. R. 1991. Biochemical events during germination and early growth of somatic embryos and seed of interior spruce (Picea glauca engelmanni complex). Seed Sci. Res. **1**: 91-97.

DMITRIEVA, M. I., and SOBOLEV, A. M. 1984. Mobilization of phytin in castor seeds during germination. Soviet plant Physiol. **31**: 799-805.

DOSTAL, J. and ELSON, C. 1980. General principles of neutron activation analysis. In Short course in neutron activation analysis in the geosciences. Vol. 5. Edited by G. K. Muecke. Mineralogical Association of Canada, Halifax. pp. 21-42.

DURZAN, D. J., MIA, A. J., and RAMAIAH, P. K. 1971. The
metabolism and subcellular organization of the jack pine
embryo (Pinus banksiana) during germination. Can. J. Bot.
49: 927-938.

EGLI, D. B., FRASER, J., LEGGETT, J. E., and PONELEIT, C. G.
1981. Control of seed growth in soya beans (Glycine max
(L.) Merrill). Ann. Bot. **48**: 171-176.

ERGLE, D. R., and GUINN, G. 1959. Phosphorus compounds of
cotton embryos and their changes during germination. Plant
Physiol. **34**: 476-481.

ESTEP, K. W., and MACINTYRE, F. 1986. Counting, sizing, and
identification of algae using image analysis. Sarsia **74**:
261-268.

FENNER, M. 1983. Relationships between seed weight, ash
content and seedling growth in twenty-four species of
Compositae. New Phytol. **95**: 697-706.

FERNANDEZ GARCIA de CASTRO, M., and MARTINEZ-HONDUVILLA, C. J.
1984. Ultrastructural changes in naturally aged Pinus pinea
seeds. Physiol. Plant. **62**: 581-588.

FLINN, B. S., WEBB, D. T., and NEWCOMB, W. 1989. Morphometric
analysis of reserve substances and ultrastructural changes
during caulogenic determination and loss of competence of
eastern White pine (Pinus strobus) cotyledons in vitro.
Can. J. Bot. **67**: 779-789.

GAYLER, K. R., and SYKES, G. E. 1985. Effects of nutritional
stress on the storage proteins of soybeans. Plant Physiol.
78: 582-585.

GIFFORD, D. J. 1988. An electrophoretic analysis of the seed
proteins from Pinus monticola and eight other species of
pine. Can. J. Bot. **66**: 1808-1812.

GIFFORD, D. J., and TOLLEY, M. C. 1989. The seed proteins of
white spruce and their mobilization following germination.
Physiol. Plant. **77**: 254-261.

GLASCOCK, M. D. 1988. Tables for neutron activation analysis.
Research Reactor Facility, University of Missouri. pp. 119.

GLASS, A. D. M. 1989. Plant nutrition: an introduction to
current concepts. Jones and Bartlett Publishers, Boston.

GORI, P. 1979. An ultrastructural investigation of protein and
lipid reserves in the endosperm of Pinus pinea L. Ann. Bot.
43: 101-105.

GORSUCH, T. T. 1959. Radiochemical investigations on the recovery for analysis of trace elements in organic and biological materials. Analyst **84**: 135-173.

GORSUCH, T. T. 1970. The destruction of organic matter. Pergamon Press, Oxford.

GREENWOOD, J. S. 1989. Phytin synthesis and deposition. <u>In</u> Recent advances in the development and germination of seeds. <u>Edited by</u> R. B. Taylorson. Plenum Press, New York. pp. 109-125.

GREENWOOD, J. S., and BEWLEY, J. D. 1984. Subcellular distribution of phytin in the endosperm of developing castor bean: a possibility for its synthesis in the cytoplasm prior to deposition within protein bodies. Planta **160**: 113-120.

GRIFFITHS, D. W., and THOMAS, T. A. 1981. Phytate and total phosphorus content of field beans (<u>Vicia</u> <u>faba</u> L.). J. Sci. Food Agric. **32**: 187-192.

GROOME, M. C., AXLER, S. R., and GIFFORD, D. J. 1991. Hydrolysis of lipid and protein reserves in loblolly pine seeds in relation to protein electrophoretic patterns following imbibition. Physiol. Plant. **83**: 99-106.

GUNNING, B. E. S., and STEER, M. W. 1975. Ultrastructure and the biology of plant cells. Edward Arnold Ltd., London.

HADER, D. 1988. Computer-assisted image analysis in biological sciences. Proc. Indian Acad. Sci. (Plant Sci.) **98**: 227-249.

HALL, J. R., and HODGES, T. K. 1966. Phosphorus metabolism of germinating oat seeds. Plant Physiol. **41**: 1459-1464.

HARTIG, T. 1855. Über das Klebermehl. Bot. Zeitschr. **13**: 881-882.

HASKIN, L. A. 1980. An overview of neutron activation analysis in geochemistry. <u>In</u> Short course in neutron activation analysis in the geosciences. Vol. 5. <u>Edited by</u> G. K. Muecke. Mineralogical Association of Canada, Halifax. pp. 1-19.

HIGGINS, T. J. V. 1984. Synthesis and regulation of major proteins in seeds. Ann. Rev. Plant Physiol. **35**: 191-221.

HIRIART, M., TEIXIDO, E., FUCHSLOCHER, R., and CUEVAS, E. 1977. Determination of minerals in forage. I. Comparison of wet and dry digestion methods. Chem. Abs. **89**: 430.

HOCKING, P. J., and PATE, J. S. 1977. Mobilization of minerals to developing seeds of legumes. Ann. Bot. **41:** 1259-1278.

HOFFMAN, E. L. 1980. Analytical geochemistry advanced by neutron activation. Can. J. Spectroscopy **25:** 23A-25A.

HOSIE, R. C. 1979. Native trees of Canada. 8th Ed. Canadian Forestry Service, Dept. of Environment. Fitzhenry and Whiteside, Ltd.

HYDE, B. B., HODGE, A. J., KAHN, A., and BIRNSTIEL, M. L. 1963. Studies on phytoferritin I. identification and localization. J. Ultrastructure Res. **9:** 248-258.

INGESTAD, T. 1979. Mineral nutrient requirements of Pinus sylvestris and Picea abies seedlings. Physiol. Plant. **45:** 373-380.

ISAAC, R. A. 1990. Phosphorus in plants: micro-method. In Official methods of analysis of the Association of Official Analytical Chemists. Vol. 1. 15th Ed. Chapter 3: Plants. Edited by K. Helrich. Assoc. Off. Anal. Chem. Inc., Virginia. pp. 56.

ISAAC, R. A., and JOHNSON, W. C. 1975. Collaborative study of wet and dry ashing techniques for the elemental analysis of plant tissue by atomic absorption spectrophotometry. J. Assoc. Off. Anal. Chem. **58:** 436-440.

JENSEN, U., and BERTHOLD, H. 1989. Legumin-like proteins in gymnosperms. Phytochemistry **28:** 1389-1394.

KIKUNAGA, S., KATOH, Y., and TAKAHASHI, M. 1991. Biochemical changes in phosphorus compounds and in the activity of phytase and α-amylase in the rice (Oryza sativa) grain during germination. J. Sci. Food Agric. **56:** 335-343.

KRUGER, P. 1971. Principles of activation analysis. John Wiley and Sons, Inc., New York.

LALONDE, L., FOUNTAIN, D. W., KERMODE, A., OUELLETTE, F. B., SCOTT, K., BEWLEY, J. D., and GIFFORD, D. J. 1984. A comparative study of the insoluble storage proteins and the lectins of seeds of the Euphorbiaceae. Can. J. Bot. **62:** 1671-1677.

LAMBERT, M. J. 1976. Preparation of plant material for estimating a wide range of elements. Forestry Commission of N.S.W., Research Note No. 29. pp. 1-51.

LAMMER, D. L., and GIFFORD, D. J. 1989. Lodgepole pine seed germination. II. The seed proteins and their mobilization

in the megagametophyte and embryonic axis. Can. J. Bot. **67:** 2544-2551.

LANGDON, O. G. 1958. Cone and seed size of south Florida slash pine and their effects on seedling size and survival. J. Forestry **56:** 122-127.

LITTLE, E. L., and CRITCHFIELD, W. B. 1969. Subdivisions of the genus _Pinus_ (pines). U. S. Dept. Agr. Forest Service, Washington. Misc. Publ. No. 1144.

LOLAS, G. M., and MARKAKIS, P. 1975. Phytic acid and other phosphorus compounds of beans (_Phaseolus_ _vulgaris_ L.). J. Agric. Food Chem. **23:** 13-15.

LOLAS, G. M., PALAMIDIS, N., and MARKAKIS, P. 1976. The phytic acid-total phosphorus relationship in barley, oats, soybeans, and wheat. Cereal Chem. **53:** 867-871.

LOPEZ-PEREZ, M. J., GIMENEZ-SOLVES, A., CALONGE, F. D., and SANTOS-RUIZ, A. 1974. Evidence of glyoxysomes in germinating pine seeds. Plant Sci. Letters **2:** 377-386.

LOTT, J. N. A. 1980. Protein bodies. _In_ The biochemistry of plants: a comprehensive treatise. Vol. 1. _Edited_ _by_ N. E. Tolbert. Academic Press, New York. pp. 589-623.

LOTT, J. N. A. 1981. Protein bodies in seeds. Nord. J. Bot. **1:** 421-432.

LOTT, J. N. A. 1984. Accumulation of seed reserves of phosphorus and other minerals. _In_ Seed physiology. Vol. 1. _Edited_ _by_ D. R. Murray. Academic Press, Sydney. pp.139-166.

LOTT, J. N. A., and BUTTROSE, M. S. 1978. Globoids in protein bodies of legume seed cotyledons. Aust. J. Plant Physiol. **5:** 89-111.

LOTT, J. N. A., and VOLLMER, C. M. 1979. Composition of globoid crystals from embryo protein bodies in five species of _Cucurbita_. Plant Physiol. **63:** 307-311.

LOTT, J. N. A., and OCKENDEN, I. 1986. The fine structure of phytate-rich particles in plants. _In_ Phytic acid: chemistry and applications. _Edited_ _by_ E. Graf. Pilatus Press, Minneapolis. pp. 43-55.

LOTT, J. N. A., SPITZER, E., and VOLLMER, C. M. 1979. Calcium distribution in globoid crystals of _Cucurbita_ cotyledon protein bodies. Plant Physiol. **63:** 847-851.

LOTT, J. N. A., GOODCHILD, D. J., and CRAIG, S. 1984. Studies

of mineral reserves in pea (<u>Pisum</u> <u>sativum</u>) cotyledons using low-water-content procedures. Aust. J. Plant physiol. **11**: 459-469.

LOTT, J. N. A., RANDALL, P. J., GOODCHILD, D. J., and CRAIG, S. 1985. Occurrence of globoid crystals in cotyledonary protein bodies of <u>Pisum</u> <u>sativum</u> as influenced by experimentally induced changes in Mg, Ca and K contents of seeds. Aust. J. Plant Physiol. **12**: 341-353.

MAGA, J. A. 1982. Phytate: its chemistry, occurrence, food interactions, nutritional significance, and methods of analysis. J. Agric. Food Chem. **30**: 1-9.

MALDONADO, S., and LOTT, J. N. A 1992. Protein bodies in <u>Datura</u> <u>stramonium</u> seeds: structure and mineral nutrient composition. Can. J. Bot. **69**: 2545-2554.

MENGDEHL, H. 1933. Studien zum Phosphorstoffwechsel in der Höheren Pflanze. I. Die Bestimmung von Pyro- und Metaphosphate, sowie von Phosphit und Hypophosphit in Pflanzenmaterial. Planta **19**: 154-169.

MENGEL, K., and KIRKBY, E. A. 1982. Principles of plant nutrition. International Potash Institute, Switzerland.

MIKA, V. 1977. Comparison of various methods of plant material mineralization employed most frequently in Czechoslovakian laboratories. Chem. Abs. **88**: 220.

MILLER, G. A., YOUNGS, V. L., and OPLINGER, E. S. 1980. Environmental and cultivar effects on oat phytic acid concentration. Cereal Chem. **57**: 189-191.

MOTOMIZU, S., WAKIMOTO, T., and TÔEL, K. 1983. Spectrophotometric determination of phosphate in river waters with molybdate and malachite green. Analyst **108**: 361-367.

MUNTER, R. C., GRANDE, R. A., and AHN, P. C. 1979. Analysis of animal tissue and food materials by inductively coupled plasma emission spectrometry in a university research service laboratory. Chem. Abs. **92**: 290.

NEUMAN, M. R., SAPIRSTEIN, H. D., SHWEDYK, E., and BUSHUK, W. 1989. Wheat grain colour analysis by digital image processing I. Methodology. J. Crop Sci. **10**: 175-182.

NINOMIYA, S., and SHIGEMORI, I. 1991. Quantitative evaluation of soybean (<u>Glycine</u> <u>max</u> L. MERRILL) plant shape by image analysis. Japan. J. Breed. **41**: 485-497.

O'KENNEDY, B. T., REILLY, C. C., TITUS, J. S., and SPLITTSTOESSER, W. E. 1979. A comparison of the storage protein (globulin) of eight species of Cucurbitaceae. Can. J. Bot. **57**: 2044-2049.

OCKENDEN, I., and LOTT, J. N. A. 1988. Mineral storage in Cucurbita embryos. I. Calcium storage in relation to embryo size. Can. J. Bot **66**: 1477-1481.

OCKENDEN, I., and LOTT, J. N. A. 1990. Elemental storage in Cucurbita embryos: X-ray microanalysis of magnesium, potassium, calcium, and phosphorus within globoid crystals. Can. J. Bot. **68**: 646-650.

OCKENDEN, I., and LOTT, J. N. A. 1991. Beam sensitivity of globoid crystals within seed protein bodies and commercially prepared phytates during x-ray microanalysis. Scanning Microsc. **5**: 767-778.

PARDOS, J. A. 1990. Morphological and chemical aspects of Pinus sylvestris L. from Spain. Holzforschung **44**: 143-146.

PATE, J. S., RASINS. E., RULLO, J., and KUO, J. 1986. Seed nutrient reserves of Proteaceae with special reference to protein bodies and their inclusions. Ann. Bot. **57**: 747-770.

PERNOLLET, J. C. 1978. Protein bodies of seeds: ultrastructure, biochemistry, biosynthesis and degradation. Phytochem. **17**: 1473-1480.

PERRY, T. O. 1976. Maternal effects on the early performance of tree progenies. In Tree physiology and yield improvement. Edited by M. Cannell and F. Last. Academic Press, London. pp. 473-482.

RABOY, V. 1990. Biochemistry and genetics of phytic acid synthesis. In Inositol metabolism in plants. Vol. 9. Edited by D. J. Morré, W. F. Boss and F. A. Loewus. Wiley-Liss, Inc., New York. pp. 55-76.

RAKOVIC, M. 1970. Activation analysis, Academia, Prague.

RUSS, J. C. 1972. Obtaining quantitative x-ray analytical results from thin sections in the electron microscope. In Proceedings of the Thin-section Microanalysis Symposium, St. Louis, Mo, November 8, 1972. Edited by J. C. Russ and B. J. Panessa. EDAX Laboratories, Raleigh, NC. pp. 115-132.

RUSS, J. C. 1990. Computer-assisted microscopy: the measurement and analysis of images. Plenum Press, New York.

SALMIA, M. A., and MIKOLA, J. J. 1975. Activities of two

peptidases in resting and germinating seeds of Scots pine, Pinus sylvestris. Physiol. Plant. **33**: 261-265.

SASAKI, S., and KOZLOWSKI, T. T. 1969. Utilization of seed reserves and currently produced photosynthates by embryonic tissues of pine seedlings. Ann. Bot. **33**: 473-482.

SANDELL, E. B. 1950. Chemical analysis. Vol. 3. Colourimetric determination of traces of metals. Interscience Publishers Inc., New York.

SECKBACH, J. 1972. Electron microscopical observations of leaf ferritin from iron-treated Xanthium plants: localization and diversity in the organelle. J. Ultrastructure Res. **39**: 65-76.

SHKOLNIK, M. Y. 1984. Trace elements in plants. Elsevier Science, Amsterdam.

SHOULDERS, E. 1961. Effect of seed size on germination, growth, and survival of slash pine. J. Forestry **59**: 576-579.

SIMOLA, L. K. 1974. The ultrastructure of dry and germinating seeds of Pinus sylvestris L. Acta Bot. Fennica **103**: 1-31.

SKILNYK, H. R. 1990. Light microscopy, electron microscopy, and elemental analyses of Cucurbita maxima and Cucurbita andreana pollen. M.Sc. thesis, Department of Biology, McMaster University, Hamilton, Ont.

SOBOLEV, A. M., and RODIONOVA, M. A. 1966. Phytin synthesis by aleurone grains in maturing sunflower seeds. Soviet Plant Physiol. **13**: 958-961.

SPITZER, E., LOTT, J. N. A., and VOLLMER, C. M. 1980. Studies of metal uptake, especially iron, into protein bodies of Capsella and Lycopersicon seeds. Can. J. Bot. **58**: 1244-1249.

SPURR, S. H. 1944. Effect of seed weight and seed origin on the early development of eastern white pine. J. Arnold Arboretum **25**: 457-480.

STEWART, A., NIELD, H., and LOTT, J. N. A. 1988. An investigation of the mineral content of barley grains and seedlings. Plant Physiol. **86**: 93-97.

STUFFINS, C. B. 1967. The determination of phosphate and calcium in feeding stuffs. Analyst **92**: 107-111.

ŠTUPAR, J., AJLEC, R., KOROSIN, J., and LOBNIK, F. 1987. A

comparison of spectroscopic methods for determination of phosphorus in plant materials, soil extracts and fertilizers. Landwirtsch. Forschung **40**: 21-31.

SUZUTANI, T. 1980. Investigations on ashing of animal tissues for the determination of trace metals by means of polarography or atomic absorption spectrometry. Biol. Abs. **70**: 7221.

SYMONS, S. J., and FULCHER, R. G. 1988. Determination of wheat kernel morphological variation by digital image analysis. I. Variation in eastern Canadian milling quality wheats. J. Cereal Sci. **8**: 211-218.

TANAKA, K., YOSHIDA, T., and KASAI, Z. 1976. Phosphorylation of myo-inositol by isolated aleurone particles of rice. Agr. Biol. Chem. **40**: 1319-1325.

THOMPSON, D. B., and ERDMAN, J.W. 1982. Structural model for ferric phytate: implications for phytic acid analysis. Cereal Chem. **59**: 525-528.

TINKER, B., and LÄUCHLI, A. 1986. Advances in plant nutrition. Vol. 2. Praeger, New York.

TOON, P. G., HAINES, R. J., and DIETERS, M. J. 1991. Relationship between seed weight, germination time and seedling height growth in Pinus caribaea Morelet var. hondurensis Barrett and Golfari. Seed Sci. and Technol. **19**: 397-402.

TUŠL, J. 1972. Spectrophotometric determination of phosphorus in biological samples after dry ashing without fixatives. Analyst **97**: 111-113.

WANG, C. H., WILLIS, D. L., and LOVELAND, W. D. 1975. Radiotracer methodology in the biological, environmental and physical sciences. Prentice-Hall Inc., New York.

WEBSTER, A. D. 1896. Hardy coniferous trees. Hutchinson and Co., London.

WEISSFLOG, J., and MENGDEHL, H. 1933. Studien zum Phosphorstoffwechsel in der Hoheren Pflanze. III. Aufnahme und Verwertbarkeit Organischer Phosphorsaureverbindungen durch die Pflanze. Planta **19**: 182-241.

WEST, M. M., and LOTT, J. N. A. 1991. A histological and elemental analysis study of the mature seed of Begonia semperflorens. Can. J. Bot. **69**: 2165-2169.

WEST, M. M., LOTT, J. N. A., and MURRAY, D. R. 1992. Studies

of storage reserves in seeds of the marine angiosperm
Zostera capricorni. Aquatic Bot. **43**: 75-85.

WILCOX, M. D. 1983. Reciprocal cross effects in *Pinus radiata*.
New Zealand J. Forestry Sci. **13**: 37-45.

WINTON, A. I., and WINTON, K. B. 1932. Nuts of the pine
family. *In* The structure and composition of foods. Vol. 1.
Cereals, starch, oil seeds, nuts, oils, forage plants. John
Wiley and Sons Inc., New York. pp. 360-365.

YATSU, L. Y., and JACKS, T. J. 1972. Spherosome membranes.
Plant Physiol. **49**: 937-943.

YEATMAN, C. W. 1966. Germinant size of jack pine in relation
to seed size and geographic origin. Joint Proceedings:
Second Genetics Workshop of the Society of American
Foresters and the Seventh Lake States Forest Tree
Improvement Conference. July, 1966. U. S. Forest Service
Research Paper NC-6. pp. 28-36.

ZAR, J. H. 1984. Biostatistical analysis. Prentice-Hall, Inc.,
Englewood Cliffs, N. J.

Table A1. Correlations between female gametophyte + embryo measurements and mineral levels within female gametophyte and embryo tissues.

	P	Mg	Ca	Na	K
female gametophyte+embryo weight vs.					
μg/g female gametophyte	ns	ns	-ve	-ve	ns
μg/female gametophyte	+ve[*]	+ve	+ve[*]	+ve[*]	+ve[*]
μg/g embryo	ns	ns	ns	-ve	ns
μg/embryo	+ve	+ve	+ve	ND	+ve

	Cl	Mn	Cu	S	Zn	Fe
female gametophyte+embryo weight vs.						
μg/g female gametophyte	ns	ns	-ve	-ve[*]	-ve[*]	-ve
μg/female gametophyte	+ve	+ve[*]	+ve[*]	+ve[*]	+ve[*]	+ve[*]
μg/g embryo	+ve	-ve	ns	ns	-ve	-ve
μg/embryo	+ve	ns	ns	+ve	+ve	+ve

Note: +ve – significant positive correlation at P=0.05

-ve – significant negative correlation at P=0.05

[*] – significant correlation at P=0.001

ns – no significant correlation

ND – correlation test not performed

Table A2. Correlations between female gametophyte measurements and mineral levels within female gametophyte tissues.

female gametophyte weight vs.

	P	Mg	Ca	Na	K
μg/g female gametophyte	ns	ns	-ve	-ve	ns
μg/female gametophyte	+ve	+ve	+ve*	+ve*	+ve*

female gametophyte weight vs.

	Cl	Mn	Cu	S	Zn	Fe
μg/g female gametophyte	ns	ns	-ve	-ve*	-ve*	-ve
μg/female gametophyte	+ve	+ve*	+ve*	+ve*	+ve*	+ve*

female gametophyte area vs.

	P	Mg	Ca	Na	K
μg/g female gametophyte	ns	ns	-ve	-ve	ns
μg/female gametophyte	+ve*	+ve*	+ve*	+ve*	+ve*

female gametophyte area vs.

	Cl	Mn	Cu	S	Zn	Fe
μg/g female gametophyte	ns	ns	-ve	-ve	-ve*	-ve
μg/female gametophyte	+ve*	+ve*	+ve*	+ve*	+ve*	+ve*

female gametophyte length vs.

	P	Mg	Ca	Na	K
μg/g female gametophyte	ns	ns	ns	-ve	ns
μg/female gametophyte	+ve*	+ve*	+ve*	+ve*	+ve*

	Cl	Mn	Cu	S	Zn	Fe
female gametophyte length vs.						
μg/g female gametophyte	ns	ns	-ve	-ve	-ve	-ve
μg/female gametophyte	+ve*	+ve	+ve*	+ve*	+ve*	+ve*

	P	Mg	Ca	Na	K
female gametophyte width vs.					
μg/g female gametophyte	ns	ns	-ve	-ve	ns
μg/female gametophyte	+ve*	+ve	+ve*	+ve	+ve*

	Cl	Mn	Cu	S	Zn	Fe
female gametophyte width vs.						
μg/g female gametophyte	ns	ns	-ve	-ve*	-ve*	-ve*
μg/female gametophyte	+ve	+ve*	+ve*	+ve*	+ve*	+ve*

Table A3. Correlations between embryo measurements and mineral levels within embryo tissues.

	P	Mg	Ca	Na	K
embryo weight vs.					
μg/g embryo	ns	ns	ns	-ve	+ve
μg/embryo	+ve	+ve*	+ve*	ND	+ve*

	Cl	Mn	Cu	S	Zn	Fe
embryo weight vs.						
μg/g embryo	+ve*	-ve	ns	ns	-ve	-ve
μg/embryo	+ve*	+ve	+ve	+ve*	+ve*	+ve*

	P	Mg	Ca	Na	K
embryo area/width vs.					
μg/g embryo	ns	ns	ns	-ve	+ve
μg/embryo	+ve*	+ve*	+ve*	ND	+ve*

	Cl	Mn	Cu	S	Zn	Fe
embryo area/width vs.						
μg/g embryo	+ve*	-ve	ns	ns	ns	-ve
μg/embryo	+ve*	+ve	+ve	+ve*	+ve*	+ve*

	P	Mg	Ca	Na	K
embryo length vs.					
μg/g embryo	ns	ns	ns	-ve	+ve
μg/embryo	+ve*	+ve*	+ve*	ND	+ve*

	Cl	Mn	Cu	S	Zn	Fe
embryo length vs.						
μg/g embryo	+ve*	-ve	ns	ns	-ve	-ve
μg/embryo	+ve*	+ve	+ve	+ve*	+ve*	+ve*

Table A4. Correlations between P levels and the levels of other elements
in female gametophyte tissues.

μg/g P vs.	Mg	Ca	Na	K	Cl	Mn	Cu	S	Zn	Fe
μg/g	+ve	ns	ns	ns	ns	ns	ns	ns	+ve	ns

μg P/female gametophyte vs.	Mg	Ca	Na	K	Cl
μg/female gametopyte	+ve*	+ve*	+ve	+ve*	+ve*

μg P/female gametophyte vs.	Mn	Cu	S	Zn	Fe
μg/female gametophyte	+ve	+ve	+ve*	+ve*	+ve

Table A5. Correlations between P levels and the levels of other elements in embryo tissues.

μg/g P vs.	Mg	Ca	Na	K	Cl	Mn	Cu	S	Zn	Fe
μg/g	+ve	ns	ns	ns	ns	ns	ns	ns	ns	ns

μg P/embryo vs.	Mg	Ca	Na	K	Cl	Mn	Cu	S	Zn	Fe
μg/embryo	+ve*	+ve*	ND	+ve*	+ve*	+ve	+ve	+ve*	+ve*	+ve*

Table A6. Correlations between various elements in female gametophyte tissues.

μg/g vs.

μg/g	Mg	Ca	Na	K	Cl	Mn	Cu	S	Zn	Fe
Ca	ns	ND								
Na	ns	ns	ND							
K	+ve	ns	ns	ND						
Cl	+ve*	ns	ns	+ve	ND					
Mn	ns	ns	ns	ns	ns	ND				
Cu	ns	ns	ns	ns	ns	+ve	ND			
S	ns	+ve	ns	ns	ns	+ve	+ve	ND		
Zn	ns	+ve	+ve	ns	ns	ns	ns	+ve	ND	
Fe	ns	ns	+ve	ns	ns	ns	+ve	+ve	+ve	ND

μg/female gametophyte vs.

μg/female gametophyte

	Mg	Ca	Na	K	Cl	Mn	Cu	S	Zn	Fe
Ca	+ve*	ND								
Na	+ve*	+ve*	ND							
K	+ve*	+ve*	+ve*	ND						
Cl	+ve*	+ve*	+ve*	+ve*	ND					
Mn	+ve	+ve	+ve	+ve*	ns	ND				
Cu	+ve	+ve*	+ve	+ve*	+ve	+ve*	ND			

S	+ve*	+ve*	+ve*	+ve*	+ve*	+ve	+ve*	ND	
Zn	+ve*	+ve*	+ve	+ve*	+ve*	+ve	+ve*	+ve*	ND
Fe	+ve	+ve*	+ve*	+ve*	+ve	+ve*	+ve*	+ve*	+ve*	ND

Table A7. Correlations between various elements in embryo tissues.

μg/g vs.	Mg	Ca	Na	K	Cl	Mn	Cu	S	Zn	Fe
μg/g Ca	+ve	ND								
Na	ns	ns	ND							
K	ns	ns	ns	ND						
Cl	ns	ns	-ve	+ve	ND					
Mn	ns	ns	ns	ns	-ve	ND				
Cu	ns	ns	+ve	ns	ns	ns	ND			
S	ns	ns	ns	ns	ns	+ve	ns	ND		
Zn	ns	ns	ns	ns	ns	ns	ns	ns	ND	
Fe	ns	ns	ns	-ve	-ve	+ve	ns	ns	+ve	ND

μg/embryo vs.

μg/embryo

	Mg	Ca	Na	K	Cl	Mn	Cu	S	Zn	Fe
Ca	+ve*	ND								
Na	ND	ND	ND							
K	+ve*	+ve*	ND	ND						
Cl	+ve*	+ve	ND	+ve*	ND					
Mn	+ve	+ve	ND	+ve	+ve	ND				
Cu	+ve	+ve	ND	+ve	+ve	+ve	ND			
S	+ve*	+ve*	ND	+ve*	+ve*	+ve	+ve	ND		
Zn	+ve*	+ve*	ND	+ve*	+ve*	+ve	+ve	+ve*	ND	
Fe	+ve*	+ve*	ND	+ve*	+ve*	+ve	+ve	+ve*	+ve*	ND

Table A8. Correlations between the levels of various elements within
female gametophyte tissues and embryo tissues.

μg/g female gametophyte vs.

μg/g embryo

P	Mg	Ca	Na	K	Cl	Mn	Cu	S	Zn	Fe
+ve	ns	ns	ns	+ve	+ve	+ve	+ve	ns	+ve	+ve

μg/female gametopyte vs.

μg/embryo

P	Mg	Ca	Na	K	Cl	Mn	Cu	S	Zn	Fe
+ve[*]	+ve[*]	+ve	ND	+ve[*]	+ve[*]	ns	+ve	+ve[*]	+ve[*]	+ve

Appendix B

Table B1. Mean (±SD) peak-to-background ratios of several elements in various tissues of P. banksiana seeds.

region analyzed	P	Mg	K	Ca	Zn	Fe	Mn	S
cell walls	0.3 ± 0.3	0.2 ± 0.2	0.4 ± 0.5	0.1 ± 0.1	0.0 ± 0.2	0.1 ± 0.2	0.0 ± 0.2	0.1 ± 0.1
lipid bodies	0.5 ± 0.4	0.1 ± 0.2	0.5 ± 0.6	0.1 ± 0.2	0.0 ± 0.2	0.2 ± 0.2	0.0 ± 0.2	0.2 ± 0.2
proteinaceous matrix of protein bodies	1.7 ± 1.0	0.3 ± 0.3	0.3 ± 0.2	0.5 ± 0.4	0.0 ± 0.1	0.1 ± 0.2	0.0 ± 0.1	1.1 ± 0.4

Table B2. Mean (±SD) peak-to-background ratios of several elements in various tissues of P. contorta seeds.

region analyzed	P	Mg	K	Ca	Zn	Fe	Mn	S
cell walls	0.2 ± 0.2	0.4 ± 0.5	0.5 ± 0.3	0.1 ± 0.1	0.1 ± 0.1	0.1 ± 0.2	0.0 ± 0.2	0.2 ± 0.2
lipid bodies	0.1 ± 0.3	0.3 ± 0.9	0.2 ± 0.2	0.1 ± 0.2	0.1 ± 0.2	0.1 ± 0.2	0.0 ± 0.2	0.1 ± 0.2
proteinaceous matrix of protein bodies	0.8 ± 0.7	0.1 ± 0.2	0.4 ± 0.3	0.2 ± 0.2	0.1 ± 0.1	0.1 ± 0.2	0.1 ± 0.2	0.8 ± 0.4

Table B3. Mean (±SD) peak-to-background ratios of several elements in various tissues of P. resinosa seeds.

region analyzed	P	Mg	K	Ca	Zn	Fe	Mn	S
cell walls	0.1 ± 0.1	0.2 ± 0.1	0.9 ± 0.9	0.1 ± 0.1	0.0 ± 0.1	0.1 ± 0.1	0.1 ± 0.2	0.2 ± 0.1
lipid bodies	0.2 ± 0.3	0.2 ± 0.2	0.2 ± 0.4	0.0 ± 0.2	0.1 ± 0.2	0.1 ± 0.2	0.0 ± 0.2	0.2 ± 0.5
proteinaceous matrix of protein bodies	1.2 ± 0.4	0.3 ± 0.2	0.6 ± 0.3	0.0 ± 0.1	0.1 ± 0.1	0.1 ± 0.2	0.0 ± 0.2	1.2 ± 0.4

Table B4. Mean (±SD) peak-to-background ratios of several elements in various tissues of P. sylvestris seeds.

region analyzed	P	Mg	K	Ca	Zn	Fe	Mn	S
cell walls	0.2 ± 0.2	0.1 ± 0.1	1.0 ± 0.5	0.2 ± 0.2	0.0 ± 0.1	0.2 ± 0.1	0.0 ± 0.1	0.2 ± 0.1
lipid bodies	0.3 ± 0.4	0.1 ± 0.1	0.2 ± 0.2	0.1 ± 0.1	0.0 ± 0.1	0.1 ± 0.2	0.0 ± 0.2	0.1 ± 0.1
proteinaceous matrix of protein bodies	1.3 ± 0.6	0.3 ± 0.2	0.4 ± 0.3	0.4 ± 0.4	0.1 ± 0.1	0.3 ± 0.1	0.1 ± 0.1	0.9 ± 0.3

Table B5. Mean (±SD) peak-to-background ratios of several elements in various tissues of P. mugo seeds.

region analyzed	P	Mg	K	Ca	Zn	Fe	Mn	S
cell walls	0.7 ± 1.5	0.3 ± 0.3	0.7 ± 0.8	0.2 ± 0.2	0.1 ± 0.1	1.9 ± 6.8	0.0 ± 0.1	0.6 ± 0.3
lipid bodies	0.7 ± 0.4	0.2 ± 0.3	0.7 ± 0.7	0.3 ± 0.4	0.1 ± 0.2	0.1 ± 0.2	0.0 ± 0.2	0.5 ± 0.3
proteinaceous matrix of protein bodies	0.8 ± 0.7	0.3 ± 0.2	0.4 ± 0.6	0.1 ± 0.1	0.1 ± 0.1	0.2 ± 0.2	0.1 ± 0.1	1.4 ± 0.6

Table B6. Mean (±SD) peak-to-background ratios of several elements in various tissues of P. strobus seeds.

region analyzed	P	Mg	K	Ca	Zn	Fe	Mn	S
cell walls	0.3 ± 0.2	0.1 ± 0.1	0.8 ± 0.6	0.2 ± 0.3	0.0 ± 0.1	0.1 ± 0.1	0.0 ± 0.2	0.2 ± 0.1
lipid bodies	0.3 ± 0.5	0.2 ± 0.2	0.4 ± 0.4	0.0 ± 0.1	0.0 ± 0.1	0.1 ± 0.2	0.0 ± 0.2	0.1 ± 0.1
proteinaceous matrix of protein bodies	1.0 ± 0.5	0.2 ± 0.1	0.7 ± 0.5	0.1 ± 0.1	0.0 ± 0.1	0.2 ± 0.1	0.0 ± 0.2	1.2 ± 0.4

Table B7. Mean (±SD) peak-to-background ratios of several elements in various tissues of P. nigra seeds.

region analyzed	P	Mg	K	Ca	Zn	Fe	Mn	S
cell walls	0.1 ± 0.1	0.1 ± 0.2	0.5 ± 0.3	0.2 ± 0.2	0.0 ± 0.1	0.1 ± 0.1	0.0 ± 0.1	0.3 ± 0.2
lipid bodies	0.4 ± 0.3	0.1 ± 0.1	0.1 ± 0.2	0.0 ± 0.2	0.1 ± 0.2	0.1 ± 0.2	0.0 ± 0.3	0.1 ± 0.2
proteinaceous matrix of protein bodies	1.0 ± 0.6	0.2 ± 0.2	0.8 ± 0.3	0.1 ± 0.1	0.0 ± 0.1	0.2 ± 0.1	0.1 ± 0.1	1.2 ± 0.4

Table B8. Mean (±SD) peak-to-background ratios of several elements in various tissues of P. ponderosa seeds.

region analyzed	P	Mg	K	Ca	Zn	Fe	Mn	S
cell walls	0.3 ± 0.2	0.2 ± 0.3	0.9 ± 0.7	0.2 ± 0.2	0.0 ± 0.1	0.1 ± 0.1	0.1 ± 0.2	0.2 ± 0.1
lipid bodies	0.0 ± 0.2	0.0 ± 0.1	0.2 ± 0.4	0.0 ± 0.1	0.0 ± 0.1	0.1 ± 0.1	0.0 ± 0.1	0.0 ± 0.1
proteinaceous matrix of protein bodies	1.2 ± 0.7	0.4 ± 0.2	0.9 ± 0.8	0.1 ± 0.2	0.1 ± 0.2	0.1 ± 0.1	0.0 ± 0.2	1.5 ± 0.5

Table B9. Mean (±SD) peak-to-background ratios of several elements in various tissues of P. coulteri seeds.

region analyzed	P	Mg	K	Ca	Zn	Fe	Mn	S
cell walls	0.2 ± 0.3	0.2 ± 0.3	0.8 ± 0.4	0.0 ± 0.2	0.0 ± 0.1	0.3 ± 0.3	0.1 ± 0.4	0.2 ± 0.2
lipid bodies	0.0 ± 0.2	0.2 ± 0.3	0.1 ± 0.2	0.1 ± 0.2	0.0 ± 0.2	0.2 ± 0.3	0.1 ± 0.3	0.0 ± 0.3
proteinaceous matrix of protein bodies	0.8 ± 0.4	0.2 ± 0.2	0.7 ± 0.4	0.1 ± 0.1	0.1 ± 0.1	0.3 ± 0.2	0.1 ± 0.1	0.8 ± 0.4

Table B10. Mean (±SD) peak-to-background ratios of several elements in various tissues of P. sabiniana seeds.

region analyzed	P	Mg	K	Ca	Zn	Fe	Mn	S
cell walls	0.2 ± 0.4	0.2 ± 0.2	0.9 ± 0.5	0.1 ± 0.1	0.0 ± 0.1	0.1 ± 0.2	0.0 ± 0.1	0.1 ± 0.2
lipid bodies	0.1 ± 0.3	0.1 ± 0.1	0.2 ± 0.3	0.0 ± 0.1	0.0 ± 0.1	0.1 ± 0.1	0.2 ± 0.2	0.1 ± 0.2
proteinaceous matrix of protein bodies	1.3 ± 0.8	0.2 ± 0.2	0.8 ± 0.4	0.0 ± 0.1	0.0 ± 0.2	0.1 ± 0.1	0.0 ± 0.2	0.6 ± 0.3

Table B11. Mean (±SD) peak-to-background ratios of several elements in various tissues of P. koraiensis seeds.

region analyzed	P	Mg	K	Ca	Zn	Fe	Mn	S
cell walls	0.2 ± 0.4	0.1 ± 0.3	0.5 ± 0.7	0.0 ± 0.1	0.0 ± 0.2	0.1 ± 0.1	0.0 ± 0.2	0.1 ± 0.4
lipid bodies	0.2 ± 0.4	0.2 ± 0.6	0.3 ± 0.5	0.1 ± 0.2	0.0 ± 0.2	0.3 ± 0.2	0.1 ± 0.3	0.4 ± 1.3
proteinaceous matrix of protein bodies	0.9 ± 0.8	0.4 ± 0.3	1.4 ± 0.9	0.1 ± 0.2	0.0 ± 0.1	0.1 ± 0.1	0.0 ± 0.1	0.6 ± 0.3

Appendix C

Table C1. Correlations between female gametophyte + embryo weight and P/B ratios of elements in globoid crystals as detected by EDX analysis.

Weight vs.	P	Mg	K	Ca	Fe
female gametophyte	-ve	ns	ns	ns	ns
root apex	ns	ns	ns	ns	ns
ground meristem					
cotyledon tip	ns	ns	ns	-ve	ns
cotyledon gr. meristem	-ve	ns	ns	ns	ns
hypocotyl	-ve*	-ve	ns	ns	ns

Note: +ve - significant positive correlation at P=0.05

-ve - significant negative correlation at P=0.05

* - significant correlation at P=0.001

ns - no significant correlation

Table C2. Correlations of female gametophyte + embryo weight to P/B ratios of elements in electron-dense particles (<0.33 μm).

weight vs.	P	Mg	K	Ca	Fe
female gametophyte	ns	ns	ns	ns	ns
root apex	ns	ns	ns	ns	-ve
shoot apex	ns	ns	ns	ns	ns

<u>protoderm</u>

cotyledon tip	ns	ns	ns	ns	-ve
cotyledon	ns	ns	ns	ns	-ve[*]
hypocotyl	ns	ns	ns	ns	-ve

<u>ground</u> <u>meristem</u>

cotyledon tip	-ve	-ve	ns	ns	-ve[*]
cotyledon	ns	ns	ns	ns	-ve
hypocotyl	-ve	ns	ns	ns	-ve[*]

<u>procambium</u>

cotyledon tip	ns	ns	ns	ns	-ve[*]
cotyledon	ns	ns	ns	ns	-ve[*]
hypocotyl	ns	ns	ns	ns	-ve[*]

Table C3. Correlations of female gametophyte measurements to P/B ratios of elements in globoid crystals of female gametophytes.

measurements vs.	P	Mg	K	Ca	Fe
weight/width	-ve	ns	ns	ns	ns
length/area	-ve[*]	ns	ns	-ve	ns

Table C4. Correlations of female gametophyte measurements to P/B ratios of elements in electron-dense particles of female gametophytes.

weight/length/width/area vs.	P	Mg	K	Ca	Fe
	ns	ns	ns	ns	ns

Table C5. Correlations of embryo measurements to P/B ratios
of elements in globoid crystals of embryos.

weight/area vs.	P	Mg	K	Ca	Fe
root apex	ns	-ve	ns	ns	ns
ground **meristem**					
cotyledon tip	ns	ns	+ve	-ve	ns
cotyledon	-ve*	-ve*	ns	ns	ns
hypocotyl	-ve*	-ve*	ns	ns	ns
length/width vs.	P	Mg	K	Ca	Fe
root apex	-ve	-ve*	ns	ns	ns
ground **meristem**					
cotyledon tip	ns	ns	ns	-ve	ns
cotyledon	-ve*	-ve*	ns	-ve	ns
hypocotyl	-ve*	-ve*	ns	-ve	ns

Table C6. Correlations of embryo measurements to P/B ratios
of electron-dense particles of embryos.

weight vs.	P	Mg	K	Ca	Fe
root apex	ns	ns	ns	ns	ns
shoot apex	-ve	ns	ns	ns	ns
protoderm					
cotyledon tip	ns	ns	ns	ns	-ve*
cotyledon	ns	ns	ns	-ve	-ve*
hypocotyl	-ve	ns	ns	ns	ns
ground **meristem**					
cotyledon tip	-ve	-ve*	ns	ns	-ve*

	P	Mg	K	Ca	Fe
cotyledon	ns	ns	ns	ns	-ve*
hypocotyl	-ve*	-ve	ns	-ve	-ve*

procambium

	P	Mg	K	Ca	Fe
cotyledon tip	ns	ns	ns	-ve	-ve*
cotyledon	ns	ns	ns	ns	-ve*
hypocotyl	ns	ns	ns	ns	-ve*
length vs.	P	Mg	K	Ca	Fe
root apex	ns	ns	ns	-ve	ns
shoot apex	-ve	ns	ns	ns	ns

protoderm

	P	Mg	K	Ca	Fe
cotyledon tip	ns	ns	ns	ns	-ve*
cotyledon	ns	ns	ns	-ve	-ve*
hypocotyl	ns	ns	ns	ns	ns

ground meristem

	P	Mg	K	Ca	Fe
cotyledon tip	-ve	-ve	ns	ns	-ve*
cotyledon	ns	ns	ns	ns	-ve
hypocotyl	-ve*	-ve	ns	-ve	-ve*

procambium

	P	Mg	K	Ca	Fe
cotyledon tip	ns	ns	ns	-ve	-ve*
cotyledon	ns	ns	ns	ns	-ve*
hypocotyl	ns	ns	ns	ns	-ve*
width vs.	P	Mg	K	Ca	Fe
root apex	-ve	ns	ns	ns	-ve
shoot apex	-ve	ns	ns	ns	-ve

protoderm

	P	Mg	K	Ca	Fe
cotyledon tip	ns	ns	ns	ns	-ve*

	P	Mg	K	Ca	Fe
cotyledon	ns	ns	ns	-ve	-ve*
hypocotyl	ns	ns	ns	ns	ns
ground meristem					
cotyledon tip	-ve	-ve	ns	ns	-ve*
cotyledon	ns	ns	ns	ns	-ve*
hypocotyl	-ve*	-ve	ns	-ve	-ve*
procambium					
cotyledon tip	ns	ns	ns	-ve	-ve*
cotyledon	ns	ns	ns	ns	-ve*
hypocotyl	ns	ns	ns	ns	-ve*
area vs.	P	Mg	K	Ca	Fe
root apex	ns	ns	ns	ns	ns
shoot apex	-ve	ns	ns	ns	ns
protoderm					
cotyledon tip	-ve	ns	ns	ns	-ve*
cotyledon	ns	ns	ns	ns	-ve*
hypocotyl	-ve	ns	ns	ns	ns
ground meristem					
cotyledon tip	-ve	-ve*	ns	ns	-ve*
cotyledon	ns	ns	ns	ns	-ve
hypocotyl	-ve*	-ve	ns	-ve	-ve*
procambium					
cotyledon tip	ns	ns	ns	-ve	-ve*
cotyledon	ns	ns	ns	ns	-ve*
hypocotyl	ns	ns	ns	ns	-ve*

Table C7. Correlations of female gametophyte + embryo weight

to K/P ratios of globoid crystals.

female gametophyte + embryo weight	vs.	K/P
female gametophyte		+ve
root apex		+ve[*]
ground meristem		
cotyledon tip		+ve[*]
cotyledon		+ve[*]
hypocotyl		+ve[*]

Table C8. Correlations of female gametophyte + embryo weight

to K/P ratios of electron-dense particles.

female gametophyte + embryo weight	vs.	K/P
female gametophyte		ns
root apex		+ve
shoot apex		ns
protoderm		
cotyledon tip		+ve
cotyledon		+ve
hypocotyl		+ve[*]
ground meristem		
cotyledon tip		+ve[*]
cotyledon		ns
hypocotyl		+ve

<u>procambium</u>

cotyledon tip		+ve
cotyledon		ns
hypocotyl		ns

Table C9. Correlations of female gametophyte measurements to
K/P ratios of globoid crystals and electron-dense
particles in female gametophytes.

female gametophyte measurement vs.	globoid crystal K/P	particle ($<0.33\mu$m) K/P
weight/width	+ve	ns
length/area	ns	ns

Table C10. Correlations of embryo measurements to K/P ratios
of globoid crystals in embryos.

weight/length vs.	K/P
root apex	+ve[*]

<u>ground</u> <u>meristem</u>

cotyledon tip	+ve
cotyledon	+ve[*]
hypocotyl	+ve[*]

width/area vs.	K/P
root apex	+ve

<u>ground</u> <u>meristem</u>

cotyledon tip	+ve
cotyledon	+ve[*]

hypocotyl   +ve*

Table C11.   Correlations of embryo measurements to K/P ratios
             of electron-dense particles in embryos.

weight/length vs.	K/P	width/area vs.	K/P
root apex	+ve	root apex	+ve
shoot apex	ns	shoot apex	+ve
protoderm		protoderm	
cotyledon tip	+ve*	cotyledon tip	+ve*
cotyledon	+ve*	cotyledon	+ve*
hypocotyl	+ve	hypocotyl	+ve*
ground meristem		ground meristem	
cotyledon tip	+ve	cotyledon tip	+ve
cotyledon	+ve*	cotyledon	+ve*
hypocotyl	+ve*	hypocotyl	+ve*
procambium		procambium	
cotyledon tip	+ve*	cotyledon tip	+ve*
cotyledon	+ve	cotyledon	+ve
hypocotyl	ns	hypocotyl	ns

Table C12.   Correlations of embryo measurements to Fe/P ratios
             of electron-dense particles in embryos

weight/length/width/area vs.	Fe/P
root apex	ns
shoot apex	ns

<u>protoderm</u>

cotyledon tip   -ve

cotyledon   ns

hypocotyl   ns

<u>ground</u> <u>meristem</u>

cotyledon tip   -ve*

cotyledon   -ve

hypocotyl   ns

<u>procambium</u>

cotyledon tip   -ve*

cotyledon   -ve

hypocotyl   ns

Table C13. Correlations of female gametophyte + embryo weight
            to various ratios created from P/B ratios of
            globoid crystals.

weight vs.	(Mg+K)	(Mg+Ca)	(Mg+Ca+Fe)	(Mg+Ca+Fe+K)
	P	P	P	P
female gametophyte	ns	ns	ns	ns
root apex	+ve*	ns	ns	ns
<u>ground</u> <u>meristem</u>				
cotyledon tip	+ve*	-ve	-ve	+ve*
cotyledon	+ve*	ns	ns	+ve
hypocotyl	+ve*	-ve*	-ve	+ve*

Table C14. Correlations of female gametophyte + embryo weight
to various ratios created from P/B ratios of
electron-dense particles.

weight vs.	(Mg+K)	(Mg+Ca)	(Mg+Ca+Fe)	(Mg+Ca+Fe+K)
	P	P	P	P
female gametophyte	ns	ns	ns	ns
root apex	+ve*	ns	-ve*	ns
shoot apex	ns	ns	ns	ns
protoderm				
cotyledon tip	+ve	ns	-ve	ns
cotyledon	+ve	ns	ns	ns
hypocotyl	+ve*	ns	-ve	ns
ground meristem				
cotyledon tip	+ve*	ns	-ve	ns
cotyledon	ns	ns	-ve	ns
hypocotyl	+ve*	ns	ns	ns
procambium				
cotyledon tip	+ve	-ve*	-ve*	-ve
cotyledon	+ve	ns	-ve	-ve
hypocotyl	+ve	ns	-ve	-ve

Table C15. Correlations of female gametophyte measurements to
various ratios created from P/B ratios of globoid
crystals in female gametophytes.

measurement vs.	(Mg+K)	(Mg+Ca)	(Mg+Ca+Fe)	(Mg+Ca+Fe+K)
	P	P	P	P
weight	ns	ns	ns	ns

length	ns	-ve	-ve	ns
width	+ve	-ve	ns	ns
area	ns	-ve	ns	ns

Table C16. Correlations of female gametophyte measurements to various ratios created from P/B ratios of electron-dense particles in female gametophytes.

measurement vs.	(Mg+K)	(Mg+Ca)	(Mg+Ca+Fe)	(Mg+Ca+Fe+K)
	P	P	P	P
weight/length	ns	ns	ns	ns
width/area	ns	ns	ns	ns

Table C17. Correlations of embryo measurements to various ratios created from P/B ratios of globoid crystals in embryos.

weight/length width/area vs.	(Mg+K)	(Mg+Ca)	(Mg+Ca+Fe)	(Mg+Ca+Fe+K)
	P	P	P	P
root apex	+ve	ns	ns	ns
ground meristem				
cotyledon tip	+ve	-ve[*]	-ve[*]	ns
cotyledon	+ve	ns	ns	ns
hypocotyl	+ve	-ve[*]	-ve[*]	ns

Table C18. Correlations of embryo measurements to various ratios created from P/B ratios of electron-dense particles in embryos.

weight vs.	(Mg+K)	(Mg+Ca)	(Mg+Ca+Fe)	(Mg+Ca+Fe+K)
	P	P	P	P
root apex	+ve	-ve	-ve	ns
shoot apex	ns	ns	ns	ns
protoderm				
cotyledon tip	+ve*	ns	-ve	ns
cotyledon	+ve*	ns	-ve	ns
hypocotyl	+ve	ns	ns	ns
ground meristem				
cotyledon tip	+ve*	ns	-ve	ns
cotyledon	ns	-ve	-ve	ns
hypocotyl	+ve*	-ve	ns	ns
procambium				
cotyledon tip	+ve	-ve*	-ve*	-ve
cotyledon	+ve*	ns	-ve	-ve
hypocotyl	ns	ns	-ve	-ve
length vs.	(Mg+K)	(Mg+Ca)	(Mg+Ca+Fe)	(Mg+Ca+Fe+K)
	P	P	P	P
root apex	+ve*	-ve	-ve	ns
shoot apex	+ve	ns	ns	ns
protoderm				
cotyledon tip	+ve*	ns	-ve*	-ve
cotyledon	+ve*	ns	-ve	ns
hypocotyl	+ve	ns	ns	ns

ground meristem

cotyledon tip	+ve*	ns	-ve	ns
cotyledon	ns	-ve	-ve	ns
hypocotyl	+ve*	-ve	ns	ns

procambium

cotyledon tip	+ve	-ve*	-ve*	-ve
cotyledon	+ve	ns	-ve	-ve
hypocotyl	ns	ns	-ve	-ve

width vs.	(Mg+K)	(Mg+Ca)	(Mg+Ca+Fe)	(Mg+Ca+Fe+K)
	P	P	P	P
root apex	+ve	ns	-ve	ns
shoot apex	ns	ns	ns	ns

protoderm

cotyledon tip	+ve*	ns	-ve	ns
cotyledon	+ve*	ns	ns	ns
hypocotyl	+ve	ns	ns	ns

ground meristem

cotyledon tip	+ve*	ns	-ve	ns
cotyledon	ns	-ve	-ve	ns
hypocotyl	+ve	ns	ns	ns

procambium

cotyledon tip	+ve	-ve	-ve*	-ve
cotyledon	+ve	ns	-ve	ns
hypocotyl	ns	ns	-ve	-ve

area vs.	(Mg+K)	(Mg+Ca)	(Mg+Ca+Fe)	(Mg+Ca+Fe+K)
	P	P	P	P
root apex	+ve	ns	-ve	ns

shoot apex	ns	ns	ns	ns

<u>protoderm</u>

cotyledon tip	+ve[*]	ns	-ve	ns
cotyledon	+ve	ns	ns	ns
hypocotyl	+ve	ns	ns	ns

<u>ground</u> <u>meristem</u>

cotyledon tip	+ve[*]	ns	-ve	ns
cotyledon	ns	-ve	-ve	ns
hypocotyl	+ve[*]	-ve	ns	ns

<u>procambium</u>

cotyledon tip	+ve	-ve	-ve[*]	-ve
cotyledon	+ve	ns	-ve	-ve
hypocotyl	ns	ns	-ve	ns